Republic of Iraq
Ministry of Higher Education
and Scientific Research
University of Kerbala
College of Science

Synthesis and Biological Activity of Bis-1,2,3-Triazole Derivatives Starting from D-Mannitol

A Thesis

Submitted to the Council of the College of Science
University of Kerbala
In Partial Fulfillment of the Requirement for the
Degree of Master of Science in Chemistry

By

Zainab Mohammed Kadhim
B.Sc. Chemistry (2015) \University of Babylon

Supervised by
Assist.Prof. Dr. Adnan Ibrahim Mohammed

2021 AD **1443 AH**

بسم الله الرحمن الرحيم

{ وَمَا أُوتِيتُم مِّنَ الْعِلْمِ إِلَّا قَلِيلًا }

صدق الله العلي العظيم

سورة الاسراء اية (85)

Supervisor Certification

I certify that this thesis is conducted under my supervision at the Department of Chemistry, College of Science, University of Kerbala, as a partial fulfillment of the requirements for the degree of Master in chemistry.

Signature:

Name: Prof. Dr. Adnan Ibrahim Mohammed

Address: University of Kerbala / College of Science

Date: / /2021

Report of the Head of Chemistry Department
Chairman of Postgraduate Studies Committee

According to the recommendation presented by the Chairman of the Postgraduate Studies Committee, I forward this thesis for discussion.

Signature:

Name: Assist. Prof. Dr. Adnan Ibrahim Mohammed

Address: University of Kerbala / College of Science

Date: / /2021

Examination Committee Certification

We, the examining committee, certify that we have read this thesis "**Synthesis, Biological Activity and Structural Study of D-Mannitol-based 1,2,3-Triazoles**" and *examined the student* (**Zainab Mohammed Kadhim**) *in its contents and that in our opinion, it is adequate as a thesis for the degree of Master of Science in chemistry.*

(Chairman)
Signature:
Name: Dr. Majed Jari Mohammed
Title: Prof.
Address: University of Kufa / College of Science
Date: / / 2021

(Member)
Signature:
Name: Dr. Muqdad Irhaeem Kadhim
Title: Prof.
Address: University of Al-Qadisiyah, College of Science
Date: / / 2021

(Member)
Signature:
Name: Dr. Haitham Dalol Hanoon
Title: Prof.
Address: University of Kerbala, College of Science
Date: / / 2021

(Member & Supervisor)
Signature:
Name: Dr. Adnan Ibrahim Mohammed
Title: Assist. Prof.
Address: University of Kerbala, College of Science
Date: / / 2021

Approved by the council of the College of Science in its Session No. in / /2021

Signature:
Name: Dr. Jasem Hannon Hashim Al-Awadi
Title: Assist. Prof.
Address: University of Kerbala - Dean of College of Science
Date: / / 202

Dedication

To **my father** and **my mother**

To **my brothers**

To **my department of chemistry, College of Science for Girls, University of Babylon**, for their advice and guidance they gave me scientifically and morally, to strive to achieve this important step, especially mention **Assist. Prof. Dr. Aseel Al-Joburri** for her continuous support to this day.

To **my loyal friend**

Acknowledgement

I would like to thank Allah for its blessings ...

I would like to thank my supervisor Assist. Prof. Dr. Adnan Ibrahim Mohammed for his guidance during the course and the idea of deep research and for the continuous laboratory follow-up. Huge thanks to Assoc. Prof. Dr. Jason Harper, the University of New South Wales for his support and analyzing the compounds.

I would like to thank whoever help me from the teaching staff at the University of Kerbala, College of science, department of chemistry,

I would like to thank the Lecturer Mrs Lamya Saleh for the useful information in the laboratory .

Table of contents

Abstract

The current work is including synthesis of new mannitol based bis-1,2,3-triazoles and study of their cytotoxicity. First, aromatic azides **99a**–**c** were synthesized in excellent yields via the reaction of corresponding benzyl bromides with sodium azide in DMSO. In a separate step, the commercially available D-mannitol was reacted with acetone in the presence of zinc chloride to give 1,2:5,6-di-*O*-isopropylidene-D-mannitol (**101**) in 54% yield, which was treated with propargyl bromide in DMF to produce 3,4-bis-*O*-propargyl-1,2:5,6-di-*O*-isopropylidene-D-mannitol (**102**) in a very good yield. The copper catalyzed cycloaddition reaction of the dialkyne **102** with azides **99a**–**c** gave the bis-1,2,3-triazole derivatives **103 a**–**c** in nearly very good yields. The final step in the synthesis was the acetal groups' removal of compounds **103 a**–**c** to afford the deprotected triazole derivatives **104 a**–**c** in quantitative yields. The synthesized compounds were characterized followed by TLC, FT-IR, NMR, COSY, HSQC, HMBC and HRMS. Compounds **103 a**–**c** were *in vitro* screened against human mesenchymal stem cells and found to possess fair cytotoxicity.

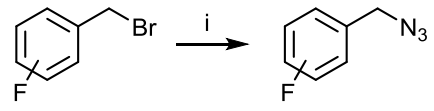

98a-c **99a-c**

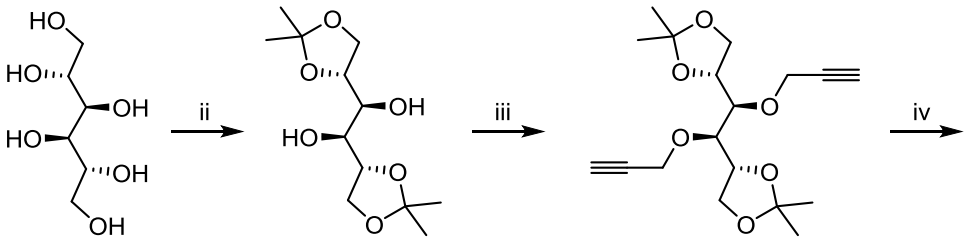

100 **101** **102**

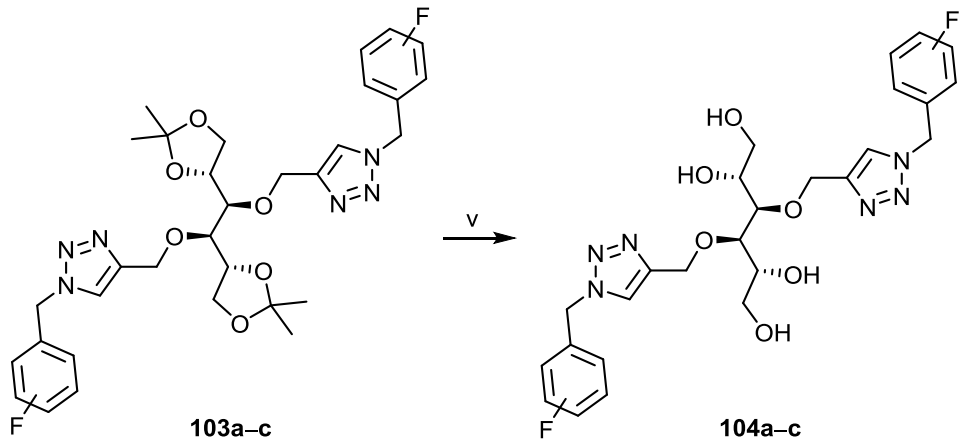

103a–c **104a–c**

Reagents and conditions: **i**] NaN_3, DMSO, 50 °C, 24 h; 88-91%ii] acetone, $ZnCl_2$, r.t., 24 h, 54%; **iii**] propargyl bromide, DMF, –20 °C–r.t.,24 h, 84%; iv] **99a–c**, Na ascorbate, $CuSO_4$•$5H_2O$, DMSO, 50 °C, 36 h, 77–81%; v] Amberlite IR 120 H+, MeOH / H_2O, 60 °C, 72 h.quantitative.

Abbreviations

^{13}C NMR	carbon nuclear magnetic resonance
^{19}F NMR	fluorine nuclear magnetic resonance
^{1}H NMR	proton nuclear magnetic resonance
2D	two dimensional
Ac	acyl
ATP	adenosine triphosphate
CAN	cerium ammonium nitrate
COSY	correlation spectroscopy
COVID	CO' stands for corona, 'VI' for virus, and 'D' for disease
CuAAC	copper(I)-catalyzed azide-alkyne cycloaddition
DCE	1,2-dichloroethane
DES	deep eutectic solvent
DMF	dimethylformamide
DMSO	dimethyl sulfoxide
EC_{50}	half maximal effective concentration
EtOAc	ethyl acetate
FBS	fetal bovine serum
FT-IR	Fourier-transform infrared
h	hour
HMBC	heteronuclear multiple bond correlation
HRMS	high-resolution mass spectrometry
HSQC	heteronuclear single quantum coherence
IC_{50}	half maximal inhibitory concentration

J	coupling constant
M	molar
m.p.	melting point
PEG	polyethylene glycol
ppm	part per million
r.t.	room temperature
$\boldsymbol{R_f}$	retention factor
TBAI	tetrabutylammonium iodide
THF	tetrahydrofuran
TLC	thin layer chromatography

CHAPTER ONE INTRODUCTION

1. Introduction

Heterocyclic compounds are one of the important classes of organic chemistry due their wide range of applications.[1–5] In addition to their cyclic nature, it should contain one or more heteroatoms rather than carbon i.e. nitrogen, oxygen, sulfur, selenium…etc. and it can be aromatic or non-aromatic.[6,7] Heterocyclic compounds are classified into three, four, five, six, seven-membered rings and they could be fused-cyclic derivatives comprises of two rings or more.[8,9] The most important categories are the five- and six-membered rings because their availability in compounds that have essential role nature such as nucleotides (adenosine triphosphate (ATP) (**1**)), carbohydrates (L-ascorbic acid (**2**)) and penicillin (**3**).[10–12]

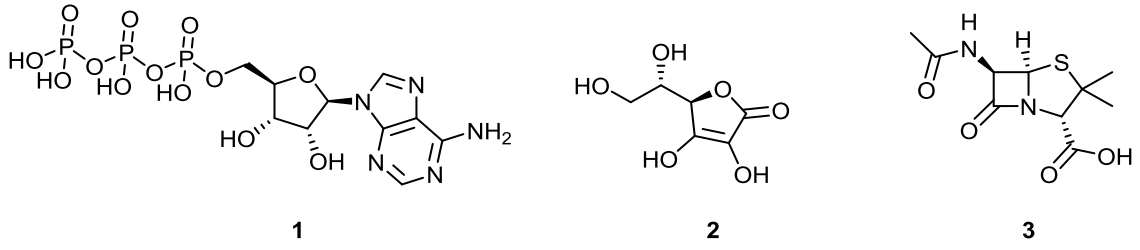

1 **2** **3**

Figure 1. Structures of ATP(1), L-ascorbic acid(2), and penicillin(3)

1.1.Five-membered ring heterocyclic compounds

There are many heterocyclic derivatives categorized under this class and varies from one to four heteroatomic molecules. The common examples of hetero-alicyclic derivatives are tetrahydrofuran (**5**), pyrrolidine (**6**) and tetrahydrothiophene (**7**). These compounds are highly consumed for industrial applications, and it produced according to the following scheme[13–15]:

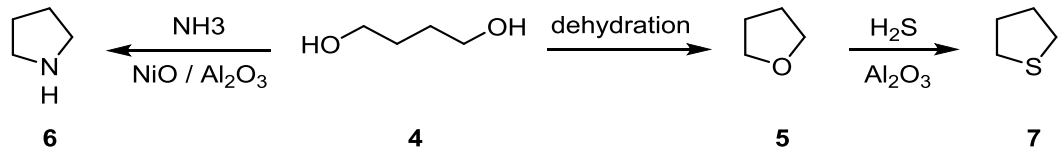

6 **4** **5** **7**

Scheme 1. Industrial production of tetrahydrofuran, tetrahydrothiophene and pyrrolidine

The aromatic counterparts: furan (**8**), pyrrole (**9**) and thiophen (**10**) of the compounds **5**–**7** are also important, and their derivatives have remarkable applications particularly in the field of drug design i.e. antimicrobial nitrofurazone (**11**)[16], antiplatelet

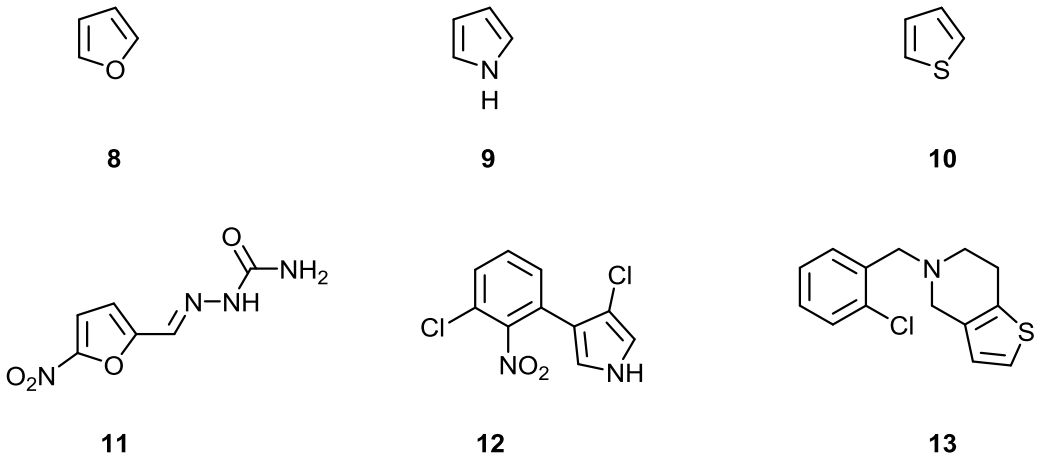

8 **9** **10**

11 **12** **13**

drug ticlopidine (**12**)[17] and antifungal pyrrolnitrin (**13**).[18]

Figure 2. Structure of furan, pyrrole, thiophene and examples of their corresponding drugs

When another carbon atom is replaced by nitrogen in the compounds **8**–**10**, a new set of diatomic heterocyclic five-membered ring is afforded, for example, isoxazole (**14**), oxazole (**15**), pyrazole (**16**), imidazole (**17**), isothiazole (**18**), and thiazole (**19**).[19,20] The position of the nitrogen regarding to the other heteroatom governs the physical and chemical properties of the molecule. Although, imidazole and pyrazole have similar

chemical formula, the former compound possess higher basicity (pK_b = 7.0) than the latter (pK_b = 11.5) and they have different physical properties.[21–23]

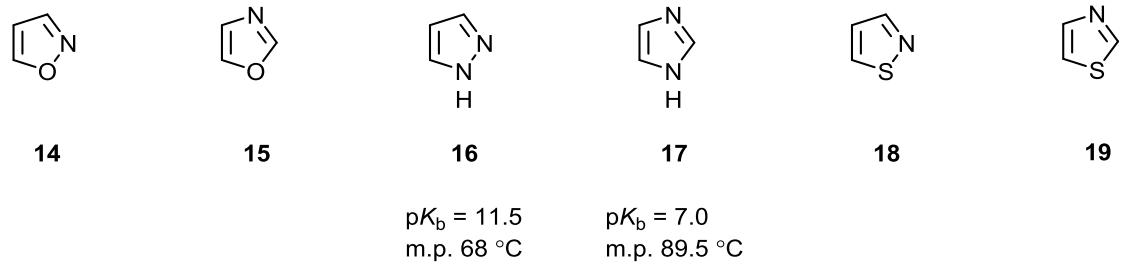

Figure 3. Structure of compounds **14**–**19**; comparison between compounds **16** and **17** in their basicity and melting points

Once again, replacing the carbon atom (adjacent to the sp^2 nitrogen) by nitrogen atom resulting in two different heterocyclic compounds; 1,2,3-triazole and 1,2,4-triazole.

1.2.Triazoles

Triazoles are available in two isomeric forms 1,2,3-triazoles (**20**) and 1,2,4-triazoles (**21**). Both have one sp^3nitrogen atom and two sp^2 or pyridine-like nitrogen atoms. This allows the two isomers to own amphoteric behavior as they can accept proton *via* the sp^2 nitrogen or subtract proton from the pyrrole-like nitrogen and stabilize by delocalization (Scheme 2).[24–26]

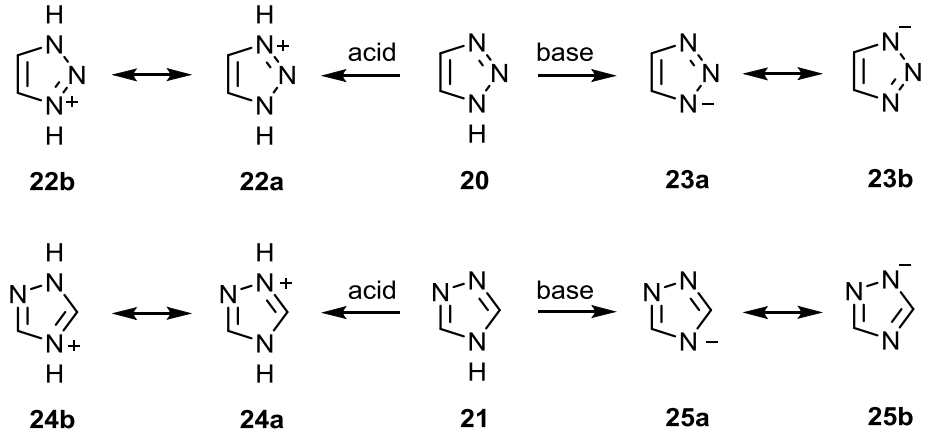

Scheme 2. The amphoteric behavior of triazoles **20** and **21**

The variety in the chemical properties of triazoles affords them wide range of applications mainly in the pharmacological domain and consequently the synthesis of triazoles draws the attention of the researchers.[27–30] There are many methods to synthesize 1,2,4-triazole and one of the earliest routs of preparation is Pellizzari method.[31] In this reaction (Scheme 3), substituted 1,3,4-triazole derivatives are synthesized by the condensation of amides and hydrazides. However, this reaction is time consuming and it requires high temperature.[32]

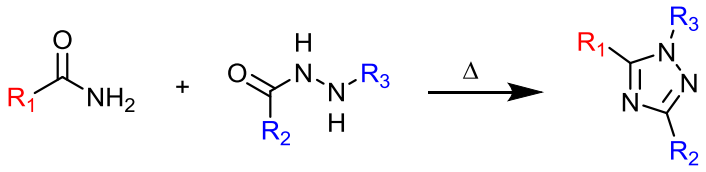

Scheme 3. Synthesis of substituted 1,3,4-triazole through Pellizzari reaction

Pellizzari method is then developed to improve the reaction conditions and regioselectivity. In the last decade, various components and green protocols have been utilized to reach the substituted 1,2,4-triazoles.[33]

The reaction of aldehydes with amidrazones in the presence of cerium ammonium nitrate (CAN) and polyethylene glycol as a reaction media yielded trisubstituted-1,2,4-triazoles in a very good yield (Scheme 4).[34]

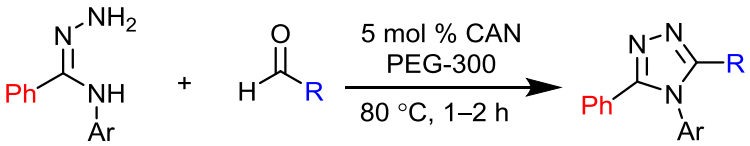

Scheme 4. Cerium ammonium nitrate (CAN) catalyzed synthesis of trisubstituted-1,2,4-triazoles

1,2,4-Triazoles can be obtained from the copper-catalyzed reaction of amidines hydrochloride with aromatic nitriles in the presence of cesium carbonate, air and using DMSO as a solvent at 120 °C for 24 h (Scheme 5).[35]

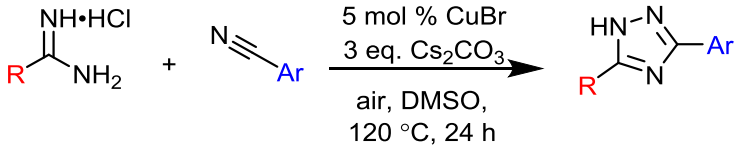

Scheme 5. Copper-catalyzed synthesis of disubstituted-1,2,4-triazoles

Liu *et al*., utilized sliver (I)[36] to promote the regioselective synthesis of 1,3-disubstituted 1,2,4-triazoles in 1,2-dichloroethane at 0 °C for 6 to 12 h. (Scheme 6). This method is highly efficient and has excellent functional group compatibility.

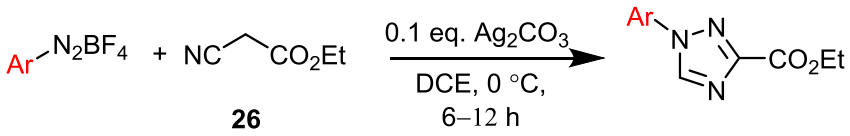

Scheme 6. Ag (I)-catalyzed regioselective synthesis of 1,3-disubstituted 1,2,4-triazoles

However, when the starting materials are reacted in the presence of a mixture of copper acetate and lithium acetate in THF at similar temperature, 1,5-disubstituted 1,2,4-triazoles are obtained instead (Scheme 7).[36]

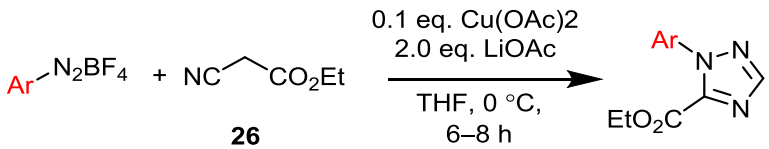

Scheme 7. Cu (II)-catalyzed regioselective synthesis of 1,5-disubstituted 1,2,4-triazoles

The environmentally tolerated synthesis of 4,5-disubstituted 3-amino-1,2,4-triazoles is achieved by the reaction of amidines and isothiocyanates in the presence of

iodine as a catalyst and water as a solvent. The reaction is performed at ambient temperature for 3 h. (Scheme 8).[37]

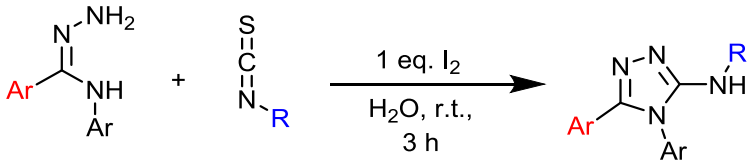

Scheme 8. Friendly-environment synthesis of 4,5-disubstituted 3-amino-1,2,4-triazoles

In addition to the interest in the synthesis and application of 1,2,4-triazoles, researchers tend to synthesize 1,2,3-triazole derivatives due to their wide applications.

1.3. 1,2,3-Triazoles

1,2,3-Triazoles are significant class of organic compounds. They are five-membered heterocyclic molecules which consist of three consecutive nitrogen atoms and two carbons.

1.3.1. Synthesis of 1,2,3-triazoles

There is a number of methods to construct 1,2,3-triazoles and they are varying from non-regioselective to regioselective protocols.[38–40]

1.3.1.1. Cycloaddition of azides to alkynes

When a 1,3-dipole reacts with dipolarphile the reaction is then called 1,3-cycloaddition or Huisgen cycloaddition due to the efforts of Rolf Huisgen[41] in the investigation and description of the 1,3-cycloaddition reaction mechanism. There are several organic compounds that process this feature because of the spread of two charge over three atoms such as azides, nitro compounds, diazo compounds, nitrones and other organic molecules (Figure 5).[42,43]

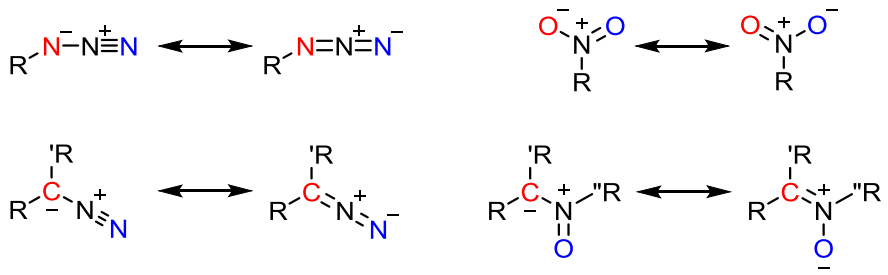

Figure 5. A number of organic 1,3-dipolar compounds

1,2,3-Triazoles can be produced by the reaction of 1,3-dipolar compound (azide) and dipolarphile (alkyne). However, this reaction affords two isomers: 1,4- and 1,5-disubstitued 1,2,3-triazoles (Scheme 9)[44,45]

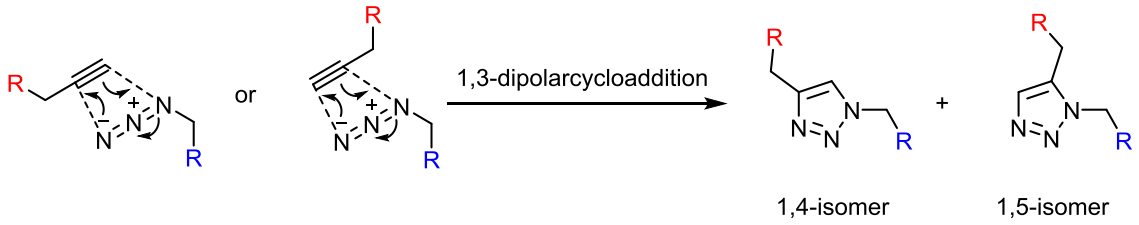

Scheme 9. 1,3-dipolarcycloaddition between organic azides and alkynes to give 1,4- and 1,5-disubstitued 1,2,3-triazoles

1.3.1.2. Cycloaddition of azides to allenes

Allenes are cumulated dienes having an *sp*-hybridized carbon atom and two sp^2-hybridized carbons. Due to their electronic properties, they tolerate [2 + 2] and [2 + 4] cycloaddition reactions.[46] For example, the reaction of allenes with aromatic azides in Deep Eutectic Solvent (DES) at 90 °C gives two different 1,4-disubstituted-1,2,3-triazole derivatives in low yield (Scheme 10).[47]

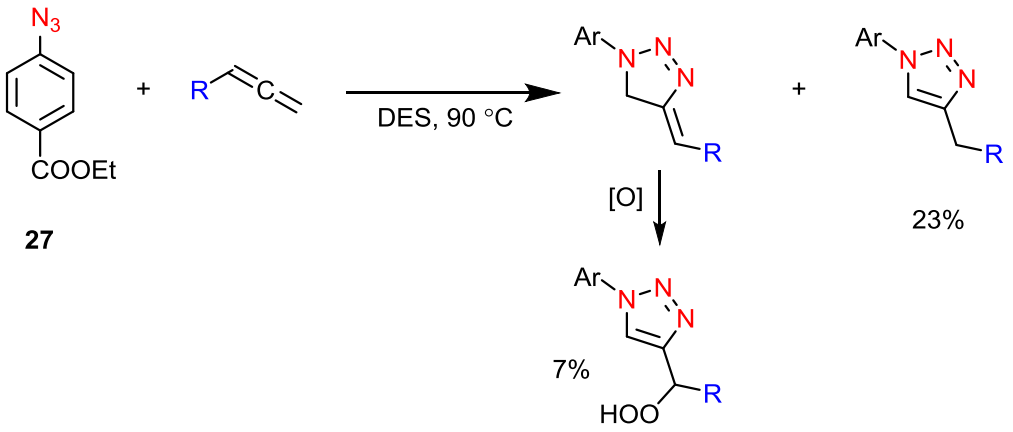

Scheme 10. Synthesis of 1,2,3-triazole derivatives from the cycloaddition of allene to aromatic azides in Deep Eutectic Solvent (DES)

Solvent-free and uncatalyzed cycloaddition of tetrasubstituted allene **28** and aromatic azide **29** affords highly substituted triazoles **30** and **31** in 25% and 3%, respectively. The reaction is non-regioselective and time consuming as it requires 14 day to obtain the products (Scheme 11).[48]

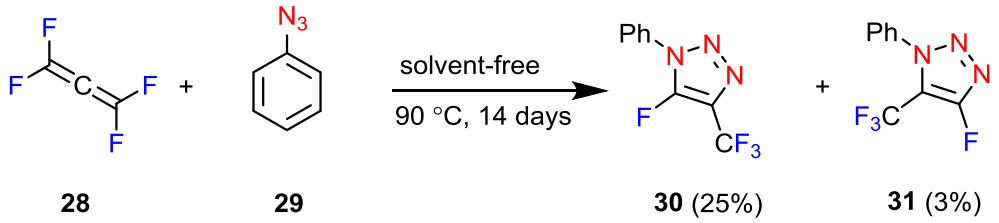

Scheme 11. Solvent-free synthesis of highly substituted 1,2,3-triazole derivatives **30** and **31**

1.3.1.3. Copper-catalyzed cycloaddition reaction (Click reaction)

The term "click chemistry" has been released in 2001 by Sharpless and coworkers[49] on the reactions that happened in nature between two substrates or more to form a joint. However, this term is not limited to bioconjugation, it can be utilized in pharmacological and chemical applications.[50,51] In chemistry, click reaction is the reaction which has relatively high yield with inoffensive byproducts and less sensitive to moisture and air. Moreover, it is a one-pot reaction.[52] In 2002, copper(I)-catalyzed

azide-alkyne cycloaddition (CuAAC) to prepare 1*H*-1,2,3-triazole was independently discovered by Sharpless[53] and Meldal[54] research groups. The reaction occurs by adding Cu(I) salts to the azide alkyne mixture or using Cu(II) slats which are mostly reduced by ascorbic acid salts *in situ* to form Cu(I). The first step in the suggested reaction mechanism (Scheme 12) demonstrates that the terminal alkyne couples with Cu(I) to form copper(I) acetylide **I**. Then, the electron-rich nitrogen donates lone pair of electrons to the copper to give complex **II** followed by the intramolecular attack of internal *sp*-carbon on terminal nitrogen of the azide moiety to form the six-membered ring intermediate **III**. Ring contraction of **III** affords intermediate **IV** that eventually releasees the copper complex to the cycle and gives the regioselective product 1,4-disubstituted-1*H*-1,2,3-triazole derivative **V**.

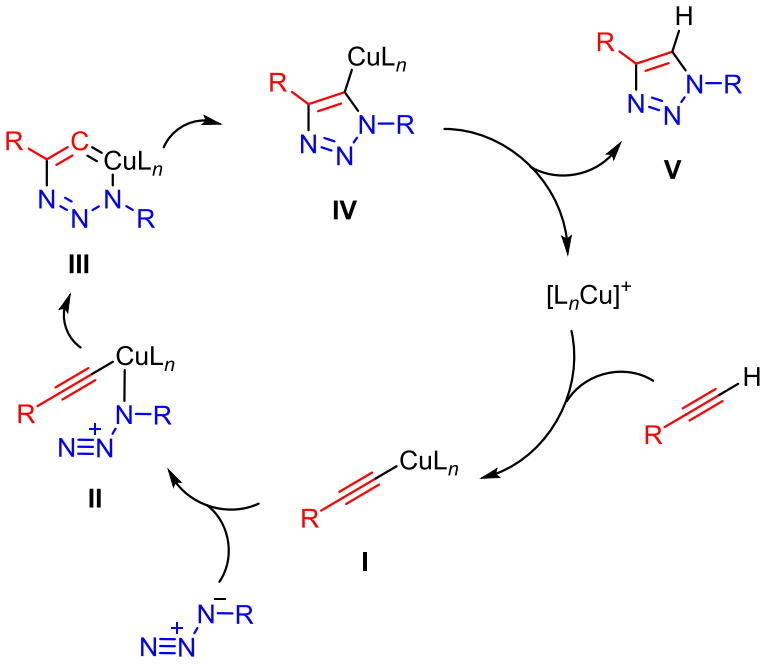

Scheme 12. Proposed mechanism copper(I)-catalyzed azide-alkyne cycloaddition (CuAAC) to prepare 1,4-disubstituted 1*H*-1,2,3-triazole derivatives.[53]

Various 1,4-disubstituted 1*H*-1,2,3-triazole derivatives have been synthesized by Sharpless and Meldal research groups in high yield at ambient temperature without minor products (Figure 6).

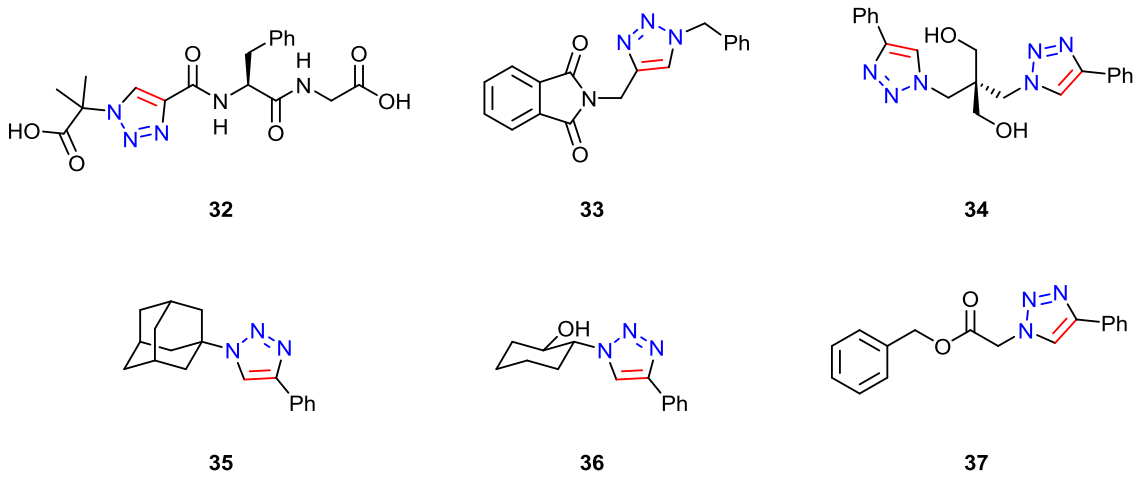

Figure 6. 1,4-Disubstituted 1*H*-1,2,3-triazole derivatives synthesized by Sharpless and Meldal research groups

1,5-disubstituted 1*H*-1,2,3-triazoles are also prepared metal-catalyzed cycloaddition. Nickel and ruthenium with suitable ligands in water or organic solvent were used for this purpose to afford regioselective 1,5-disubstitued product.[55,56] The proposed mechanism of nickel-catalyzed alkyne-azide cycloaddition NiAAC reaction is illustrated in Scheme 13:

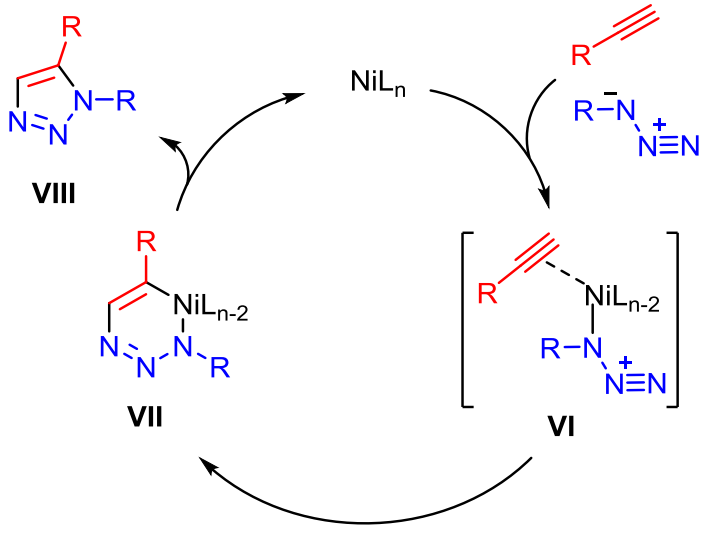

Scheme 13. The proposed mechanism of nickel-catalyzed alkyne-azide cycloaddition NiAAC reaction[55]

1.3.2. Applications of 1,2,3-triazole derivatives

Due to their unique structural properties and high stability towards various conditions, 1,2,3-triazoles have many applications starting from drug discovery to material science.[57] One of the significant features of 1,2,3-triazoles is their behavior as a hydrogen bond donor owning to the H-5 that is attached to an sp^2 carbon atom and as a hydrogen bond acceptor due to the existence of pyridine- and pyrrole-like nitrogen atom in their structure (Figure 7). This improves their ability in the biological and other fields of research.[58,59]

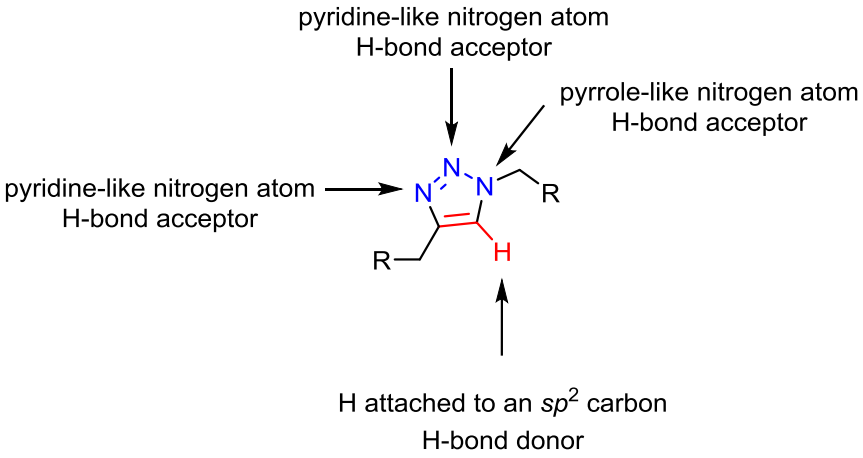

Figure 7. Hydrogen bond donor and acceptor events in 1,2,3-triazoles

1.3.2.1. Biological and medicinal applications

Triazole core is considered as amide bioisostere and it can replace the peptide bond in proteins and peptide (Figure 8). However, computational studies found that the hydrogen bonds formed by amide are stronger than those created by triazole analogues and this will alter the peptide or protein activity in biological application.[60]

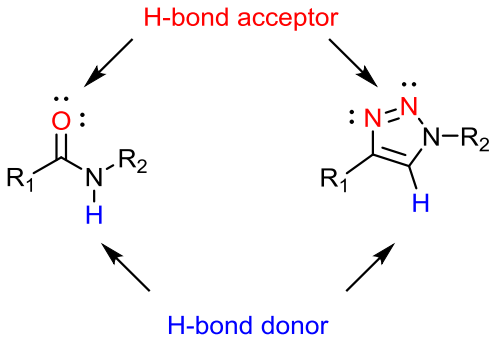

Figure 8. Structure similarity between amide and its triazole analogue

Consequently, triazole derivatives are extensively synthesized for drug discovery applications. A recent study found that substituting of amide in Lumacaftor (VX 809) **38** by 1,2,3-triazole analogue maintains hydrogen bonding. However, the calculations revealed that triazole analogue **39** formed weaker hydrogen bonds than its amide counterpart **38** and this may eliminate some of the intermolecular interaction which in turn affect the drug activity (Figure 9).[61]

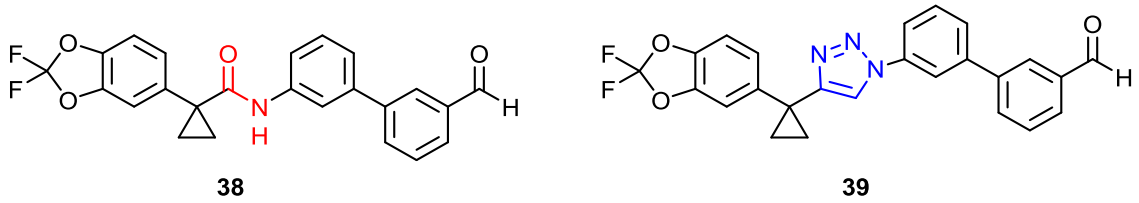

38 **39**

Figure 9. Structures of Lumacaftor (VX 809) **38** which is used for the treatment of cystic fibrosis, and its triazole analogue **39**

Mohammed *et al*.,[62–64] synthesized a collection of sugar-based 1,2,3-tiazoles **40**, bistriazole **41** and tetrakistriazole **42** derivatives. All compounds exhibited moderate to good antibacterial activity and this activity is attributed to the presence of triazole moiety (Figure 10).

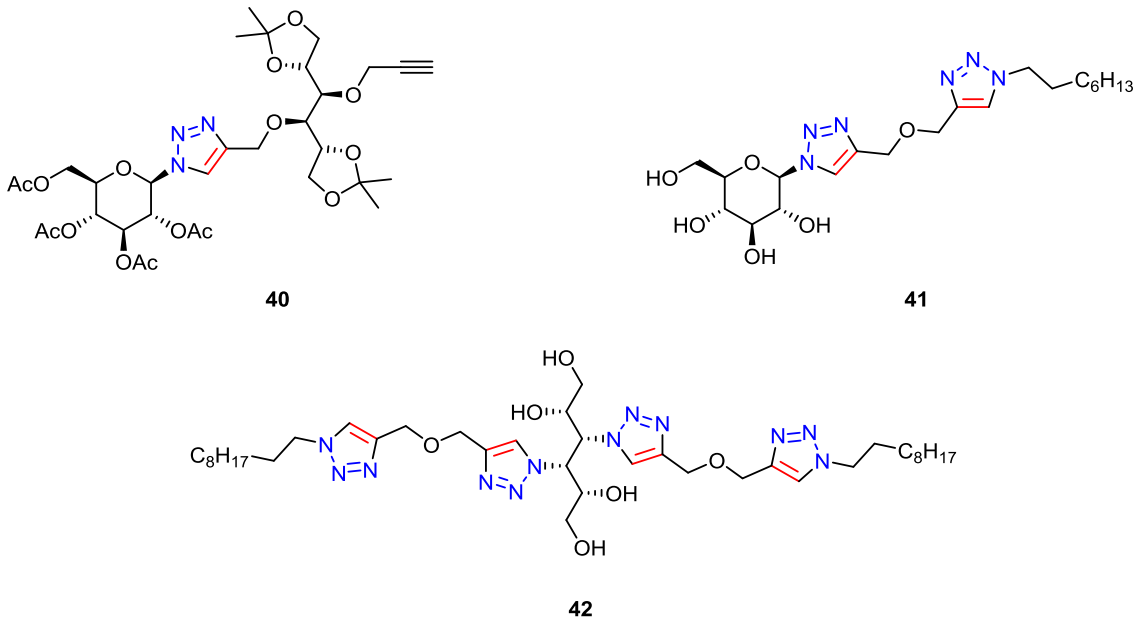

Figure 10. Sugar-based 1,2,3-tiazoles **40**, bistriazole **41** and tetrakistriazole **42** derivatives that have antibacterial activity

A novel set of uracil-containing bistriazole derivatives having silatrane moiety are tailored and screened *in vitro* against *E.coli*, *B. subtillus*, *V. cholera* and *S. aureus*. The antibacterial study showed these compounds are promising in the drug design (Figure 11).[65]

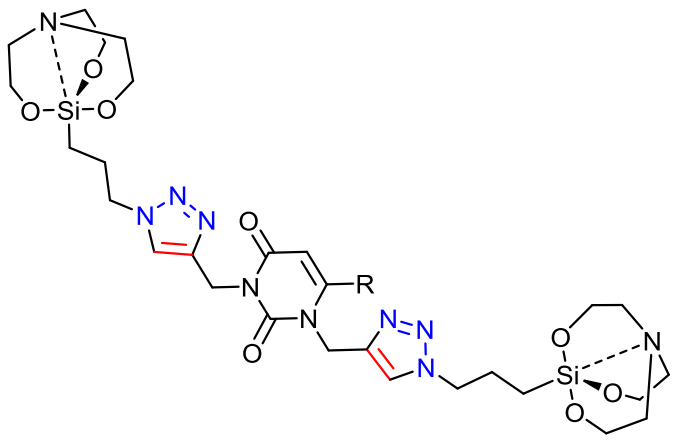

Figure 11. Uracil-containing bistriazole derivatives having silatrane moiety

Gondru *et al.*,[66] synthesized a new hybrid series of 1,2,3-triazole-thiazole derivatives and they examined their antibacterial and antifungal activity. It is found that

the designed compounds have promising *in vitro* toxicity against *B. subtilis*, *S. aureus* and *Candida* strains (Figure 12).

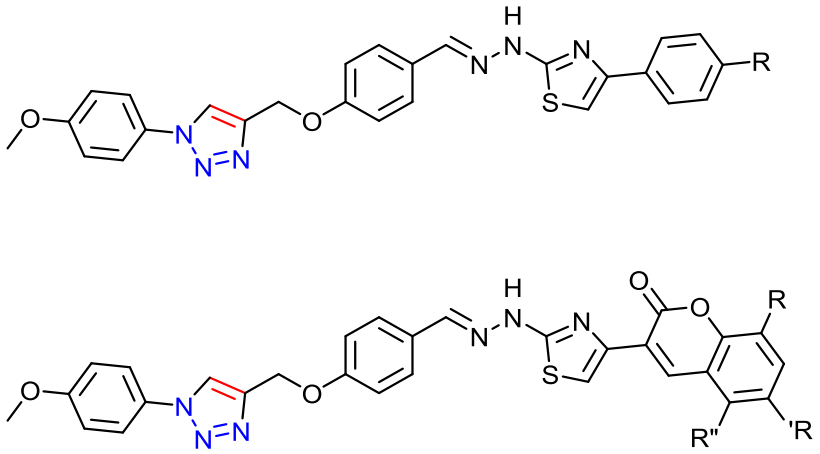

Figure 12. Hybrid 1,2,3-triazole-thiazole derivatives that have antibacterial and antifungal activity

Composites of quinoline–1,2,3-triazole **46** and **47** have been prepared through click reaction of propargyl quinoline ether **43** and alcohol or tosylated alcohol azides **44** and **45**, respectively (Scheme 14). Compound **47** was screened *in vitro* against bacterial and fungal pathogens; *K. pneumoniae*, *P. aeruginosa*, *C. albicans* and *C. neoformans*, and it exhibited more than 80% inhibition to the microbial growth.[67]

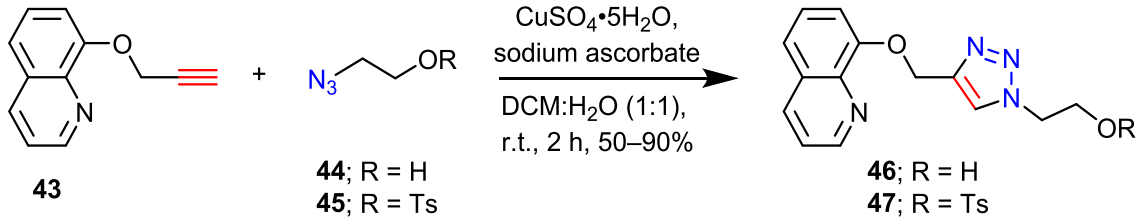

Scheme 14. Synthesis of quinoline–1,2,3-triazole hybrids **46** and **47** *via* click chemistry

Claisen-Schmidt condensation has been employed to couple 1,2,3-triazole-containing aldehydes and indolin-2-ones derivatives (Scheme 15). The resulting compounds were tested *in vivo* as vascular endothelial growth factor receptors VEGFR-2 inhibitors and the best kinase inhibition activity (IC_{50} = 26.38 nM) is recorded for compound **48**.[68]

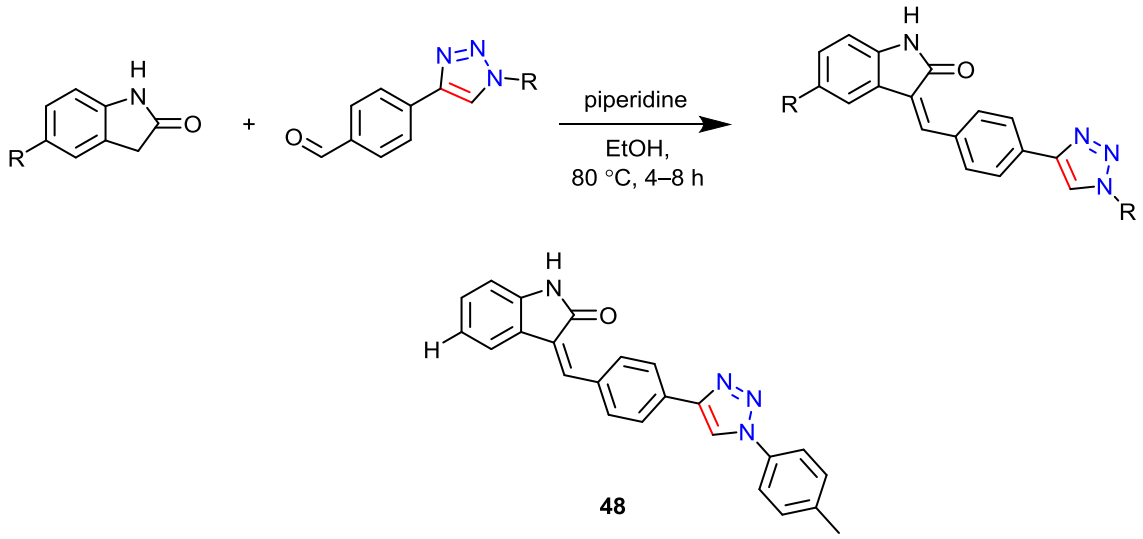

Scheme 15. Claisen-Schmidt condensation of indolin-2-ones derivatives with 1,2,3-triazole-containing aldehydes; structure of compound **48**

Vo *et al.*,[69] designed and synthesized new series of fluorinated 1,2,3-triazole analogues of the antidiabetic medication sitagliptin **49** using click conditions. The inhibitory activity of the synthesized derivatives was examined *in vitro* against the human dipeptidyl peptidase 4 (hDDP-4) and two of them **50**–**51** showed remarkable potency against the enzyme IC50 = 28 and 14 nM respectively (Figure 13).

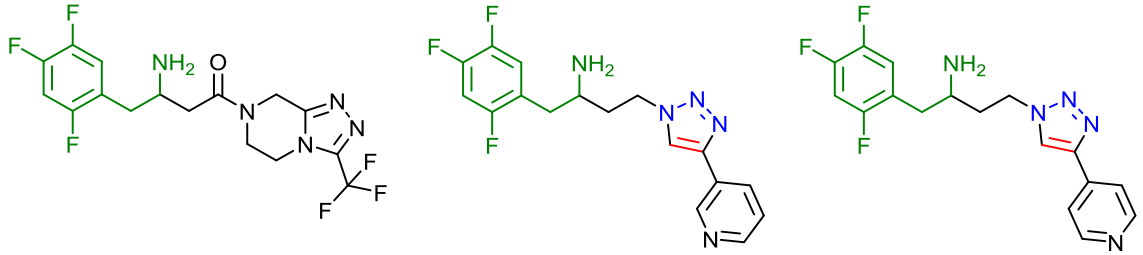

Figure 13. Comparison between the structure and the inhibitory activity against (hDDP-4) of sitagliptin **49** and its triazole analogues **50**–**51**

A novel set of piperidine-based bis-1,2,3-trizoles have been tailored using computational studies. The derivatives were then synthesized by double-click reaction of dipropargyl piperidine **52** with α-azido amides **53**–**55**. The antitubercular activity were evaluated and it is demonstrated that the bis-1,2,3-trizole derivatives possess promising antitubercular activity. However, three of the prepared compounds **56**–**58**

were assigned as the best agent as they required low minimum inhibitory concentration (MIC = 12.5 µg / L) compared to the other derivatives (Scheme 16).[70]

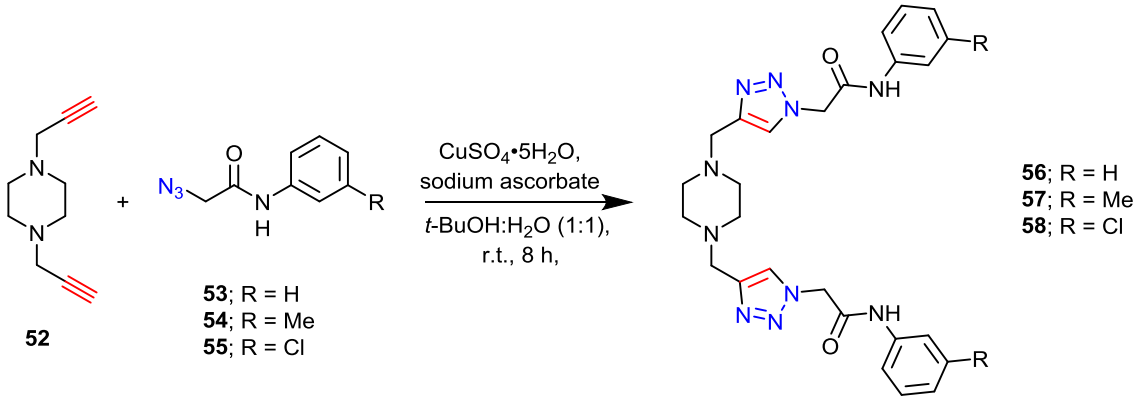

Scheme 16. Synthesis of piperidine-based bis-1,2,3-trizoles *via* click chemistry

Huang *et al.*,[71] synthesized quinoline–1,2,3-triazole hybrids through copper-catalyzed cycloaddition reaction. The structure activity relationship (SAR) and the antimalarial activity of the prepared derivatives have been profiled and it was revealed that compound **59** has the best antimalarial activity (EC_{50} = 40 nM) among the synthesized derivatives (Figure 14).

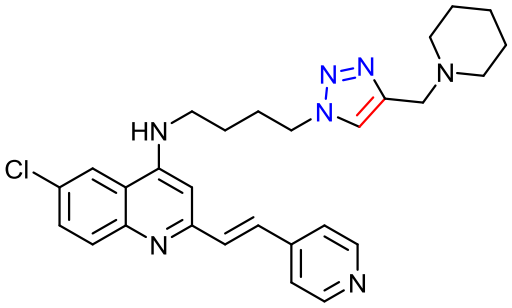

Figure 14. Structure and EC_{50} of compound **59**

Recently, Nerella and co-workers[72] reported the synthesis of carbohydrate-based 1,2,3-triazoles *via* silver (I)-*N*-heterocyclic carbene **60** (Ag(I)-NHC)-catalyzed

cycloaddition. Among the synthesized hybrids, sugar triazoles **61** and **62** demonstrated notable anticancer activity against prostate and breast cancer cell lines (Figure 15).

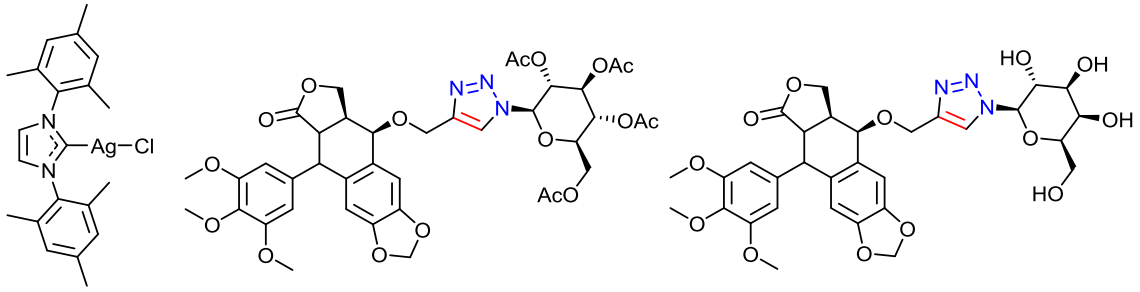

60 **61** IC_{50} = 1.02 ± 0.02 µM **62** IC_{50} = 1.25 ± 0.02 µM

Figure 15. Structure of silver (I)-*N*-heterocyclic carbene **60**; structures and IC_{50} of derivates **61** and **62**

One-pot synthesis and anticancer activity of arylacetamides based 1,4-disubstituted 1,2,3-triazoles have been reported. The anticancer activity against four human tumor cell lines; prostate cancer, lung cancer, liver cancer and breast epithelial exhibited significant antitumor activity of the compounds bearing phenyl **63** and naphthyl **64** group which possess IC_{50} = 4.0 and 3.5 µg / mL respectively (Figure 16).[73]

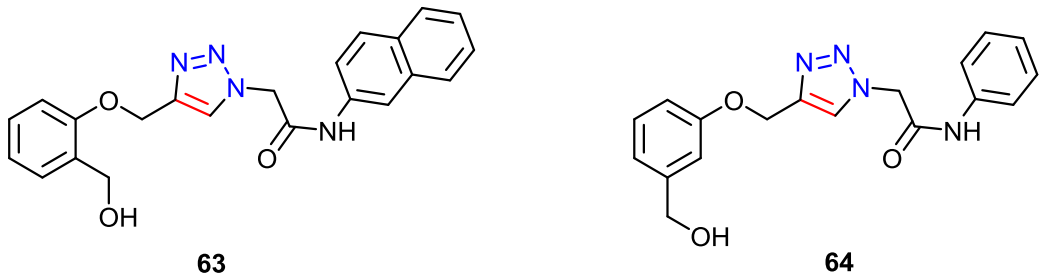

63 IC_{50} = 4.0 µg / mL **64** IC_{50} = 3.5 µg / L

Figure 16. Arylacetamides based 1,4-disubstituted 1,2,3-triazoles that have antitumor activity

Moderate anticancer activity of monosaccharide-containing 1,2,3-triazoles when screened against human liver, breast and lung cancer cells. The triazole derivatives **68**

and **69** were synthesized via Cu(I) catalyzed cycloaddition between *N*-propargyl imidazolopyrimidine **65** and glycosyl azides **66** and **67** (Scheme 17).[74]

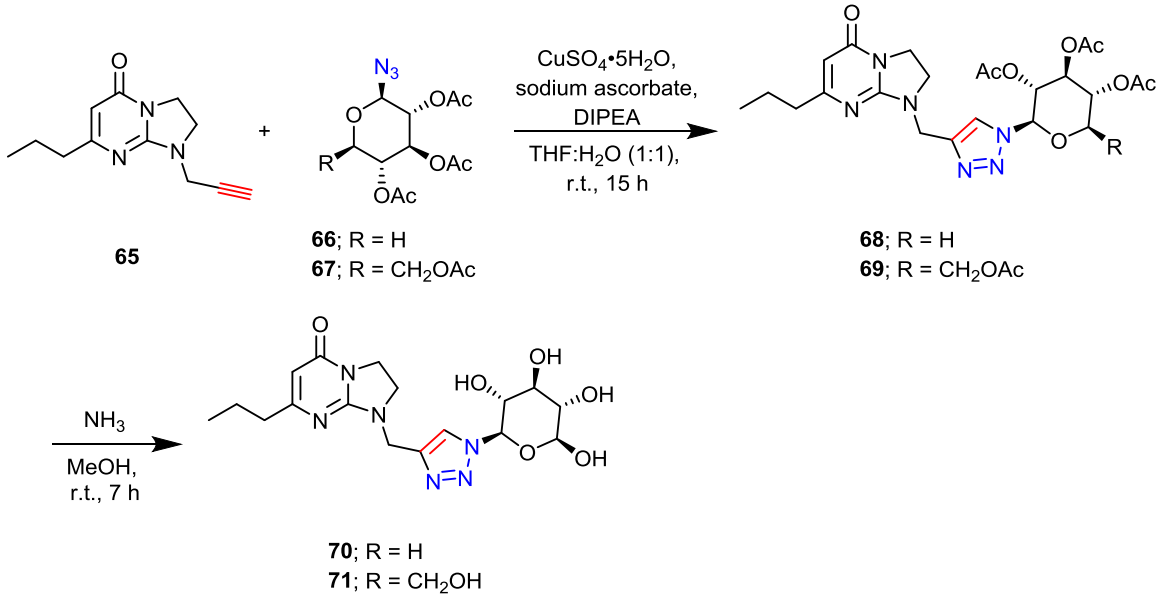

65

66; R = H
67; R = CH_2OAc

68; R = H
69; R = CH_2OAc

70; R = H
71; R = CH_2OH

Scheme 17. Monosaccharide-containing 1,2,3-triazoles **68** and **69**

Seghetti and co-workers[75] functionalized the naturally occurring curcumin **70** with 1,2,3-triazole moiety at position 4 using click chemistry approach. The effects of the synthesized derivative on the cancer apoptosis pathway have been studied and it is revealed that compound **71** is the most potent derivative because its IC_{50} against leukemia cell growth was 3.13 μM after 48 h compared with parent curcumin (IC_{50} = 10.51 μM) (Figure 17).

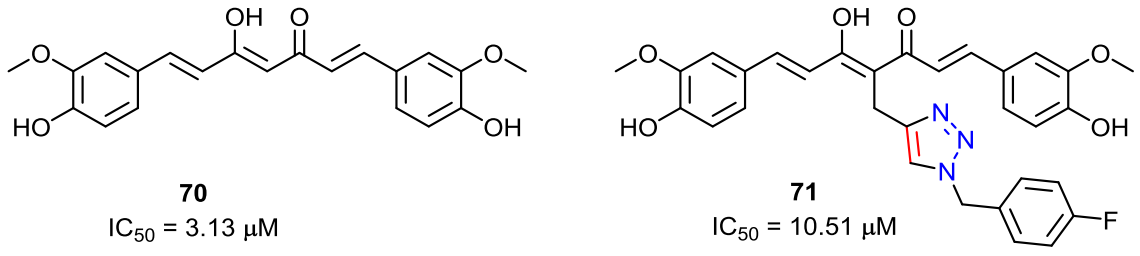

70
IC_{50} = 3.13 μM

71
IC_{50} = 10.51 μM

Figure 17. Curcumin **70**, its analogue **71** and their IC_{50}

A recent *in silico* study of a library of phthalimide-based 1,2,3-triazoles demonstrated that these derivatives **72**–**78** (Figure 18) can be active against viruses.

Moreover, they are promising drug for treatment of COVID-19 through the interruption of virus spike, protease or nucleocapsid proteins.[76]

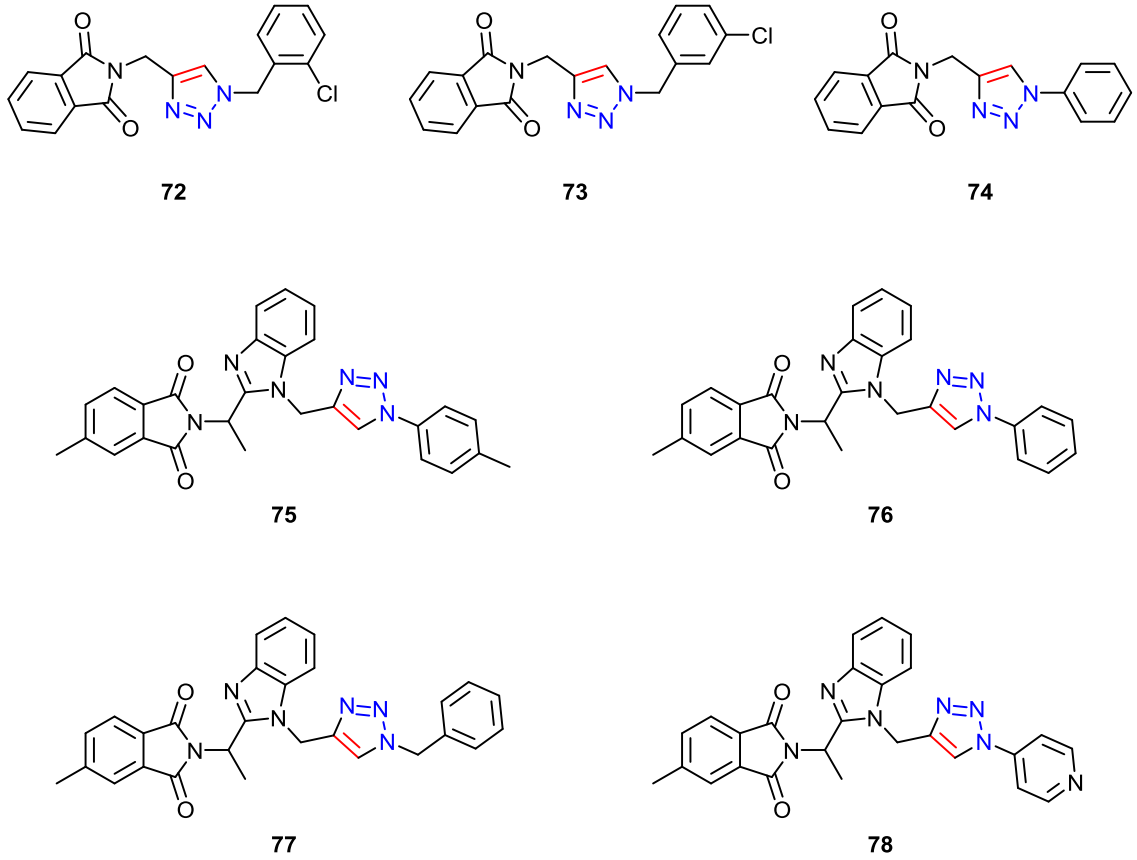

Figure 18. Structure of phthalimide-based 1,2,3-triazole derivatives **72**–**78**

1.3.2.2. Other applications

Apart from biological and pharmaceutical applications, 1,2,3-triazole derivatives are widely used in the material sciences due to their physicochemical properties. Several studies demonstrate the use of 1,2,3-triazole compounds as chemosensors for different species.[77–79]

Kamble *et al.*,[80] synthesized helicenoid bis-1,2,3-triazole **81** starting from dipropargyl derivative **79** and azide **80** by Cu(I)-catalyzed cycloaddition approach. Then compound **81** was converted to compound **82** by Williamson etherification. The target

compound has been utilized as a sensor for iodide and its sensing ability was followed by ^{1}H NMR titration with tetrabutylammonium iodide TBAI (Scheme 18).

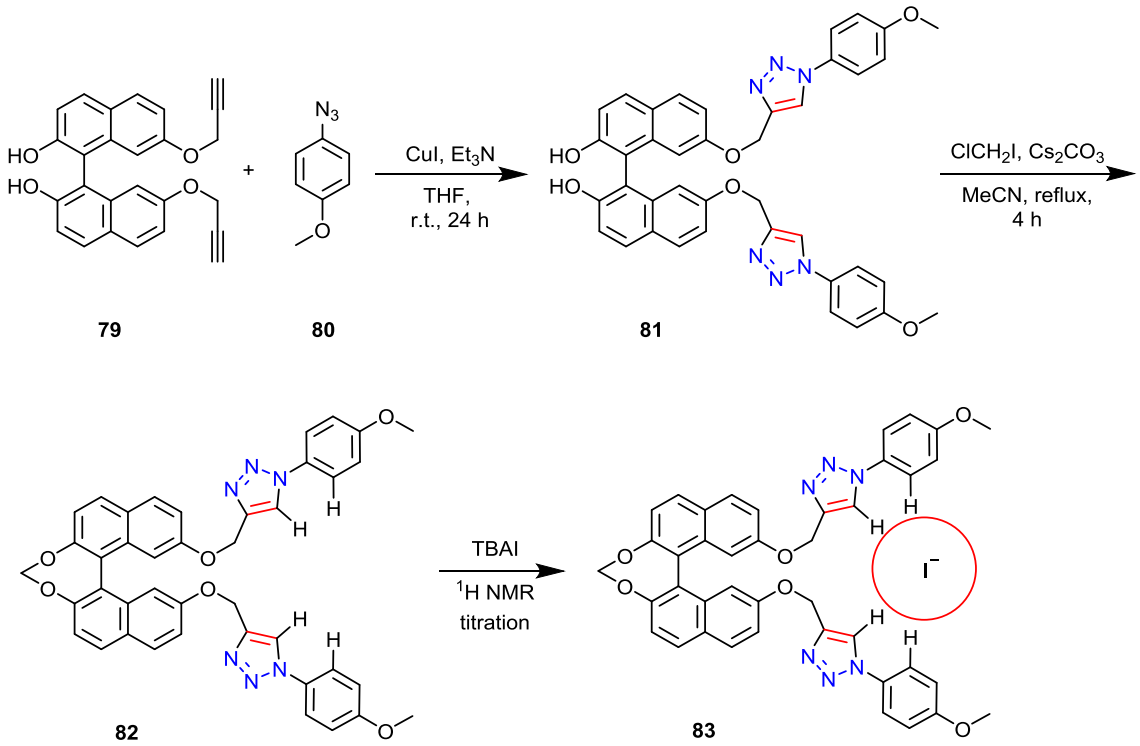

Scheme 18. Synthesis of helicenoid bis-1,2,3-triazole **82** and its complex with iodide **83**

Niskanen and co-workers,[81] prepared 1,2,3-triazole-based polyionic liquids bearing organic counterion **84**. The thermal stability and electrical properties of the synthesized polymer have been characterized. It was suggested that such polymer can be used in organic electronics (Figure 19).

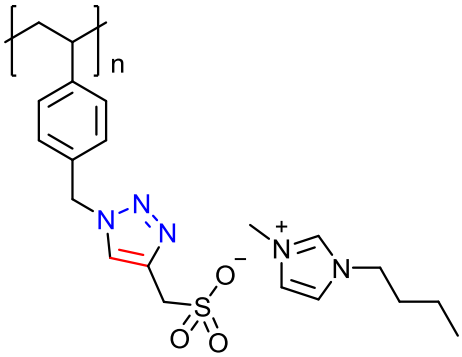

84

Figure 19. Structure of polymer **84**

In the field of catalysis, 1,2,3-triazole ligands were employed to aid the formation of other triazole derivative through cycloaddition in the presence of copper iodide. It was revealed that adding 0.5 mol% of the ligands **87** and **88** to the reaction of phenyl acetylene **85** with benzyl azide **86** produce the corresponding triazole **89** in quantitative yields (Scheme 19).

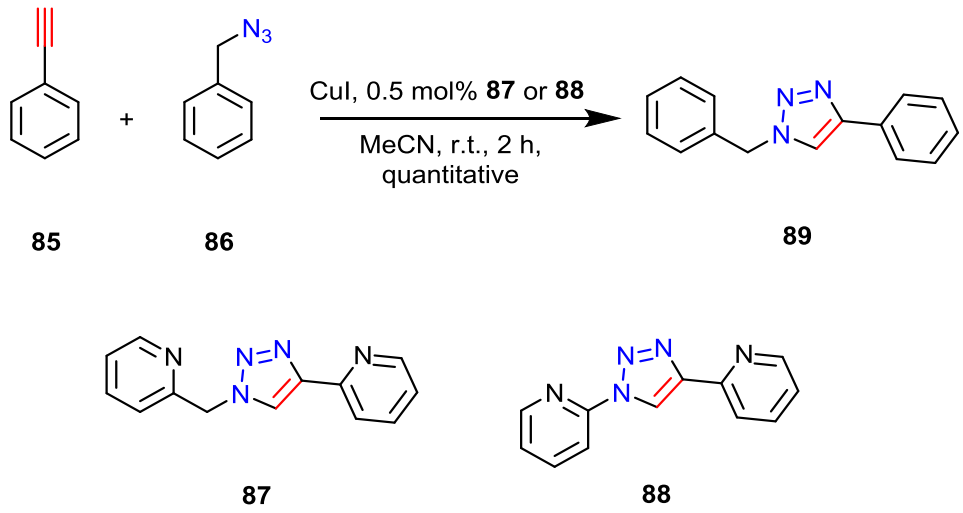

85 **86** **89**

87 **88**

Scheme 19. Copper-catalyzed cycloaddition of phenyl acetylene **85** and benzyl azide **86** in the presence of catalytic amounts of ligands **87** or **88**

Nahle *et al.*,[82] synthesized a couple of 1,2,3-triazole derivatives using click protocol and investigated their anticorrosion activity by different electrochemical

measurements. It was demonstrated that the corrosion of mild steel was inhibited by 95.3% and 95% when triazole compounds **90** and **91** were employed in 1.0 HCl (Figure 20).

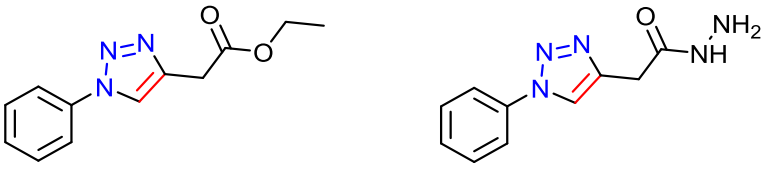

90 **91**

Figure 20. Structures of anticorrosion triazole **90** and **91**

Finally, as liquid crystals, 1,2,3-triazoles have been successfully utilized as a spacer to join two cholesteryl moieties (Figure 21). The prepared dimers were examined by polarising optical microscopy and differential scanning calorimetry to display enantiotropic mesophases, nematic or smectic phases.[83]

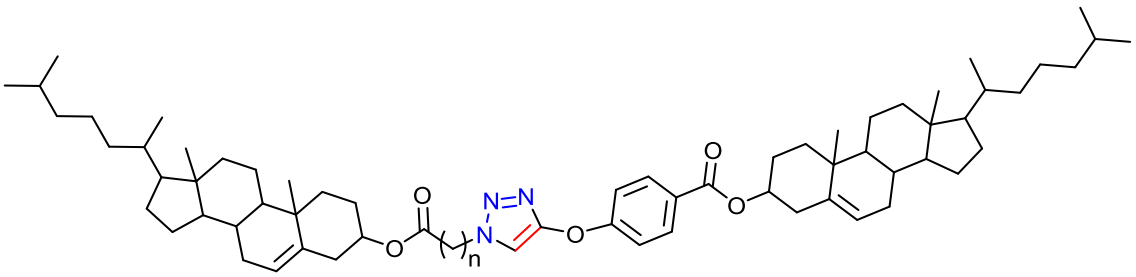

92; n = 5 **95**; n = 8
93; n = 6 **96**; n = 9
94; n = 7 **97**; n =10

Figure 21. Structure of compounds **92**–**97** that have liquid crystal properties

1.4.Aim of this work

The aim of the current work is:

1- Synthesis of new bis-1,2,3-triazole derivative starting from D-mannitol *via* copper-catalyzed cycloaddition reaction.

2- Characterization of the synthesized molecules by TLC in addition to spectroscopic techniques; FT-IR, ^{1}H NMR, ^{13}C NMR, ^{19}F NMR, COSY, HSQC and HRMS.

3- Examining the cytotoxicity of the synthesized compounds against mesenchymal stem cells MSCs.

Chapter Two

Experimental Part

2. Experimental Part

2.1. General methods

The reagents and solvents were purchased from different chemicals' suppliers and they were used as supplied. All reactions were carried out in oven-dried glassware unless stated otherwise. The progress of performed reactions was monitored by a Thin Layer of Chromatography using Merck aluminium-backed silica 60 F_{254} (0.2 mm) TLC plates and the spots were visualised by $KMnO_4$ staining solutions. Silica gel 40–63 mesh was utilized in the column chromatography as stationary phase and the stated eluting solvents were used as mobile phase. Melting points were measured using Stanford Research System Optimelt automated melting point apparatus. IR spectra were collected using Shimadzu FTIR spectrometer, University of Karbala, Iraq. 1D and 2D NMR spectra were recorded at 298 K (± 1 K) using Bruker Advance III, 500 or 600 MHz instruments, Nuclear Magnetic Resonance Facility, Mark Wainwright Analytical Centre, The University of New South Wales UNSW, Sydney, Australia. Residual solvents peaks were utilised to calibrate ^{1}H NMR and ^{13}C NMR spectra. Chemical shifts were reported in part per million (ppm). High resolution mass spectra HRMS were recorded at the Bioanalytical Mass Spectrometry Facility, Mark Wainwright Analytical Centre, The University of New South Wales UNSW, Sydney, Australia using Orbitrap LTQ XL ion trap MS in positive ion mode using electrospray ionisation (ESI) source.

2.2. Synthetic procedures and characterization

General procedure 1: Synthesis fluorobenzyl azides 99a–c (Modified procedure)[84]

Sodium azide (1.95 g, 30 mmol) was added to the stirred solution of the appropriate fluorobenzyl bromide **98 a–c** (10 mmol) in DMSO (25 mL) and the suspension was stirred at 50 °C for 24 h. The reaction mixture was diluted with water

(50 mL) and extracted with EtOAc (3 × 50 mL). The combined organic layers were washed with saturation solution of NaCl (2 × 50 mL), water (50 mL), dried over Na_2SO_4 and evaporated to dryness under reduced pressure to give a yellow liquid. Column chromatography of the residue (silica gel, n-hexane / EtOAc; 10:0 → 9:1,) afforded the appropriate fluorobenzyl azide.

1-(Azidomethyl)-2-fluorobenzene (99a)

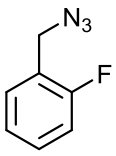

Colorless liquid (1.35 g, 89%). R_f = 0.75 (EtOAc). FTIR (KBr) cm^{-1}: 3053, 2937, 2881, 2100, 1616, 1587, 1492, 1454, 1348, 1236, 1180, 1103, 1031, 941, 883, 839, 756, 669, 588, 551, 520, 424. **^{1}H NMR** (600 MHz, $CDCl_3$) δ ppm: 7.36–7.32 (m, 2H, Ar−H), 7.17 (td, J = 7.6, 1.0 Hz, 1H, Ar−H), 7.11 (t, J = 9.1 Hz, 1H, Ar−H), 4.41 (s, 2H, Ar−C**H**$_2$). **^{13}C NMR** (150 MHz, $CDCl_3$) δ ppm: 161.0 (d, J = 247.4 Hz, Ar**C**), 130.5 (d, J = 4.1 Hz, Ar**C**), 130.4 (d, J = 8.6 Hz, Ar**C**), 124.5 (d, J = 3.4 Hz, Ar**C**), 122.8 (d, J = 15.3 Hz, Ar**C**), 115.8 (d, J = 21.7 Hz, Ar−**C**), 48.6 (d, J = 3.2 Hz, Ar−**C**H$_2$). **^{19}F NMR** (564 MHz, $CDCl_3$) δ ppm: −117.9 (m, 1F, Ar−**F**).

1-(Azidomethyl)-3-fluorobenzene (99b)

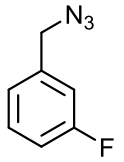

Colorless liquid (1.22 g, 81%). R_f = 0.75 (EtOAc). FTIR (KBr) cm^{-1}: 3064, 2933, 2879, 2102, 1616, 1593, 1487, 1450, 1344, 1259, 1139, 1103, 1078, 943, 891, 860, 785, 750, 690, 557, 524, 443. **^{1}H NMR** (600 MHz, $CDCl_3$) δ ppm: 7.36 (m, 1H, Ar−H), 7.11 (m, 1H, Ar−H), 7.06–703 (m, 2H, Ar−H), 4.34 (s, 2H, Ar−C**H**$_2$). **^{13}C NMR** (150 MHz, $CDCl_3$) δ ppm: 163.0 (d, J = 246.6 Hz, Ar**C**), 138.0 (d, J = 7.1 Hz, Ar**C**), 130.5 (d, J = 8.6 Hz, Ar**C**), 123.7 (d, J = 3.0 Hz, Ar**C**), 115.3 (d, J = 21.1 Hz, Ar**C**), 115.1 (d, J = 22.0 Hz, Ar−**C**), 54.2 (Ar−**C**H$_2$). **^{19}F NMR** (564 MHz, $CDCl_3$) δ ppm: −112.3 (m, 1F, Ar−**F**).

1-(Azidomethyl)-4-fluorobenzene (99c)

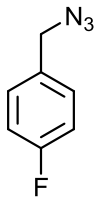

Colorless liquid (1.35 g, 1.40%). R_f = 0.75 (EtOAc). FTIR (KBr) cm^{-1}: 3045, 2933, 2879, 2100, 1602, 1510, 1450, 1344, 1226, 1157, 1097, 1016, 941, 881, 852, 823, 767, 665, 540, 480, 420. **^{1}H NMR** (600 MHz, $CDCl_3$) δ ppm: 7.32–7.28 (m, 2H, Ar−H), 7.01–7.05 (m, 2H, Ar−H), 4.31 (s, 2H, Ar−C**H**$_2$). **^{13}C NMR** (150 MHz, $CDCl_3$) δ ppm: 162.7 (d, J = 248.1 Hz, Ar**C**), 131.3 (d, J = 3.2 Hz, Ar**C**), 130.1 (d, J = 8.1 Hz, Ar**C**), 115.8 (d, J = 21.9 Hz, Ar−**C**), 54.1 (Ar−**C**H_2). **^{19}F NMR** (564 MHz, $CDCl_3$) δ ppm: −113.6 (m, 1F, Ar−**F**).

Synthesis of 1,2:5,6-di-*O*-isopropylidene-D-mannitol (101)[85]

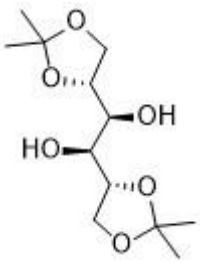

Anhydrous zinc chloride (60 g, 0.44 mol) was suspended in acetone (300 mL) in closed flask at room temperature then D-mannitol (**100**) (10 g, 0.055 mol) was added, and the resulting white suspension stirred vigorously for 24 h at 25 ˚C. The reaction mixture was poured onto a solution of K_2CO_3 (70 g, 0.506 mol) in (70 mL) of H_2O and covered with (300 mL) of Et_2O. The mixture is stirred for 2h, then filtered and the organic layer was washed with (100 mL) of ($(CH_3)_2CO$ / Et_2O, 1:1) and the combined filtrates evaporated to dryness on a rotary evaporator at 40˚C. The dry residue was yellow oil extracted with ether (5 × 250 mL), the combined filters evaporated and slowly cooled to give crystals. The product was purified by re-crystallization with *n*-hexane to yield compound **101** as tiny white crystals (7.8 g, 54%). R_f = 0.3 (EtOAc), m.p. 120–121 ˚C. FTIR (KBr) cm^{-1}: 3464, 3317, 2989, 2935, 2881, 1485. 1458, 1417, 1379, 1255, 1211, 1155, 1072, 1041, 997, 852, 781, 698, 646, 592, 516. ^{1}H NMR (600 MHz, MeOH-d_4) δ ppm: 4.14 (ddd, J = 8.3, 6.0, 6.0 Hz, 2H, 2 × (−C**H**O−CH_2O)), 4.08 (dd, J = 8.3, 6.3 Hz, 2H, 2 × (−CHO−C**H**$_2$O)), 3.97 (dd, J = 8.4, 5.3 Hz, 2H, 2 × (−CHO−C**H**$_2$O)), 3.64 (d, J = 8.2

Hz, 2H, 2 × (−C**H**OH)), 1.37 (s, 6H, 2 × (−C(C**H**$_3$)$_2$)), 1.33 (s, 6H, 2 × (−C(C**H**$_3$)$_2$)). **^{13}C {^{1}H} NMR** (150 MHz, MeOH-d_4) δ ppm: 110.2 (2 × (−**C**(CH$_3$)$_2$)), 76.5 (2 × (−**C**HO−CH$_2$O)), 72.2 (2 × (−CHO−**C**H$_2$O)), 68.2 (2 × (−**C**HOH)), 27.2 (2 × (−C(**C**H$_3$)$_2$)), 25.7 (2 × (−C(**C**H$_3$)$_2$)). HRMS-ESI [M + Na]$^+$ calculated for $C_{12}H_{22}O_6Na^+$: 285.1308; found: 285.1306.

Synthesis of 3,4-Bis-*O*-propargyl-1,2:5,6-di-*O*-isopropylidene-D-mannitol (102)[86]

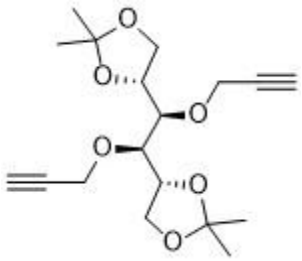

1,2:5,6-Di-O-isopropylidene-D-mannitol (**101**) (0.787 g, 3 mmol) was dissolved in DMF (30 mL) in a dry flask and crushed NaOH (0.48 g, 12 mmol) was added. The flask was cooled in an ice–salt bath at –20 °C and the contents stirred for 10 min before propargyl bromide (0.76 mL, 8.54 mmol) was added dropwise over one minute. The mixture was then allowed to stir for a further 24 h, while gradually warming to r.t. Then, the mixture was quenched with H_2O (30 mL) and extracted with Et_2O (3 × 30 mL). The combined organic layers were washed with aqueous saturated NH_4Cl (3 × 20 mL) and H_2O (30 mL), dried over Na_2SO_4 and filtered. The solvent was evaporated under reduced pressure to yield a pale-yellow oil. Column chromatography (silica gel, *n*-hexane / EtOAc; 9:1–3:1) afforded 3,4-bis-*O*-propargyl-1,2:5,6-di-*O*-isopropylidene-D-mannitol (**102**) as white prismatic crystals (0.85 g, 84%); m.p. 51–52 °C; R_f = 0.56 (EtOAc). FTIR (KBr) cm^{-1}: 3252, 2985, 2931, 2904, 2115, 1456, 1379, 1348, 1265, 1213, 1163, 1109, 1060, 1018, 964, 918, 862, 817, 675, 515. **^{1}H NMR** (500 MHz, $CDCl_3$) δ ppm: 4.60 (dd, J = 16.0, 2.2 Hz, 2H, 2 × (−C**H**$_2$C≡CH)), 4.35 (dd, J = 16.0, 2.3 Hz, 2H, 2 × (−C**H**$_2$C≡CH)), 4.21 (dd, J = 11.0, 6.2 Hz, 2H, 2 × (−C**H**O−CH$_2$O)), 4.11 (dd, J = 8.5, 6.3 Hz, 2H, 2 × (−CHO−C**H**$_2$O)), 4.03 (dd, J = 8.0, 6.9 Hz, 2H, 2 × (−CHO−C**H**$_2$O)), 3.84 (d, J = 4.3 Hz, 2H, 2 × (−C**H**O−CH$_2$C≡CH)), 2.45 (t, J = 2.0 Hz, 2H, 2 × (−CH$_2$C≡C**H**)), 1.39 (s, 6H, 2 × (−C(C**H**$_3$)$_2$)), 1.32 (s, 6H, 2

× (−C(C**H**$_3$)$_2$)). **^{13}C NMR** (125 MHz, $CDCl_3$) δ ppm: 108.5 (2 × (−**C**$(CH_3)_2$)), 79.9 (2 × (−CH_2**C**≡CH)), 78.6 (2 × (−CH_2C≡**C**H)), 76.5 (2 × (−**C**HO−CH_2O)), 74.9 (2 × (−CHO−**C**H_2O)), 66.2 (2 × (−**C**HO−CH_2C≡CH)), 59.7 (2 × (−**C**H_2C≡CH)), 26.6 (2 × (−C(**C**$H_3)_2$)), 25.3 (2 × (−C(**C**$H_3)_2$)). HRMS-ESI $[M + Na]^+$ calculated for $C_{18}H_{26}O_6Na$: 361.1621; found: 361.1621.

General procedure 2: Synthesis of bis-1,2,3-triazoles 103 a–c (Modified procedure)[87]

A suspension of sodium ascorbate (0.0396 g, 0.2 mmol) and $CuSO_4{\cdot}5H_2O$ (0.025 g, 0.01 mmol) in DMSO (2 mL) was added to a solution of propargyl ether **102** (0.34 g, 1.0 mmol) in DMSO (2 mL) and the mixture was stirred for 10 min. Next, appropriate fluorobenzyl azide **99 a**–**c** (0.35 g, 2.5 mmol) was added, and the mixture heated at 50 °C with stirring for 36 h. The mixture was diluted with H_2O (30 mL), extracted with EtOAc (3 × 30 mL), the combined organic layers washed with saturated NaCl (2 × 20 mL), dried over Na_2SO_4 and evaporated under reduced pressure. The residue was flash chromatographed (silica gel, *n*-hexane / EtOAc; 2:1 → 1:2,) to yield the corresponding bis-1,2,3-triazole.

3,4-Bis-*O*-((2-fluorobenzyl-1*H*-1,2,3-triazole-4-yl)methyl)1,2:5,6-di-*O*-isopropylidene-D-mannitol (103a)

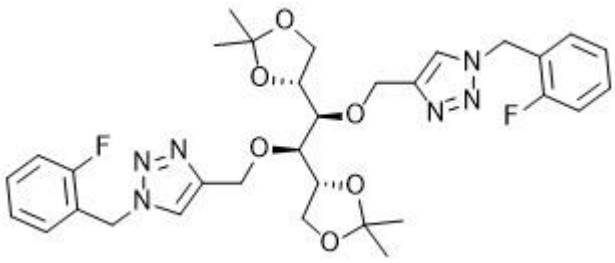

White solid (0.49 g, 77%); m.p. 98–101 °C; R_f = 0.53 (EtOAc). FTIR (KBr) cm^{-1}: 3138, 2987, 2935, 2877, 1620, 1589, 1544, 1494, 1458, 1375, 1232, 1072, 1041, 1024, 889, 846, 761, 655, 513. **^{1}H NMR** (600 MHz, $CDCl_3$) δ ppm: 7.54 (s, 2H, 2 × H triazole)), 7.34 (dddd, *J* = 13.6, 7.3, 5.4, 1.7 Hz, 2H, 2 ×

(Ar−H)), 7.25 (td, *J* = 7.5, 1.7 Hz, 2H, 2 × (Ar−H)), 7.13 (td, *J* = 7.6, 1.1 Hz, 2H, 2 × (Ar−H)), 7.10 (dd, *J* = 8.4, 0.9 Hz, 2H, 2 × (Ar−H)), 5.55 (s, 4H, 2 × (Ar−C**H**$_2$−triazole)), 4.79 (d, *J* = 12.2 Hz, 2H, 2 × (−CHO−C**H**$_2$−triazole)), 4.785 (d, *J* = 12.2 Hz, 2H, 2 × (−CHO−C**H**$_2$−triazole)), 4.17 (dd, *J* = 12.4, 6.2 Hz, 2H, 2 × (−C**H**O−CH$_2$O)), 3.96 (dd, *J* = 8.5, 6.4 Hz, 2H, 2 × (−CHO−C**H**$_2$O)), 3.86 (dd, *J* = 8.5, 6.2 Hz, 2H, 2 × (−CHO−C**H**$_2$O)), 3.77−3.75 (m, 2H, 2 × (−C**H**O−triazole)), 1.36 (s, 6H, 2 × (−C(C**H**$_3$)$_2$)), 1.29 (s, 6H, 2 × (−C(C**H**$_3$)$_2$)). **^{13}C NMR** (150 MHz, $CDCl_3$) *δ* ppm: 160.7 (d, *J* = 248 Hz, 2 × (Ar**C**)), 145.6 (2 × (−**C** triazole)), 131.0 (d, *J* = 8.2 Hz, 2 × (Ar**C**)), 130.1 (d, *J* = 3.2 Hz, 2 × (Ar**C**)), 125.0 (d, *J* = 3.7 Hz, 2 × (Ar**C**)), 122.9 (d, *J* = 1.3 Hz, 2 × (−**C** triazole)), 122.0 (d, *J* = 14.5 Hz, 2 × (Ar**C**)), 116.0 (d, *J* = 21.1 Hz, 2 × (Ar−**C**)), 108.8 (2 × (−**C**(CH$_3$)$_2$)), 80.3 (2 × (−**C**HO−CH$_2$−triazole)), 75.7 (2 × (−**C**HO−CH$_2$O)), 66.7 (2 × (−CHO−**C**H$_2$O)), 66.2 (2 × (−CHO−**C**H$_2$−triazole)), 47.7 (d, *J* = 4.4 Hz, 2 × (Ar−**C**H$_2$−triazole)), 26.7 (2 × (−C(**C**H$_3$)$_2$)), 25.3 (2 × (−C(**C**H$_3$)$_2$)). **^{19}F NMR** (564 MHz, $CDCl_3$) *δ* ppm: −118.2 (m, 2F, Ar−**F**). HRMS-ESI $[M + Na]^+$ calculated for $C_{32}H_{38}F_2N_6O_6Na^+$: 663.2713; found: 663.2708.

3,4-Bis-*O*-((3-fluorobenzyl-1*H*-1,2,3-triazole-4-yl)methyl)1,2:5,6-di-*O*-isopropylidene-D-mannitol (103b)

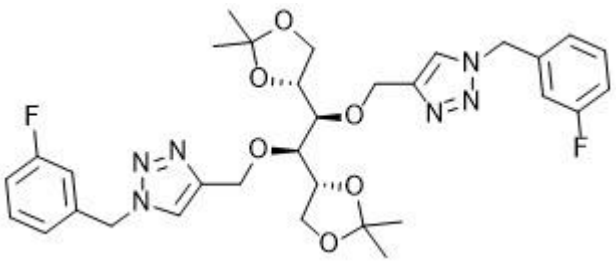

White solid (0.52 g, 81%); m.p. 116–118 °C; R_f = 0.57 (EtOAc). FTIR (KBr) cm^{-1}: 3136, 3072, 2987, 2937, 2877, 1647, 1593, 1544, 1492, 1485, 1454, 1373, 1249, 1114, 1024, 887, 783, 750, 682, 513. **^{1}H NMR** (600 MHz, $CDCl_3$) *δ* ppm: 7.50 (s, 2H, 2 × H triazole)), 7.33 (ddd, *J* = 13.8, 7.8, 5.9 Hz, 2H, 2 × (Ar−H)), 7.03 (td, *J* = 7.5, 7.5, 1.7 Hz, 4H, 2 × (2Ar−H)), 6.94 (dt, *J* = 9.2, 1.8 Hz, 2H, 2 × (Ar−H)), 5.48 (s, 4H, 2 × (Ar−C**H**$_2$−triazole)), 4.80 (d, *J* = 12.1 Hz, 2H, 2 ×

(−CHO−C**H**$_2$−triazole)), 4.797 (d, *J* = 12.1 Hz, 2H, 2 × (−CHO−C**H**$_2$−triazole)), 4.18 (dd, *J* = 12.0, 6.0 Hz, 2H, 2 × (−C**H**O−CH$_2$O)), 3.96 (dd, *J* = 8.4, 6.4 Hz, 2H, 2 × (−CHO−C**H**$_2$O)), 3.87 (dd, *J* = 8.4, 6.3 Hz, 2H, 2 × (−CHO−C**H**$_2$O)), 3.75 (broad d, *J* = 5.5 Hz 2H, 2 × (−C**H**O−triazole)), 1.36 (s, 6H, 2 × (−C(C**H**$_3$)$_2$)), 1.29 (s, 6H, 2 × (−C(C**H**$_3$)$_2$)). **^{13}C NMR** (150 MHz, CDCl$_3$) *δ* ppm: 163.1 (d, *J* = 247.6 Hz, 2 × (Ar**C**)), 145.8 (2 × (−**C** triazole)), 137.2 (d, *J* = 7.1 Hz, 2 × (Ar**C**)), 130.9 (d, *J* = 8.4 Hz, 2 × (Ar**C**)), 123.7 (d, *J* = 3.1 Hz, 2 × (Ar**C**)), 122.8 (2 × (−**C** triazole)), 115.9 (d, *J* = 21.0 Hz, 2 × (Ar**C**)), 115.1 (d, *J* = 22.7 Hz, 2 × (Ar−**C**)), 108.9 (2 × (−**C**(CH$_3$)$_2$)), 80.3 (2 × (−**C**HO−CH$_2$−triazole)), 75.7 (2 × (−**C**HO−CH$_2$O)), 66.6 (2 × (−CHO−**C**H$_2$O)), 66.2 (2 × (−CHO−**C**H$_2$−triazole)), 53.6 (2 × (Ar−**C**H$_2$−triazole)), 26.7 (2 × (−C(**C**H$_3$)$_2$)), 25.3 (2 × (−C(**C**H$_3$)$_2$)). **^{19}F NMR** (564 MHz, CDCl$_3$) *δ* ppm: −111.6 (ddd, *J* = 14.6, 8.6, 5.7 Hz, 2F, Ar−**F**). HRMS-ESI [M + Na]$^+$ calculated for $C_{32}H_{38}F_2N_6O_6Na$: 663.2713; found: 663.2715.

3,4-Bis-*O*-((4-fluorobenzyl-1*H*-1,2,3-triazole-4-yl)methyl)1,2:5,6-di-*O*-isopropylidene-D-mannitol (103c)

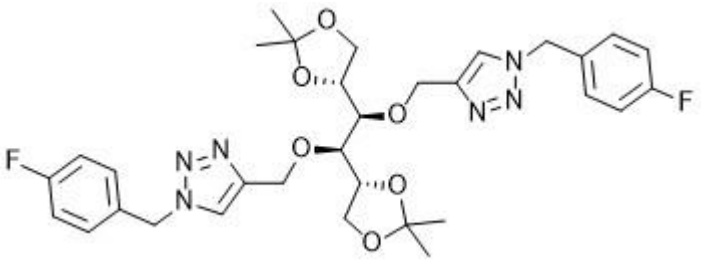

White solid (0.5 g, 78%); m.p. 105–107 °C; R_f = 0.51 (EtOAc). FTIR (KBr) cm^{-1}: 3136, 3074, 2985, 2877, 1606, 1512, 1460, 1375, 1224, 1072, 1024, 844, 748, 599, 499. **^{1}H NMR** (600 MHz, CDCl$_3$) *δ* ppm: 7.45 (s, 2H, 2 × H triazole)), 7.25 (dd, *J* = 8.6, 3.5 Hz, 4H, 2 × (2Ar−H)), 7.05 (t, *J* = 8.6 Hz, 4H, 2 × (2Ar−H)), 5.46 (s, 4H, 2 × (Ar−C**H**$_2$−triazole)), 4.783 (d, *J* = 12.1 Hz, 2H, 2 × (−CHO−C**H**$_2$−triazole)), 4.78 (d, *J* = 12.1 Hz, 2H, 2 × (−CHO−C**H**$_2$−triazole)), 4.17 (dd, *J* = 12.3, 6.1 Hz, 2H, 2 × (−C**H**O−CH$_2$O)), 3.94 (dd, *J* = 8.5, 6.4 Hz, 2H, 2 × (−CHO−C**H**$_2$O)), 3.85 (dd, *J* = 8.4, 6.3 Hz, 2H, 2 ×

(−CHO−C**H**$_2$O)), 3.75 (broad d, *J* = 5.9 Hz 2H, 2 × (−C**H**O−triazole)), 1.36 (s, 6H, 2 × (−C(C**H**$_3$)$_2$)), 1.29 (s, 6H, 2 × (−C(C**H**$_3$)$_2$)). **^{13}C NMR** (150 MHz, $CDCl_3$) δ ppm: 163.0 (d, *J* = 248.4 Hz, 2 × (Ar**C**)), 145.7 (2 × (−**C** triazole)), 130.6 (d, *J* = 3.2 Hz, 2 × (Ar**C**)), 130.9 (d, *J* = 8.4 Hz, 2 × (Ar**C**)), 130.1 (d, *J* = 8.2 Hz, 2 × (Ar**C**)), 122.6 (2 × (−**C** triazole)), 116.3 (d, *J* = 21.6 Hz, 2 × (Ar**C**)), 108.8 (2 × (−**C**(CH$_3$)$_2$)), 80.3 (2 × (−**C**HO−CH$_2$−triazole)), 75.8 (2 × (−**C**HO−CH$_2$O)), 66.6 (2 × (−CHO−**C**H$_2$O)), 66.2 (2 × (−CHO−**C**H$_2$−triazole)), 53.5 (2 × (Ar−**C**H$_2$−triazole)), 26.7 (2 × (−C(**C**H$_3$)$_2$)), 25.3 (2 × (−C(**C**H$_3$)$_2$)). **^{19}F NMR** (564 MHz, $CDCl_3$) δ ppm: −112.7 (tt, *J* = 8.5, 5.2 Hz, 2F, Ar−**F**). HRMS-ESI $[M + Na]^+$ calculated for $C_{32}H_{38}F_2N_6O_6Na$: 663.2713; found: 663.2712.

General procedure 3: Acetal removal of bis-1,2,3-triazoles[88]

To the solution of protected triazole (0.186 g, 0.29 mmol) in MeOH / H_2O (1:1, 5 mL), Amberlite IR 120 H^+ (0.29 g, 1.0 g.mol^{-1}) was added and the mixture was stirred at 60 °C for 72 h. The resin was filtered and washed with MeOH (3 × 5 mL). The filtrate was evaporated to yield the deprotected triazole as a white gum.

3,4-Bis-*O*-((2-fluorobenzyl-1*H*-1,2,3-triazole-4-yl)methyl)-D-mannitol (104a)

White gum (0.162 g, 77%); R_f = 0.15 (DCM / MeOH, 9:1). FTIR (KBr) cm^{-1}: 3360, 2924, 2856, 1653, 1592, 1562, 1498, 1386, 1226, 1128, 1041, 767, 650, 609, 522, 492. HRMS-ESI $[M + H]^+$ calculated for $C_{26}H_{31}F_2N_6O_6^+$: 561.2267; found: 561.2269.

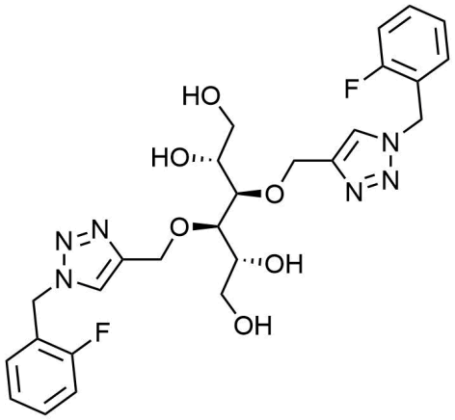

3,4-Bis-*O*-((3-fluorobenzyl-1*H*-1,2,3-triazole-4-yl)methyl)-D-mannitol (104b)

White gum (0.161 g, 77%); R_f = 0.17 (DCM / MeOH, 9:1). FTIR (KBr) cm^{-1}: 3396, 2926, 2856, 1579, 1421, 1340, 1203, 1132, 1047, 1012, 925, 833, 786, 650, 617, 509, 468. HRMS-ESI $[M + Na]^+$ calculated for $C_{26}H30F_2N_6O_6Na^+$: 583.2087; found: 583.2086.

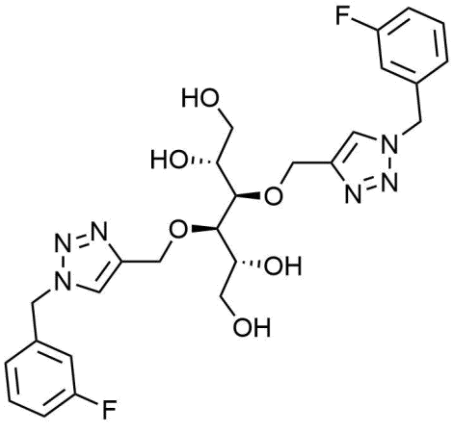

3,4-Bis-*O*-((4-fluorobenzyl-1*H*-1,2,3-triazole-4-yl)methyl)-D-mannitol (104c)

White gum (0.160 g, 77%); R_f = 0.16 (DCM / MeOH, 9:1). FTIR (KBr) cm^{-1}: 3433, 2924, 2856, 1653, 1610, 1514, 1460, 1371, 1226, 1168, 1122, 1039, 1003, 837, 781, 707, 599, 449. HRMS-ESI $[M + Na]^+$ calculated for $C_{26}H30F_2N_6O_6Na^+$: 583.2087; found: 583.2087.

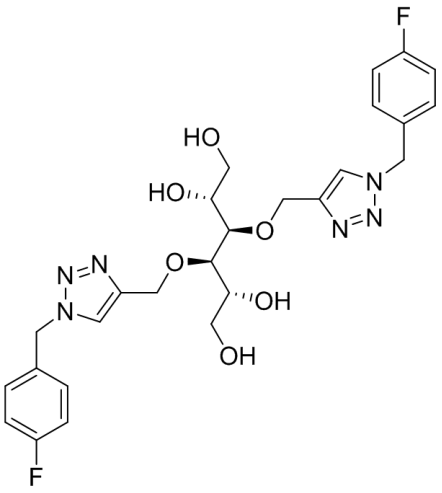

2.3. Cytotoxicity of triazoles (Modified Procedure)[89]

Sample preparation: all compounds were dissolved in 10% DMSO. Briefly 20 µL was added to all samples until they were completely dissolved, and the volume was completed to 200 µL with MiliQ water to make up 1 mM stock solution. The latter was subsequently diluted to make 0.5 mM solutions.

Cell maintenance: Mesenchymal stem cells were harvested in passage 14 when they reached 80% confluency by adding pre-warmed 0.25% Trypsin-EDTA (catalog #: 15050065, Thermo Fisher scientific) Then, incubated at 37 °C incubator supplied with

5% CO_2 for 5 minutes. When cells were completely detached form the flask, the trypsinization were neutralized by adding cell growth media (10% FBS, 1% penicillin/streptomycin in Dulbecco's Modified Eagle Medium). Cell suspension was transferred in 15 mL tube and centrifuged at 600 rpm for 6 minutes. The supernatant was discarded, and cell pellet was then re-suspended in 1 mL cell growth media.

Cell culture: 1 mM and 0.5 mM samples were deposited in triplicate in polystyrene 96 well plate (COSTAR) and 5000 cells/well added atop of samples. The control included untreated cells in the same cell density. The plate was left overnight in 37 °C incubator supplied with 5% CO_2. The viability rate was then quantified with alamarBlue assay (catalog # DAL1025, Thermo Fisher scientific). Briefly, 10% alamarBlue in DMEM solution was added on each well. Samples were placed in incubator for 4 hours and the fluorescence with 560 Excitation /590 Emission was recorded using CLARIOstar plate reader.

Chapter Three

Results and discussion

3. Results and discussion

Heterocyclic compounds have a wide range of applications particularly in the synthesis of pharmaceuticals and medications. One of those important derivatives that comprise of three nitrogen atoms are triazoles. It has been increasingly synthesized since the discovery of copper-catalyzed alkyne azide 1,3-dipolar cycloaddition reaction in the early of the last decade.[90–92]

In the current project, three novel D-mannitol-based 1,2,3-triazole derivatives have been prepared starting from the alcoholic monosaccharide D-mannitol (Scheme 20).

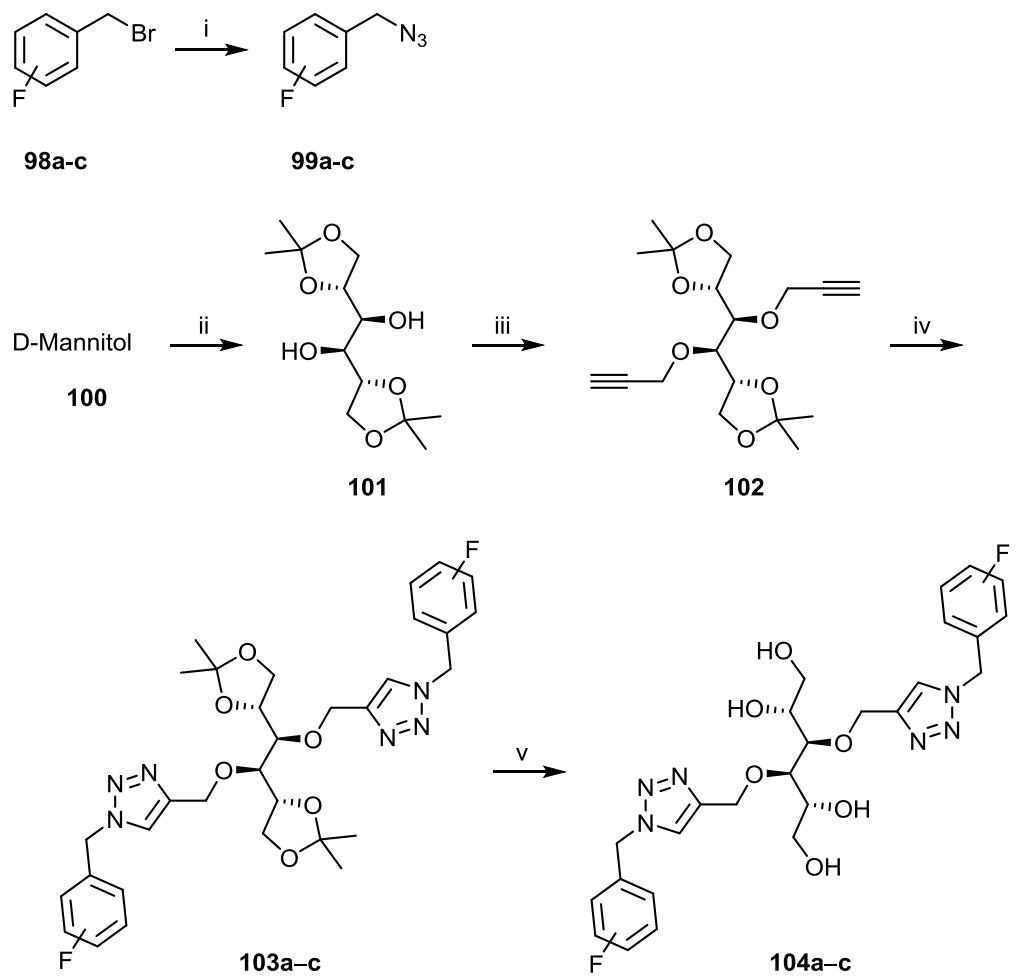

Reagents and conditions: **i**] NaN_3, DMSO, 50 °C, 24 h; 88-91%ii] acetone, $ZnCl_2$, r.t., 24 h, 54%; **iii**] propargyl bromide, DMF, –20 °C–r.t.,24 h, 84%; iv] **99a–c**, Na ascorbate, $CuSO_4$•$5H_2O$, DMSO, 50 °C, 36 h, 77–81%; v] Amberlite IR 120 H+, MeOH / H_2O, 60 °C, 72 h.quantitative.

Scheme 20. Synthesis of D-mannitol-based 1,2,3-triazole derivatives

3.1.Synthesis of fluorine-containing benzyl azides

Fluorine-containing benzyl bromides **98a**–**c** were reacted with sodium azide via S_N2 mechanism[93,94] in DMSO at 50 °C for 24 h to afford the corresponding benzyl azides **99a**–**c** in 88–91% yields (Scheme 21).

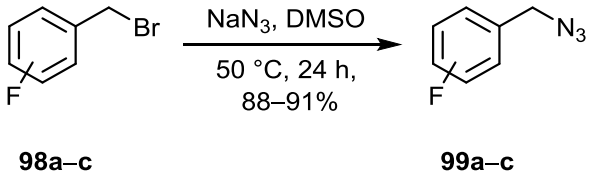

Scheme 21. Synthesis of fluorine-containing benzyl azides **99a**–**c**

FT-IR spectra of compounds **99a**–**c** (Figures 22–24) showed C–H aromatic stretching bands above 3000 cm^{-1} in addition to the characteristic $–N_3$ stretching band around 2100 cm^{-1} and the C=C aromatic stretching bands above 1600 cm^{-1} and 1580 cm^{-1}. Other important bands are shown above 1220 cm^{-1} attributed to stretching of the C–F aromatic.

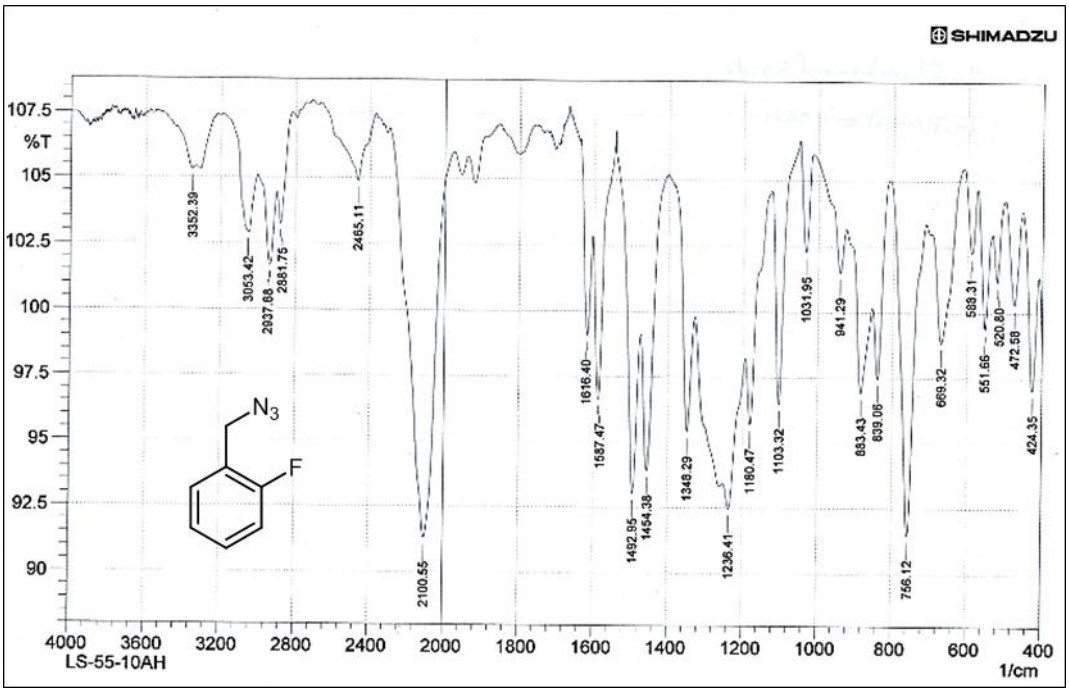

Figure 22. FT-IR spectrum of compounds **99a**

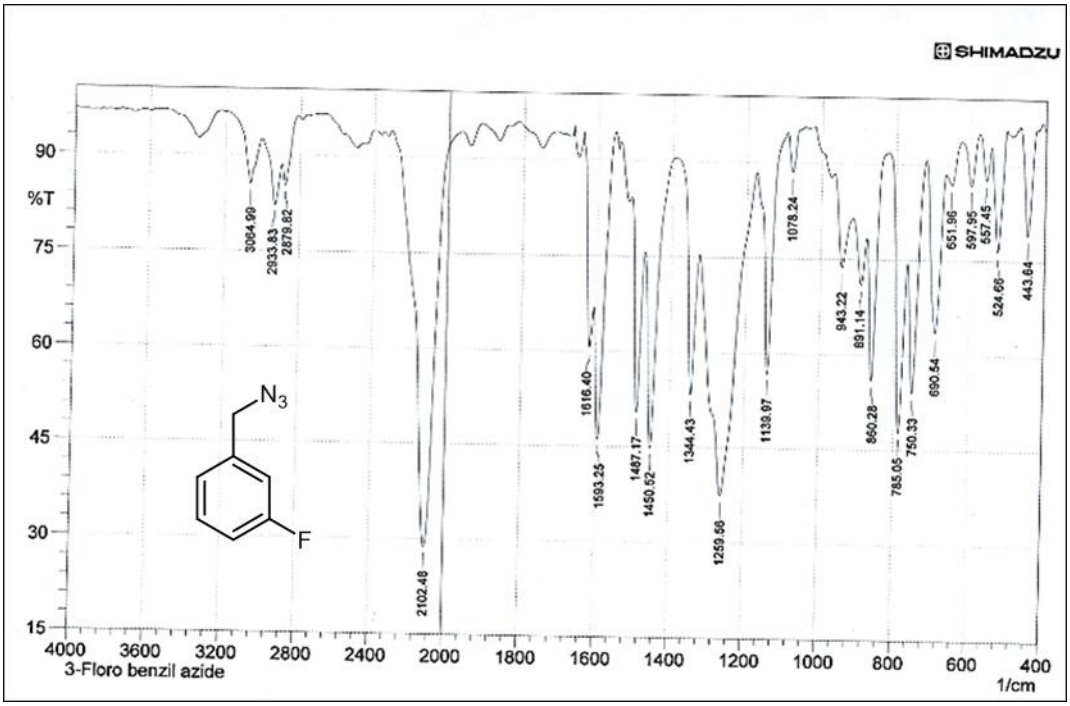

Figure 23. FT-IR spectrum of compounds **99b**

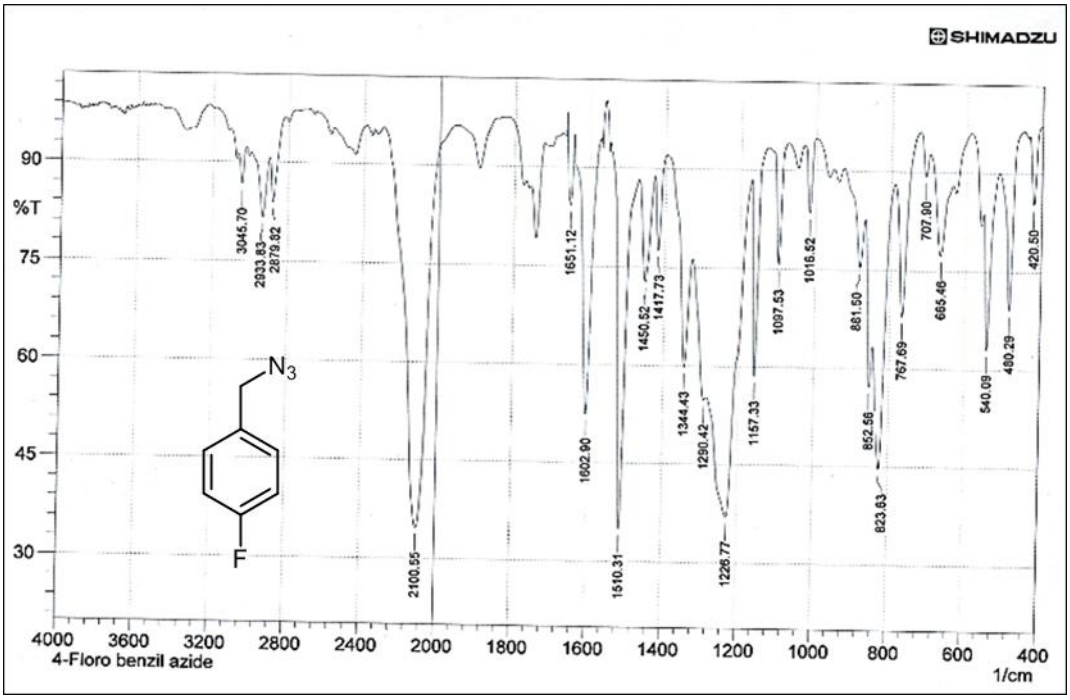

Figure 24. FT-IR spectrum of compounds **99c**

The synthesized benzyl azide derivatives **99a–c** were also characterized by NMR technique. ^{1}H NMR spectra (Figures 25–27) of these compounds displayed multiplet signals integrated for four protons at δ 7.50–7.00 ppm belong to the aromatic

protons and singlets between δ 4.41 ppm and 4.31 ppm attributed to the methylene protons.

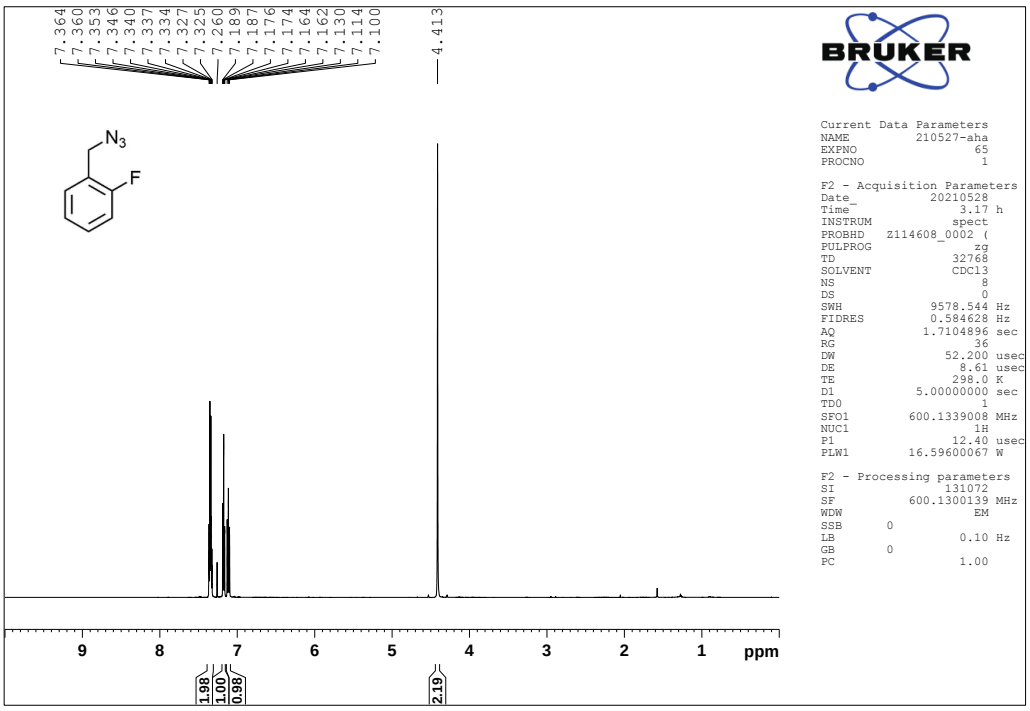

Figure 25. ^{1}H NMR spectrum ($CDCl_3$, 600 MHz) of compound **99a**

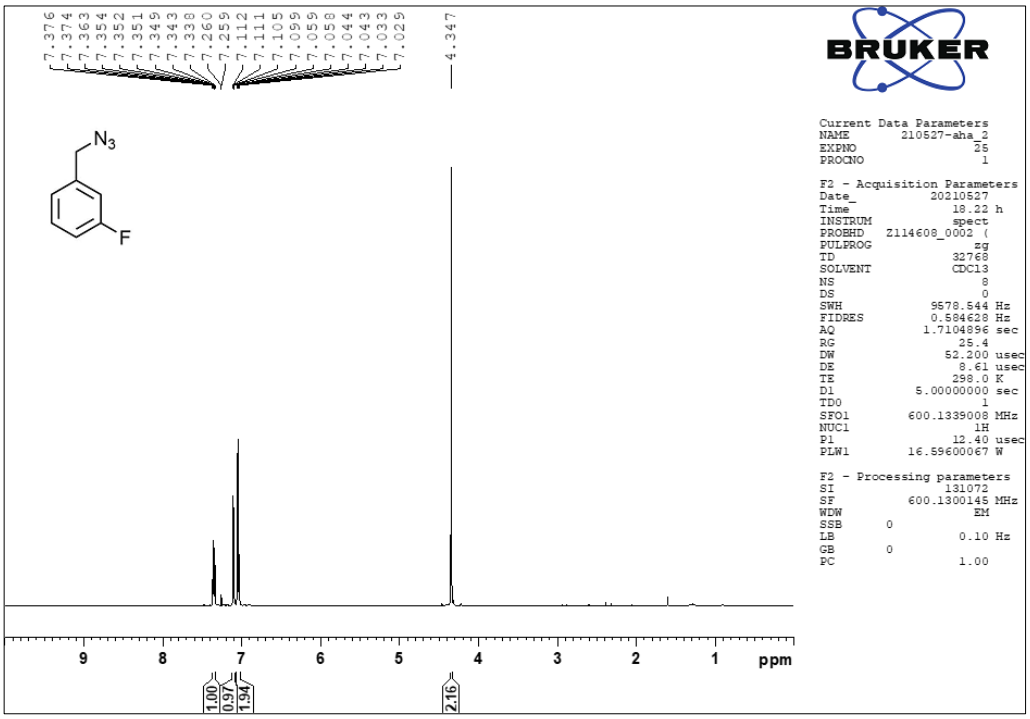

Figure 26. ^{1}H NMR spectrum ($CDCl_3$, 600 MHz) of compound **99b**

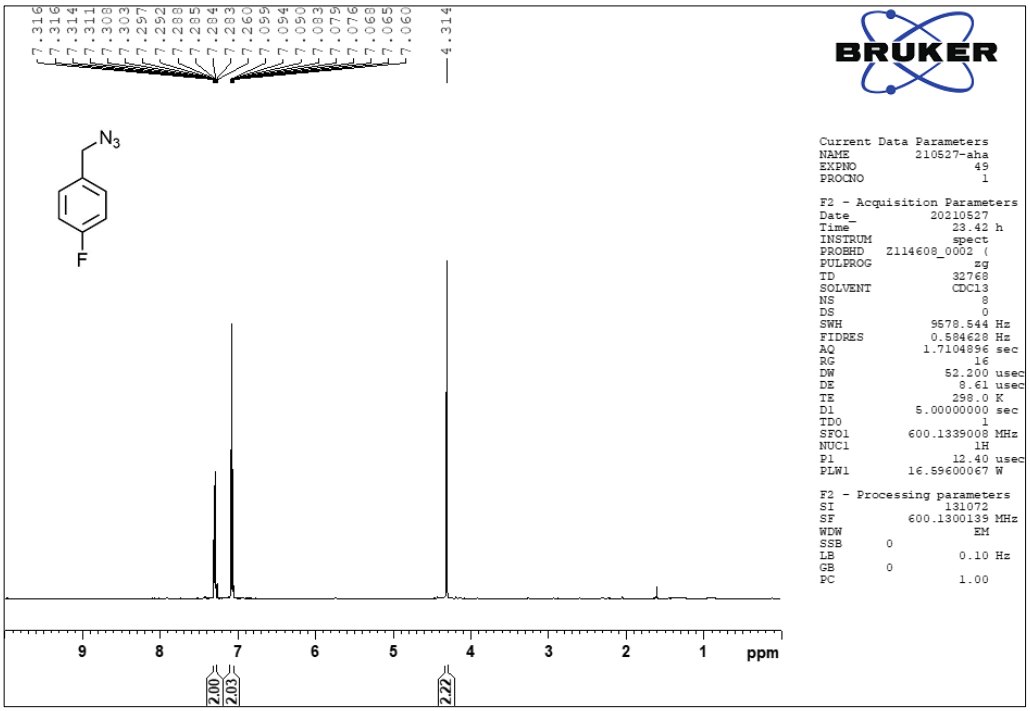

Figure 27. ^{1}H NMR spectrum ($CDCl_3$, 600 MHz) of compound **99c**

^{13}C NMR spectra of compounds **99a**–**c** (Figures 28–30) demonstrated that all aromatic carbon signals have been splitting due to the fluorine effect[95] particularly the signal of the quaternary carbon attached to the fluorine around 162 ppm with coupling constant higher than 245 Hz. In addition, the benzylic carbon signal of the *meta* and *para* isomers appeared around 54.2 ppm and 54.1 ppm respectively while that of *ortho* counterpart was observed at 48.6 ppm. ^{19}F NMR spectra of the azide derivatives **99a**–**c** (Figures 31–33) showed one multiplet at δ −117.9 ppm, −112.3 ppm and −113.6 ppm assigned to one fluorine atom for 2-, 3- and 4-fluorobenzyl azide, respectively.

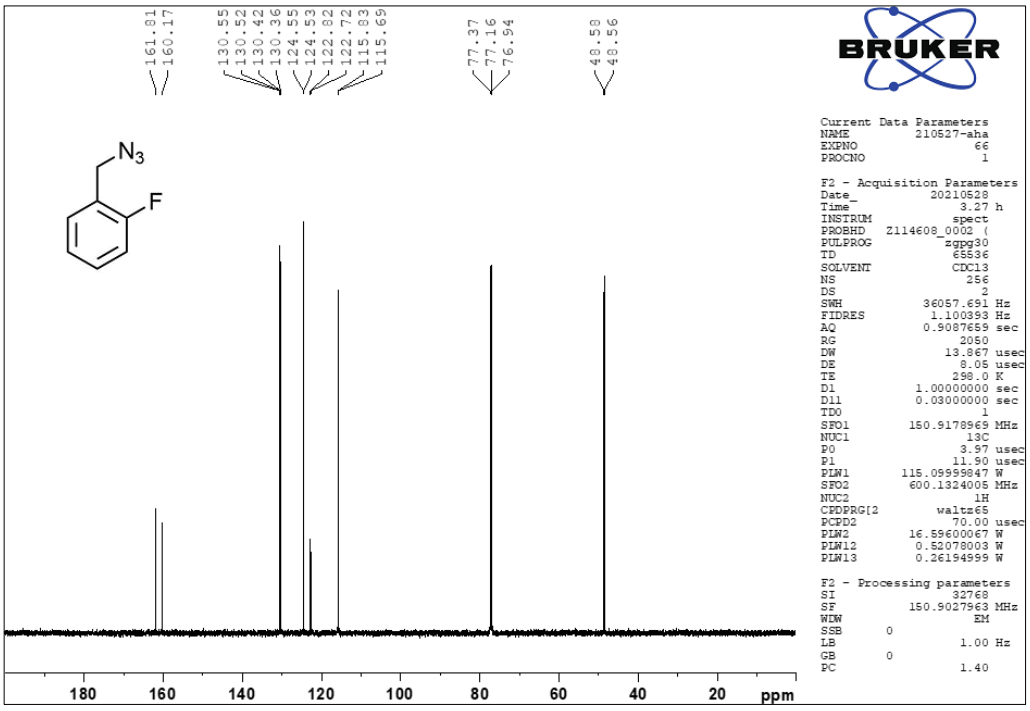

Figure 28. $^{13}C\{^{1}H\}$ NMR spectrum ($CDCl_3$, 150 MHz) of compound **99a**

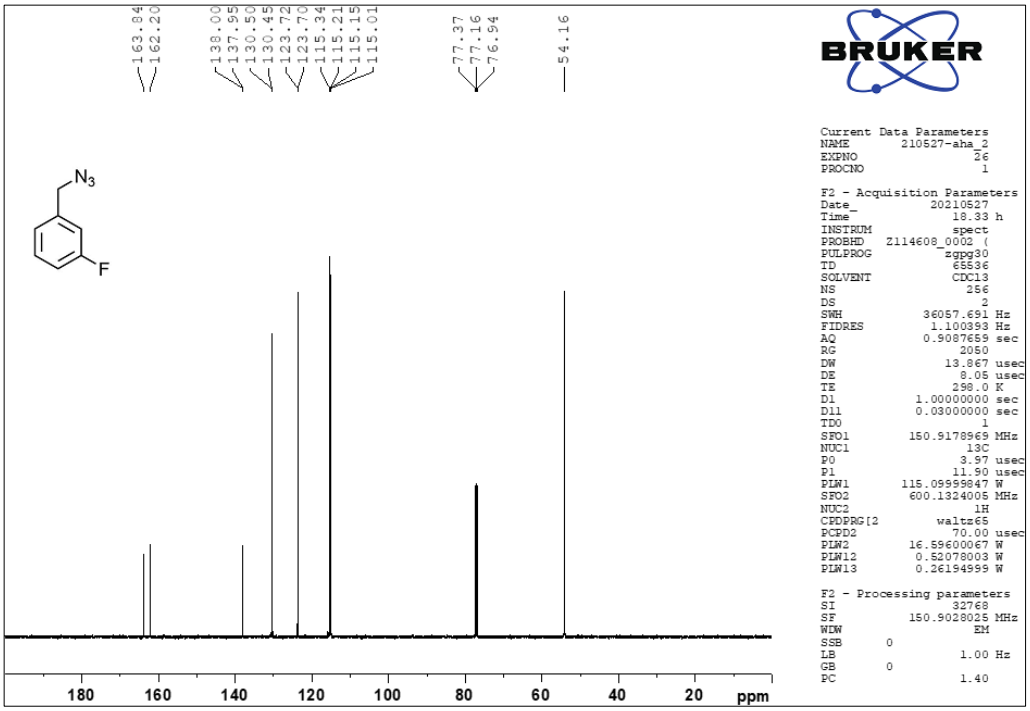

Figure 29. $^{13}C\{^{1}H\}$ NMR spectrum ($CDCl_3$, 150 MHz) of compound **99b**

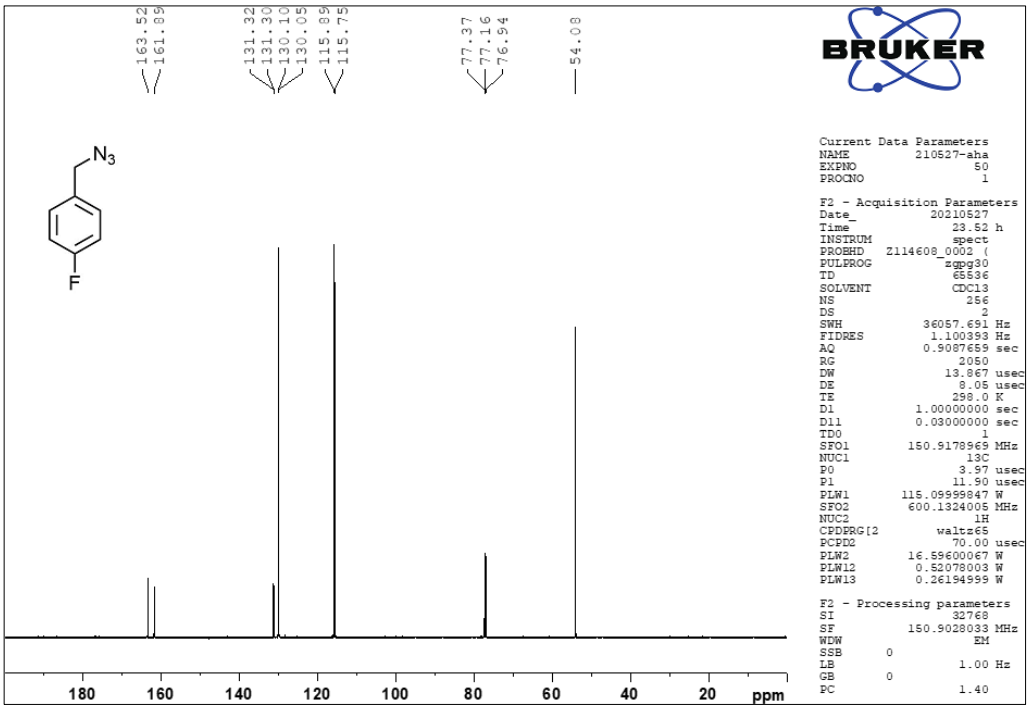

Figure 30. $^{13}C\{^{1}H\}$ NMR spectrum ($CDCl_3$, 150 MHz) of compound **99c**

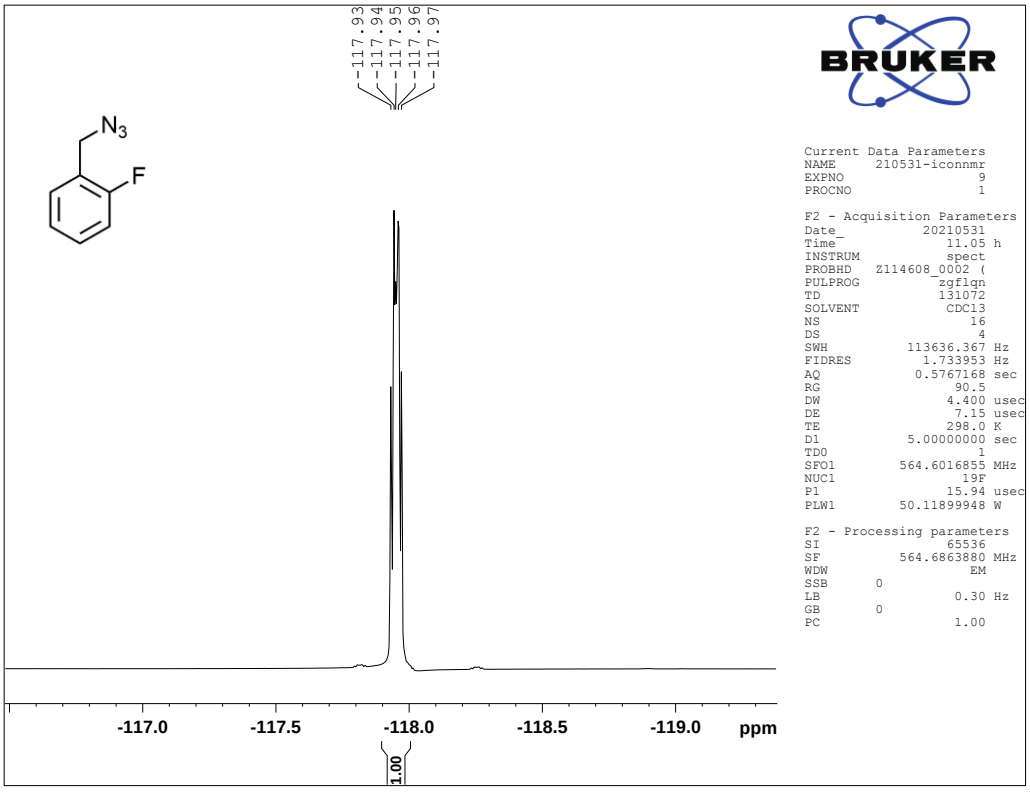

Figure 31. ^{19}F NMR spectrum ($CDCl_3$, 564 MHz) of compound **99a**

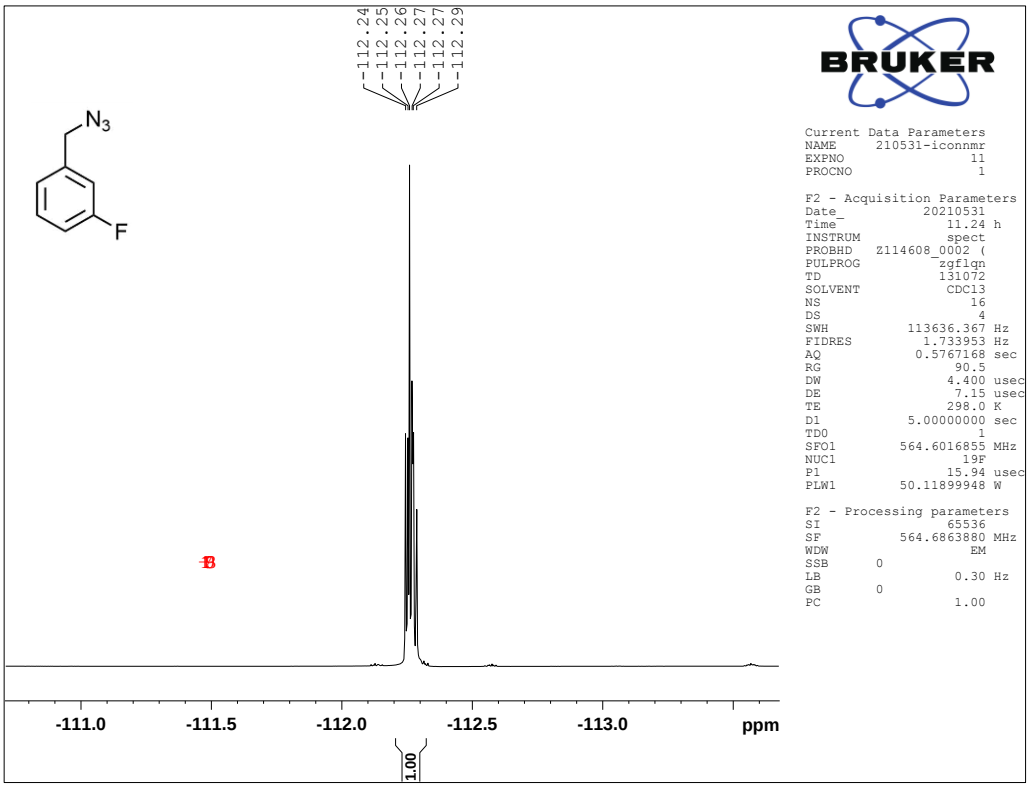

Figure 32. ^{19}F NMR spectrum ($CDCl_3$, 564 MHz) of compound **99b**

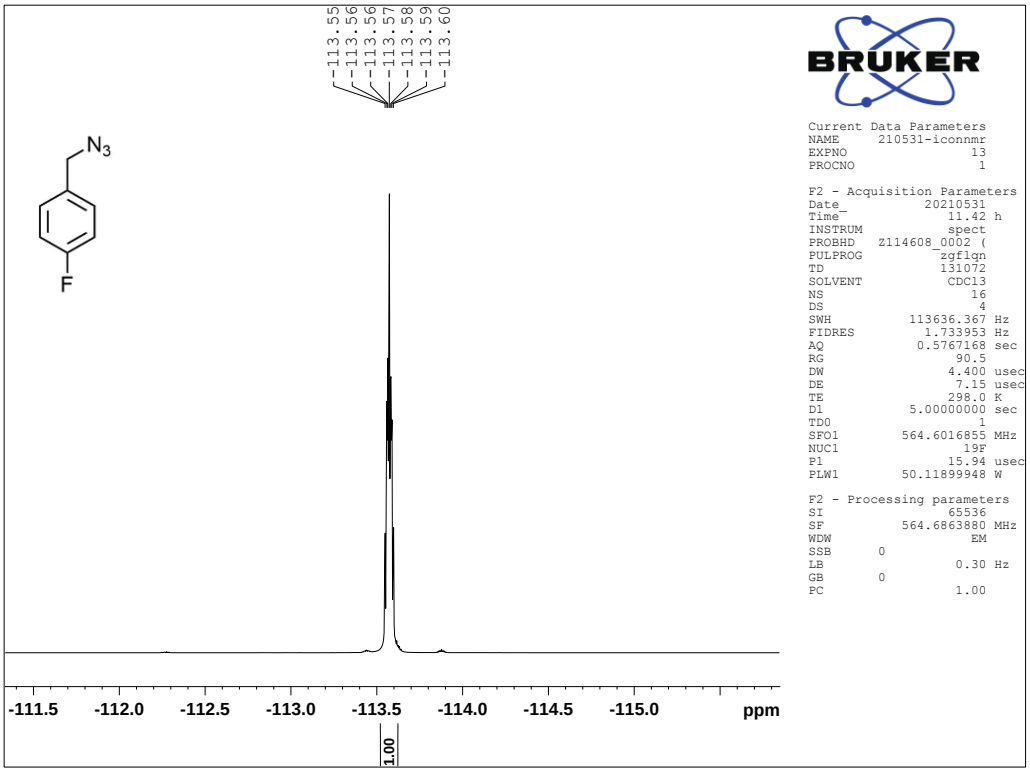

Figure 33. ^{19}F NMR spectrum ($CDCl_3$, 564 MHz) of compound **99c**

3.2.Synthesis of dipropargyl derivative

Next, four hydroxyl groups of D-mannitol (**100**) are protected using excess of $(CH_3)_2CO$ in the presence of $ZnCl_2$ at room temperature for 24 h to produce 1,2:5,6-di-O-isopropylidene-D-mannitol (**101**) in 54% yield (Scheme 22).

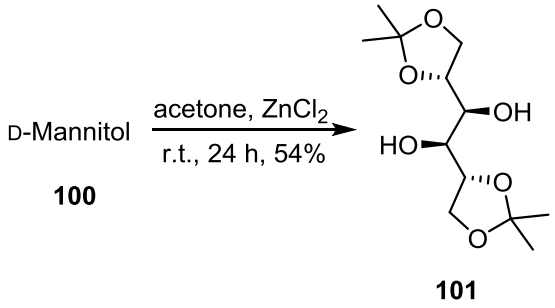

Scheme 22. Synthesis of 1,2:5,6-di-*O*-isopropylidene-D-mannitol (**101**)

The mechanism of the acetal formation is catalyzed by Lewis acid (zinc chloride).[96] Initially, the oxygen atom of the carbonyl group forms coordination bond with zinc, and this will promote the attack of the hydroxyl group of the diol by increasing the electrophilicity of the carbon atom of the carbonyl to form tetrahedral intermediate followed proton transfer then the attack of the second hydroxyl group and elimination of zinc complex. Finally, oxonium ion is deprotonated to afford the cyclic acetal.[97]

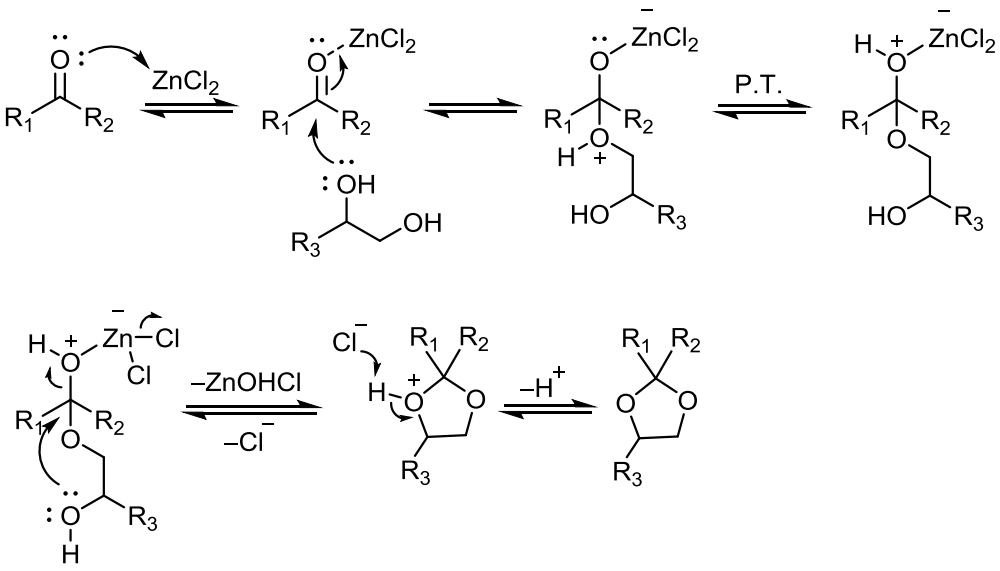

Scheme 23. Proposed mechanism of the cyclic acetal formation

The formation of compound **101** is confirmed by FT-IR spectrum (Figure 34) that shows characteristic O–H stretching bands at 3464 cm^{-1} and 3317 cm^{-1}. Also, intense C–H stretching bands appeared at 2989 cm^{-1}, 2935 cm^{-1} and 2881 cm^{-1} in addition to various C–O stretching bands between 1255 cm^{-1} and 1072 cm^{-1}.

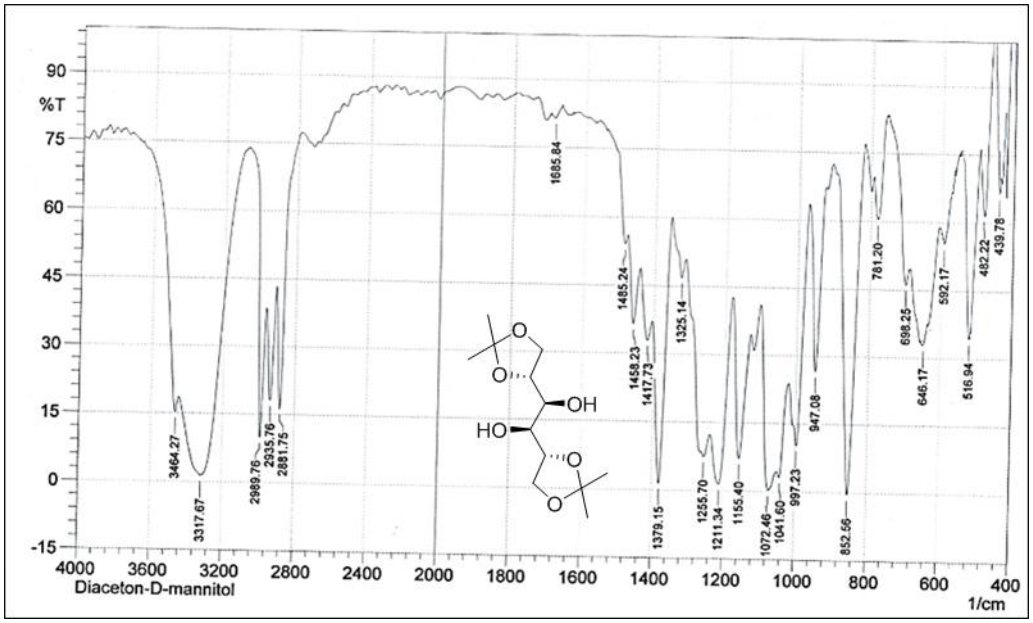

Figure 34. FT-IR spectrum of compound **101**

^{1}H NMR spectrum of compound **101** (Figure 35) displayed a doublet of doublet of doublet centred at 4.14 ppm attributed to H-2 and H-5, two doublets of doublet belong to H-1ab and H-6 ab at 4.08 ppm and 3.97 ppm, a doublet at 3.64 ppm assigned for H-3 and H-4, and two singlets of isopropylidene protons at 1.37 ppm and 1.33 ppm. ^{13}C NMR spectrum of compound **101** (Figure 36) showed six signals that confirm the suggested structure; a signal at δ 110.2 ppm belongs to the quaternary carbon of the isopropylidene moiety, 76.5 ppm for C-2 and C-5, 72.2 ppm for C-1 and C6, 68.2 for C-3, and signals at δ C-4, 27.2 ppm and 25.7 ppm that assigned for CH_3 carbon atoms of the isopropylidene protecting group. The accurate assignment of the proton and carbon signals was also verified by 2D NMR spectra (Figures 37 and 38). Finally, HRMS analysis (Figure 39) afforded a base peak at *m*/*z* 285.1306, consistent with the formula $C_{12}H_{22}O_6Na^+$.

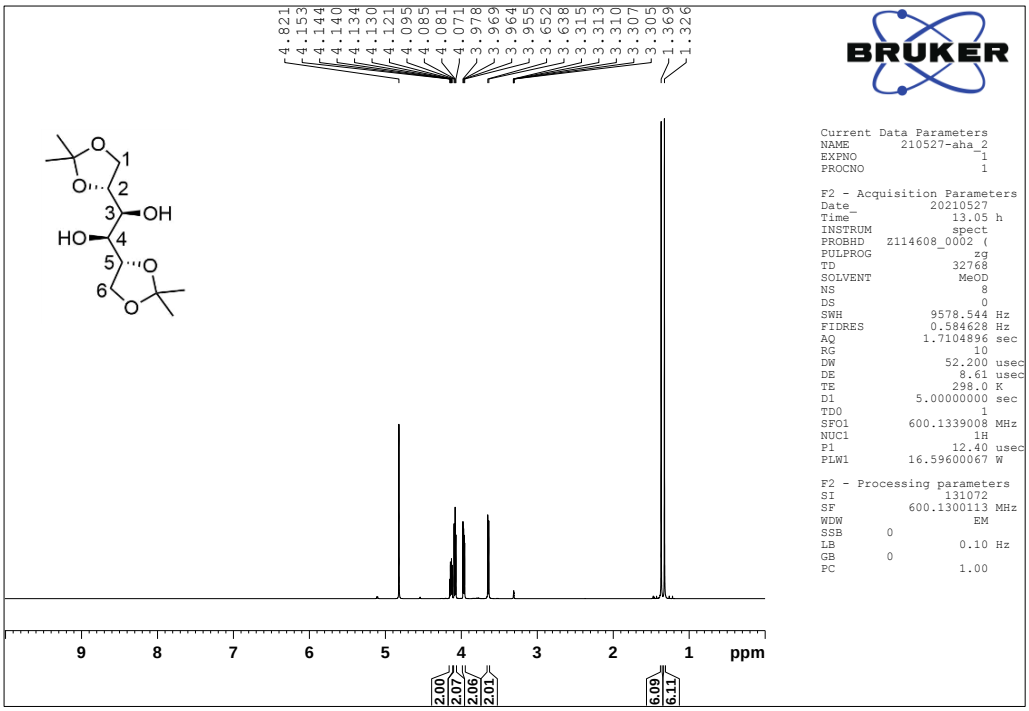

Figure 35. ^{1}H NMR spectrum (MeOH-d_4, 600 MHz) of compound **101**

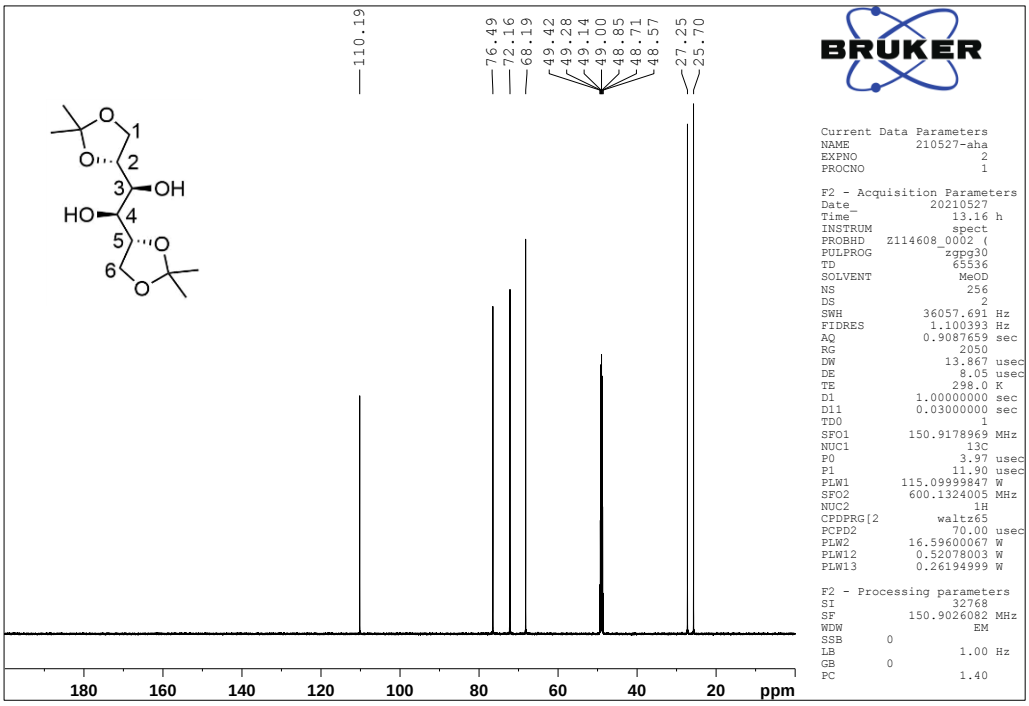

Figure 36. $^{13}C\{^{1}H\}$ NMR spectrum (MeOH-d_4, 150 MHz) of compound **101**

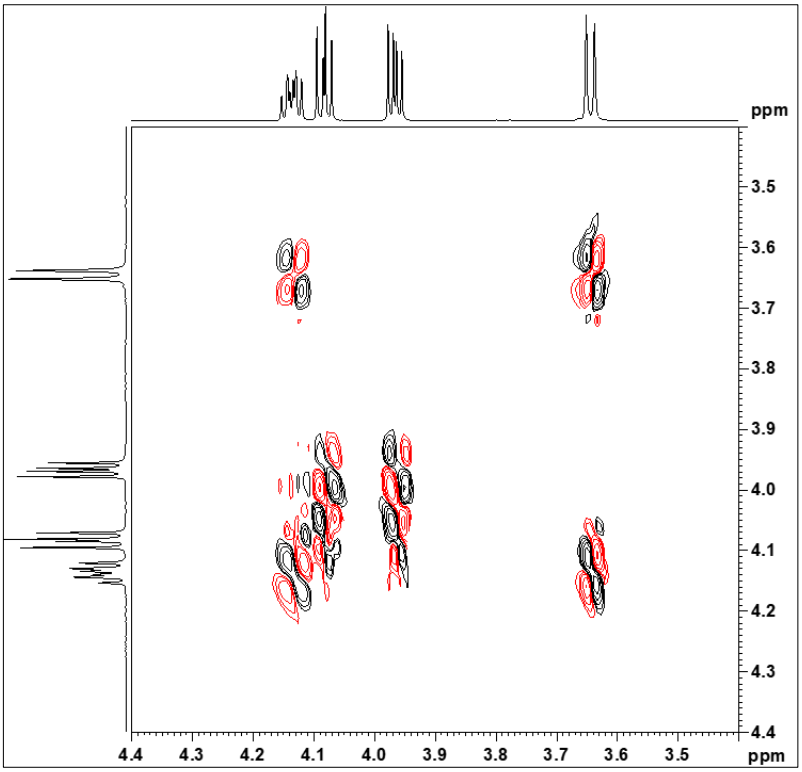

Figure 37. $^{1}H–^{1}H$ COSY (600 MHz, MeOH-d_4) of compound **101**

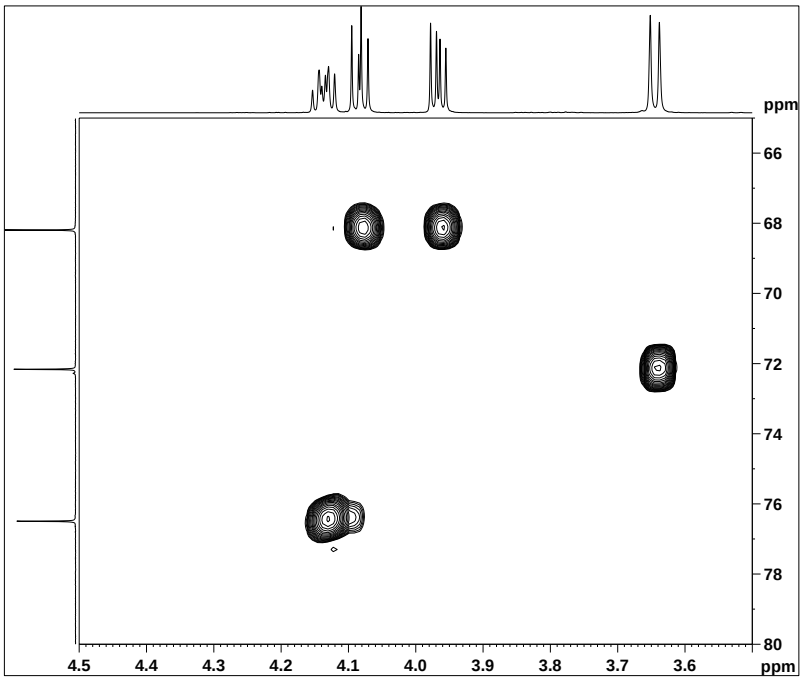

Figure 38. $^{1}H–^{13}C$ HSQC (600 MHz, MeOH-d_4) of compound **101**

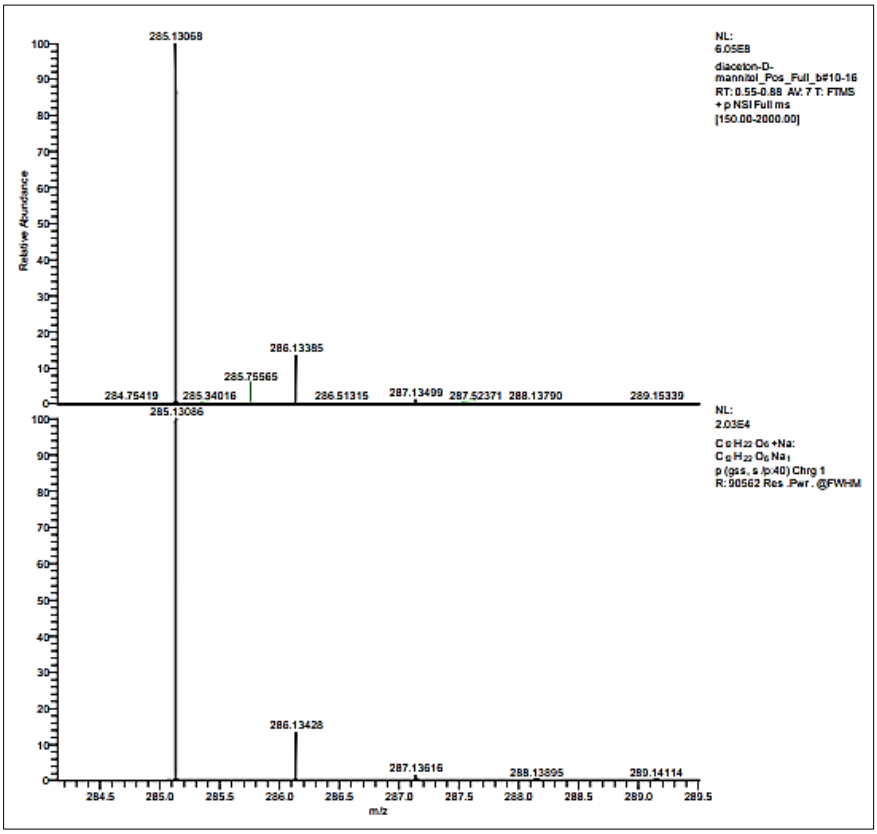

Figure 39. HRMS of compound **101**

The reaction of the diol **101** with using propargyl bromide in DMF at –20 °C to the ambient temperature for 24 h afforded 3,4-bis-*O*-propargyl-1,2:5,6-di-*O*-isopropylidene-D-mannitol (**102**) in very good yield (Scheme 24).

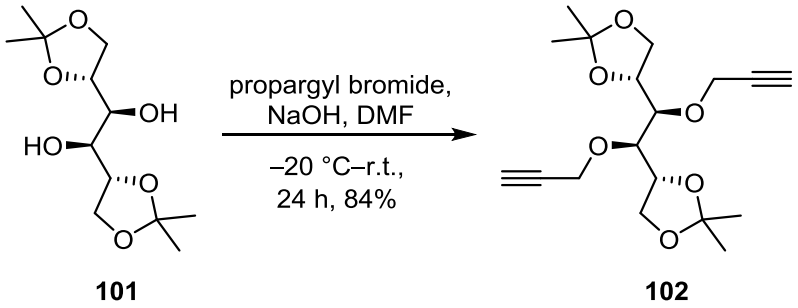

Scheme 24. Synthesis of 3,4-bis-*O*-propargyl-1,2:5,6-di-*O*-isopropylidene-D-mannitol (**102**)

The suggested mechanism of the formation of compound **102** is Williamson etherification.[98] First, the sp^3 carbon atom of propargyl bromide has been directly attacked by the hydroxyl group of an alcohol through S_N2 mechanism to form a transition state followed by NaOH-assisted elimination of HBr to form the desired product (Scheme 25).

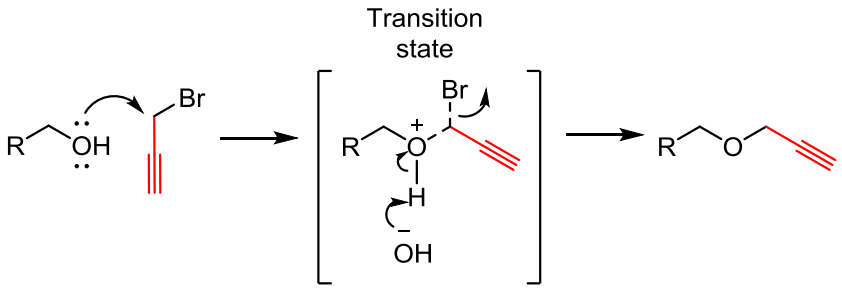

Scheme 25. Suggested mechanism of the alkyl propargyl ether formation

The formation the dipropargyl ether **102** is confirmed FT-IR (Figure 40) which showed strong absorption band at 3252 cm^{-1} due to the terminal alkyne C–H stretching and weak absorption band at 2115 cm^{-1} of the C≡C stretching. Moreover, all hydroxyl

absorption bands disappeared in the spectrum, which also confirms the dipropargyl ether formation.

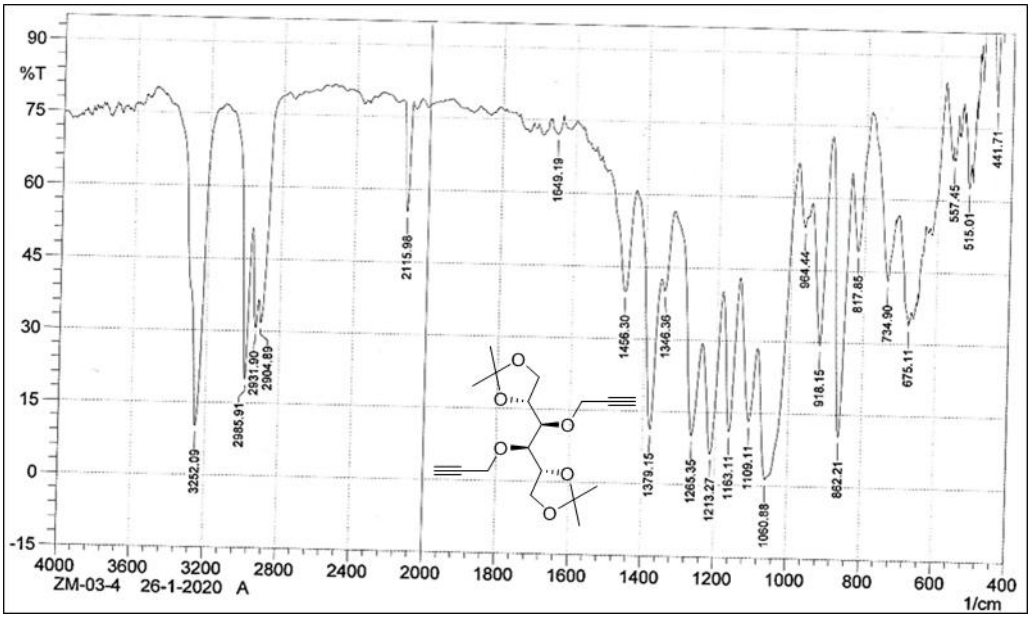

Figure 40. FT-IR spectrum of compound **102**

^{1}H NMR spectrum (Figure 41) has also added a further evidence for the formation of compound **102**. New signals belong to the propargyl moiety appeared in the spectrum. The first two doublet of doublets at 4.38 ppm and 4.33 ppm having similar coupling constants 16.0 Hz and 2.2 Hz due to the methylene protons (H-7 and H-10) and a triplet at 2.45 ppm with coupling constant 2.0 Hz attributed to the acetylenic protons (H-9 and H-12). In the ^{13}C NMR spectrum (Figure 42), three new signals appeared at 78.9 ppm, 78.6 and 59.7 which ascribed to *sp* carbon atoms (C-8, C-9, C-11 and C-12) and methylene carbons (C-7 and C-10) respectively. Finally, HRMS analysis (Figure 43) afforded a base peak at *m*/*z* 361.1621, consistent with the formula $C_{18}H_{26}O_6Na^+$.

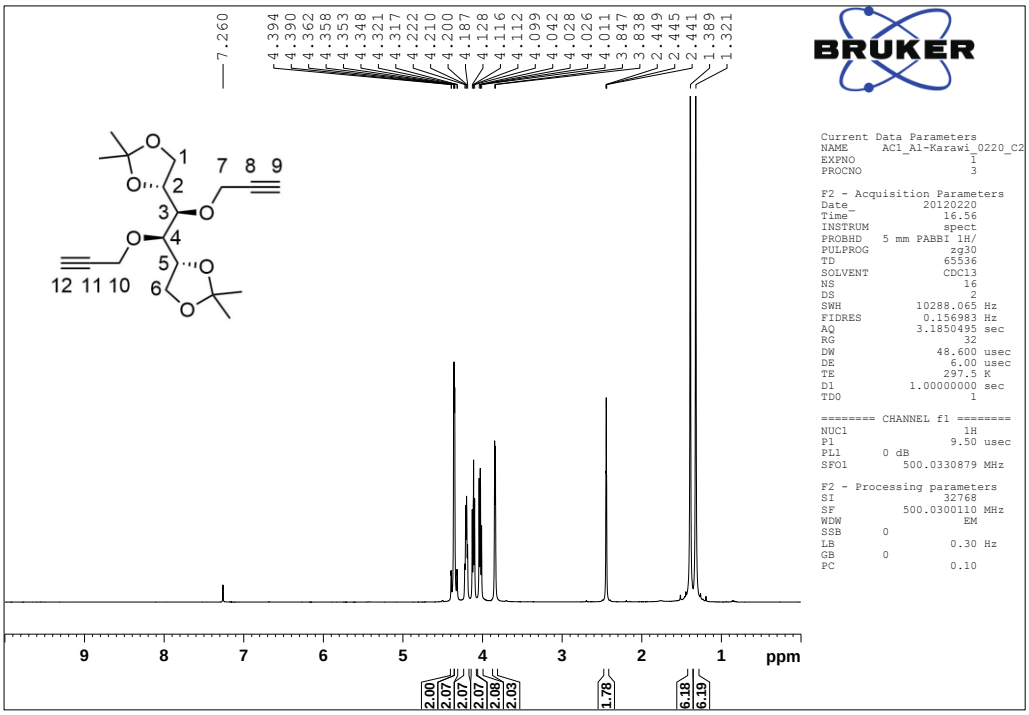

Figure 41. ^{1}H NMR spectrum ($CDCl_3$, 500 MHz) of compound **102**

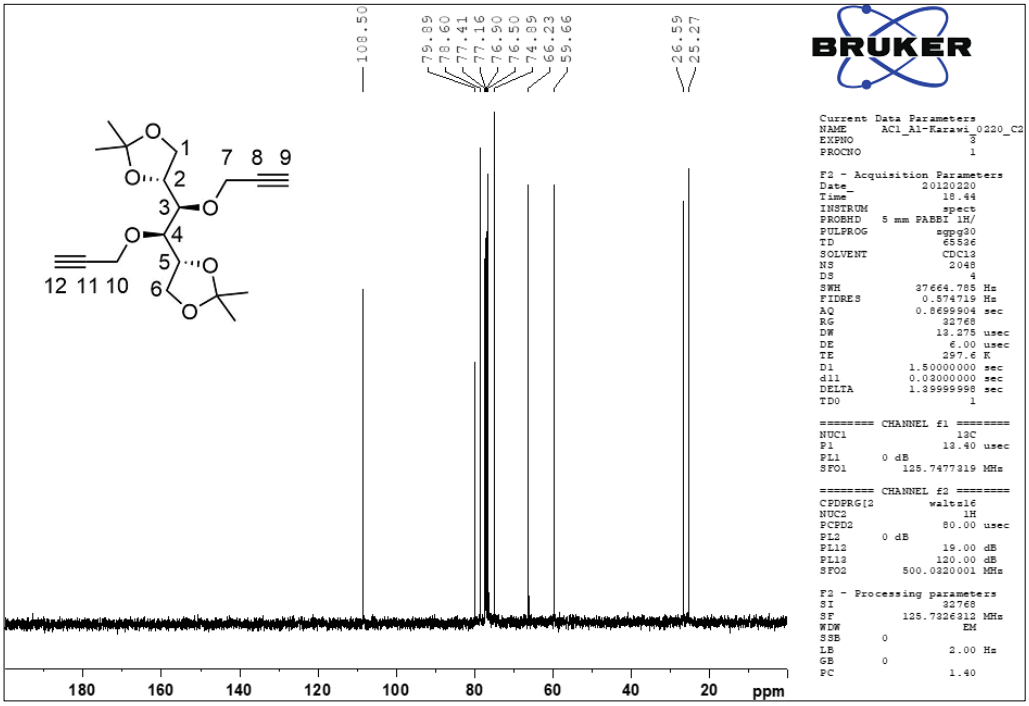

Figure 42. $^{13}C\{^{1}H\}$ NMR spectrum ($CDCl_3$, 125 MHz) of compound **102**

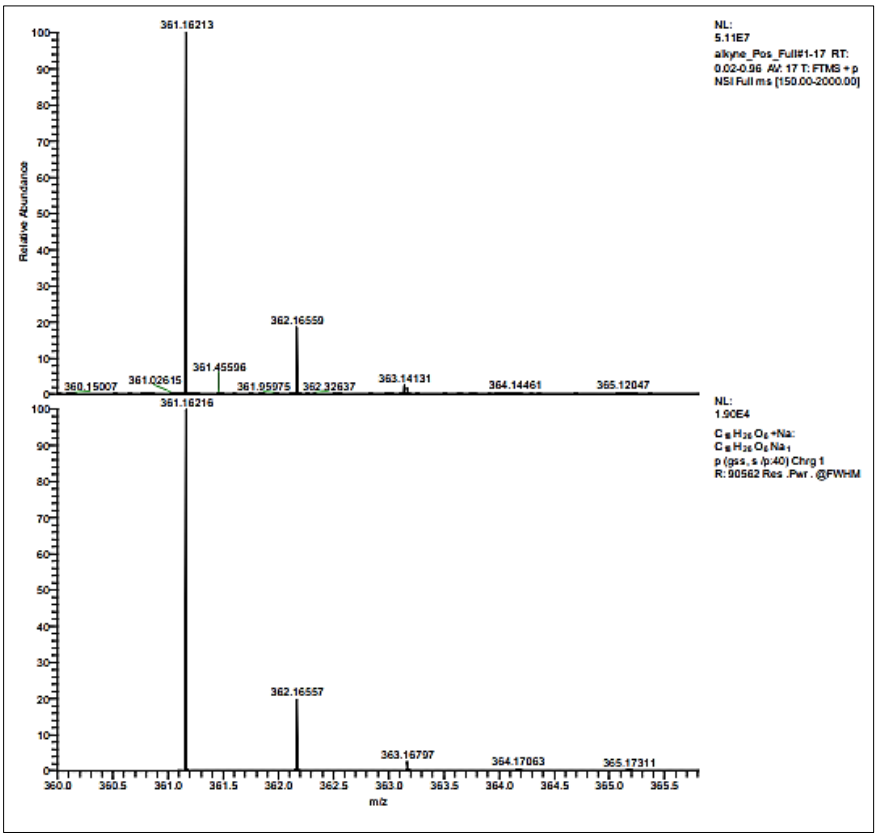

Figure 43. HRMS of compound **102**

3.3.Synthesis of bistriazoles

The last stage in the synthetic protocol in the current work is the combination of the aromatic azides **99a**–**c** with the dipropargyl sugar derivative **102**. For this purpose, aromatic azides **99a**–**c** were separately reacted with the compound **102** in DMSO[99] in the presence of sodium ascorbate and copper sulphate pentahydrate at 50 °C for 36 h to produce bis-1,2,3-triazoles **103 a**–**c** in approximately very good yield (Scheme 26).

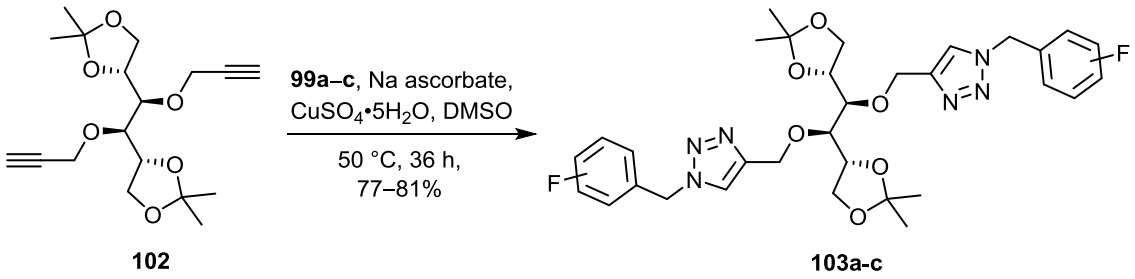

Scheme 26. Synthesis of bis-1,2,3-triazoles **103 a**–**c**

The mechanism of copper(I)-catalyzed azide-alkyne cycloaddition (CuAAC) is illustrated in Chapter 1 (Scheme 12). The first step in the suggested reaction mechanism is the generation Cu(I) *in situ* through the reduction of Cu(II) by sodium ascorbate. Then, the terminal alkyne couples with Cu(I) to form copper(I) acetylide **I** followed by the complexation of copper with the electron-rich nitrogen. Afterwards, the terminal nitrogen of the azide is intramolecularly attacked by internal *sp*-carbon to form the six-membered ring intermediate **III**. Ring contraction of **III** affords intermediate **IV** that eventually release the copper complex to the cycle and gives the regioselective product 1,4-disubstituted-1*H*-1,2,3-triazole derivative **V**.

The formation of the triazole derivatives **103 a**–**c** is confirmed by FT-IR spectra (Figures 44–46) that displayed C–H triazole stretching band at 3136 cm^{-1}, C–H aromatic stretching band around 3072 cm^{-1}, C=C stretching bands around 1610 cm^{-1} and 1500 cm^{-1} and the characteristic sharp C–F stretching band from 1240–1220 cm^{-1}.

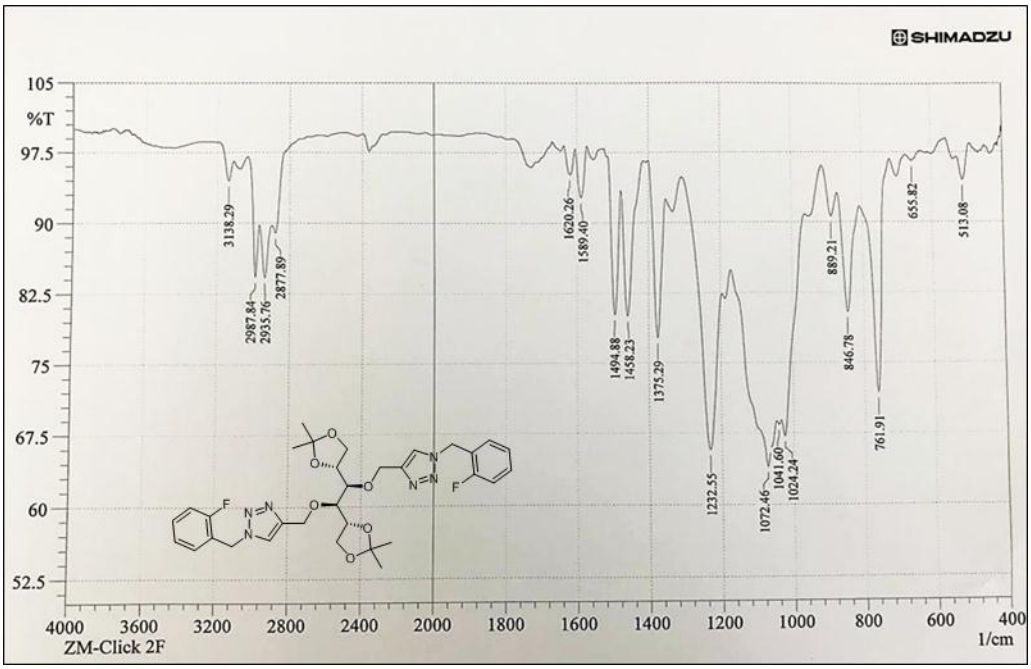

Figure 44. FT-IR spectrum of compounds **103a**

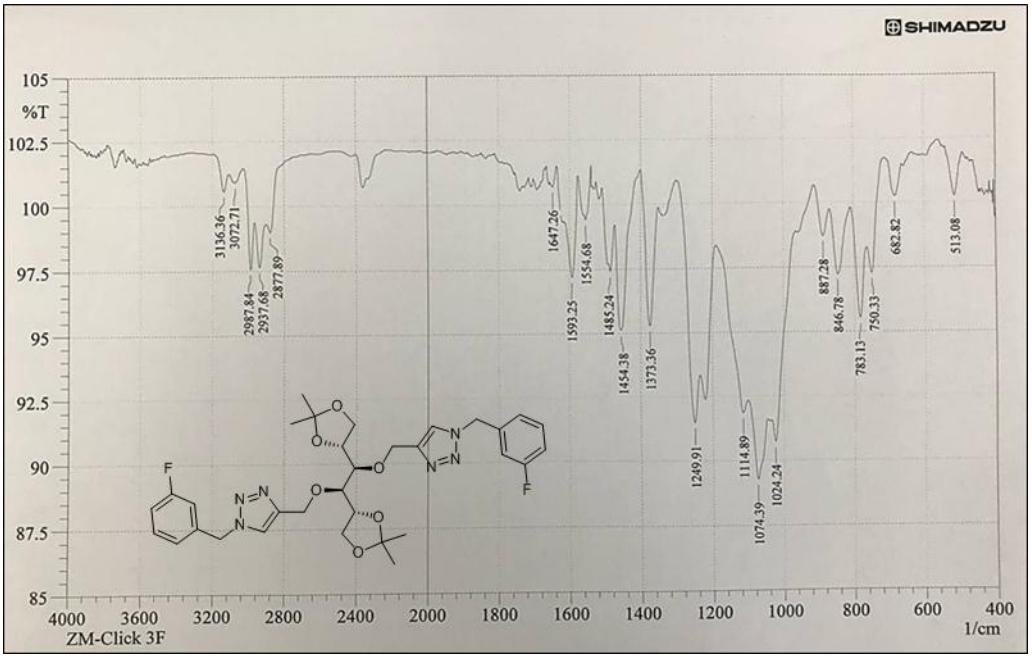

Figure 45. FT-IR spectrum of compounds **103b**

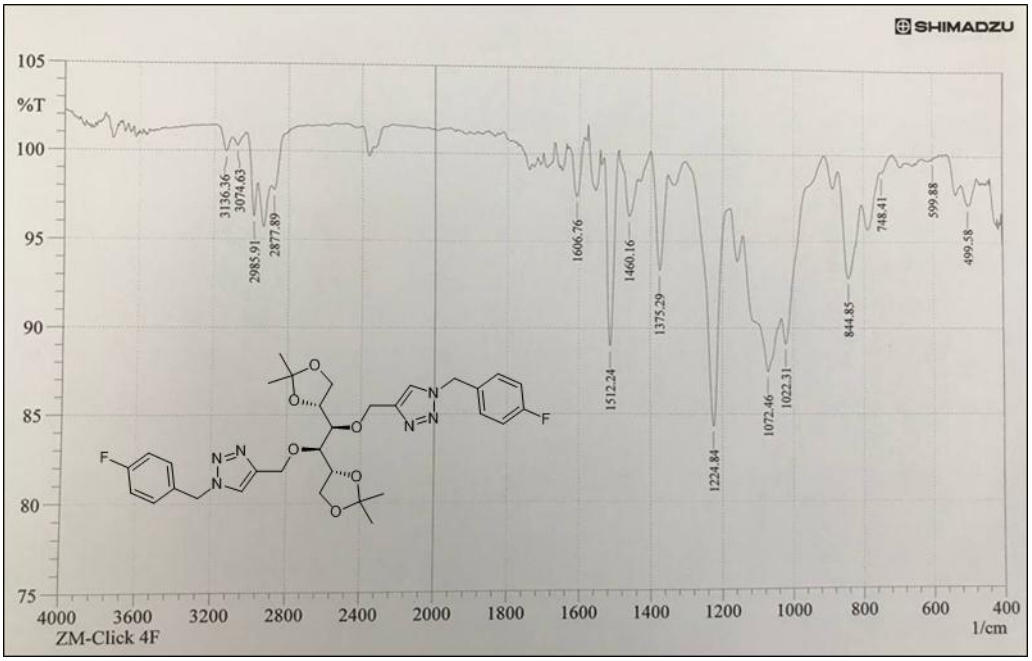

Figure 46. FT-IR spectrum of compounds **103c**

Moreover, ^{1}H NMR spectra (Figures 47–49) of compounds **103a**–**c** confirm the formation of 1,4-disubstited triazole by affording one singlet between 7.53 ppm and 7.45 ppm that indicates the presence of one triazole isomer. Furthermore, the appearance of the aromatic signals between 7.50 ppm and 7.00 ppm and the benzylic protons singlet around 5.50 ppm is an excellent proof of the azide-alkyne cycloaddition.

There is also significant shift downfield of the –O–CH_2– protons doublet of doublet from 4.36 ppm in alkyne **102** to 4.79 ppm in the spectra of triazoles **103a–c**. The ^{13}C NMR spectra (Figures 50–52) of triazole derivatives **103a–c** demonstrated the formation and the high purity of the produced compounds as it has the exact number of carbon signals corresponding to each derivative. First, the aromatic region includes all phenylene signals between 161 ppm and 115 ppm in addition to the triazole carbon signal around 145 ppm and 122 ppm. It is important to mention that the isopropylidene protecting groups did not affect by click reaction condition due to the presence of the isopropylidene carbon signals at 108.8 ppm, 26.7 ppm and 25.3 ppm. All other signals in ^{13}C NMR spectra are attributed either to the sugar backbone carbon signals or to the methylene carbons.

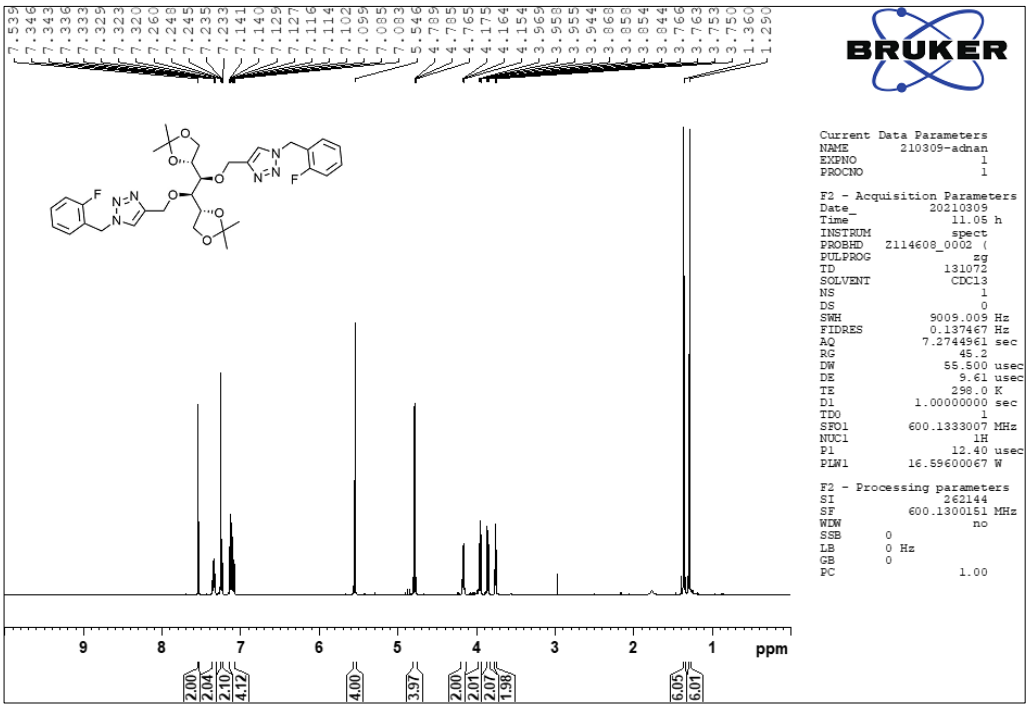

Figure 47. ^{1}H NMR spectrum ($CDCl_3$, 600 MHz) of compound **103a**

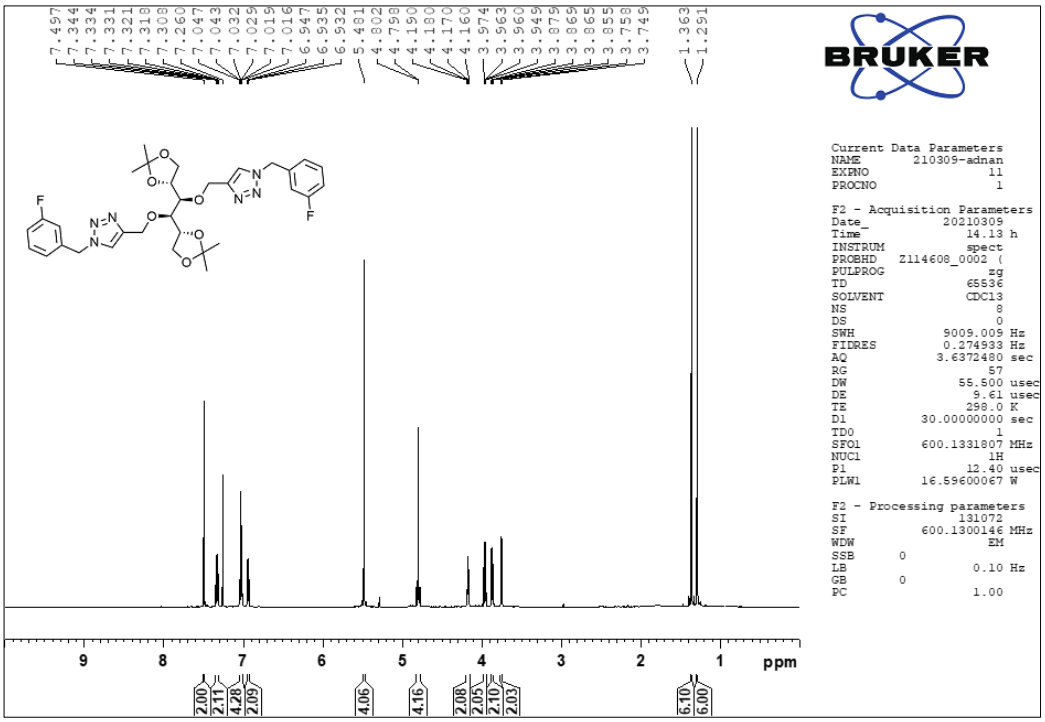

Figure 48. ^{1}H NMR spectrum ($CDCl_3$, 600 MHz) of compound **103b**

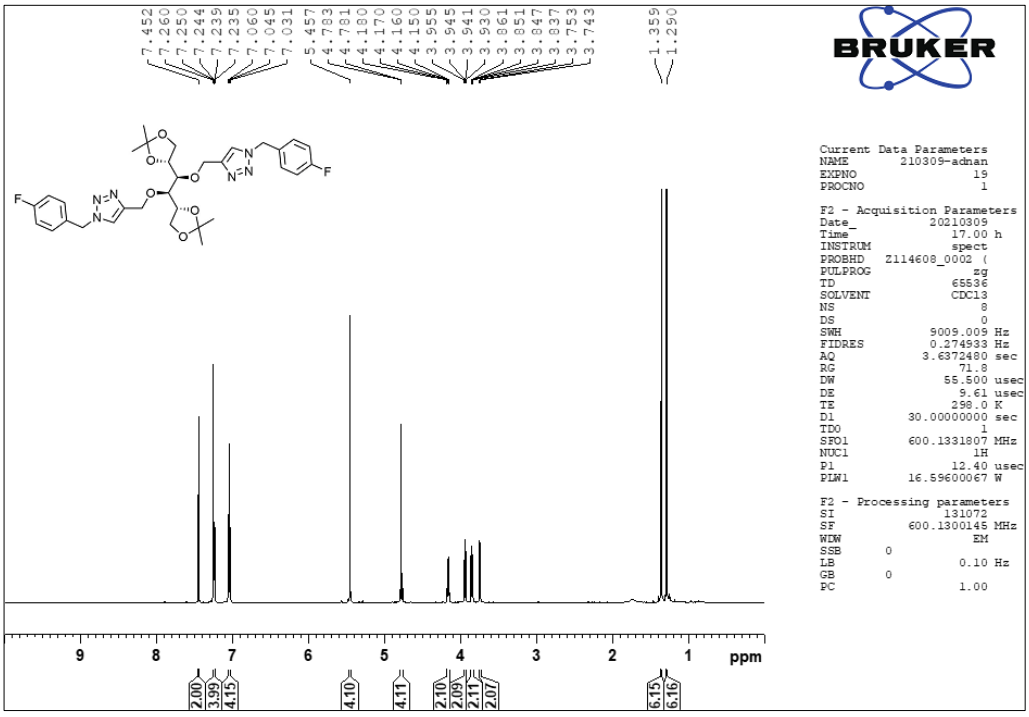

Figure 49. ^{1}H NMR spectrum ($CDCl_3$, 600 MHz) of compound **103c**

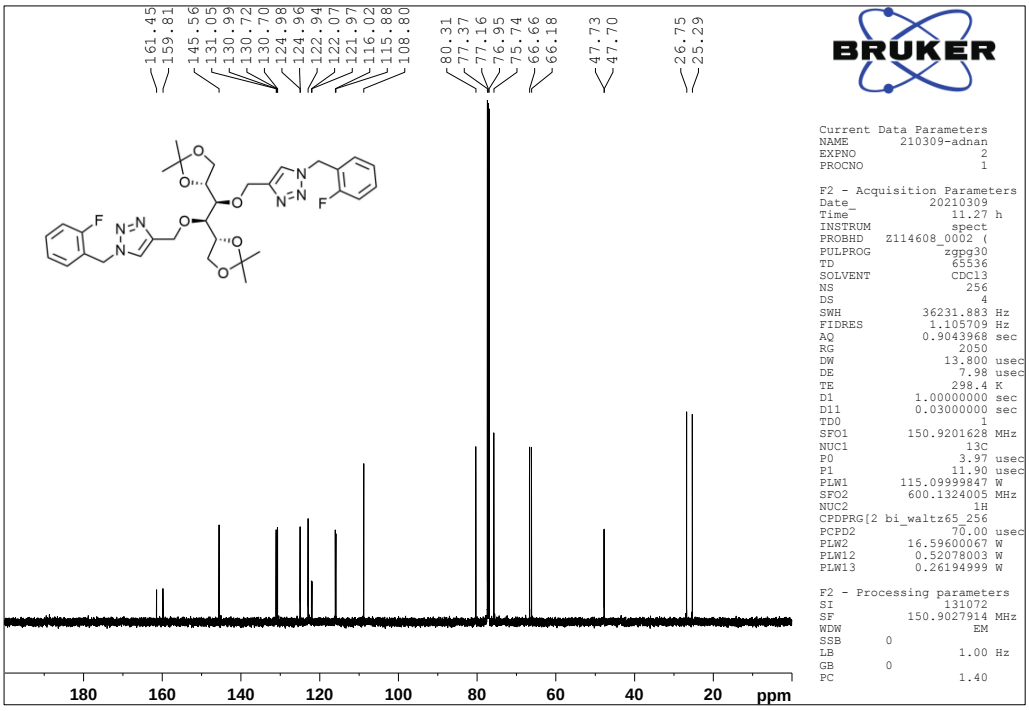

Figure 50. $^{13}C\{^{1}H\}$ NMR spectrum ($CDCl_3$, 150 MHz) of compound **103a**

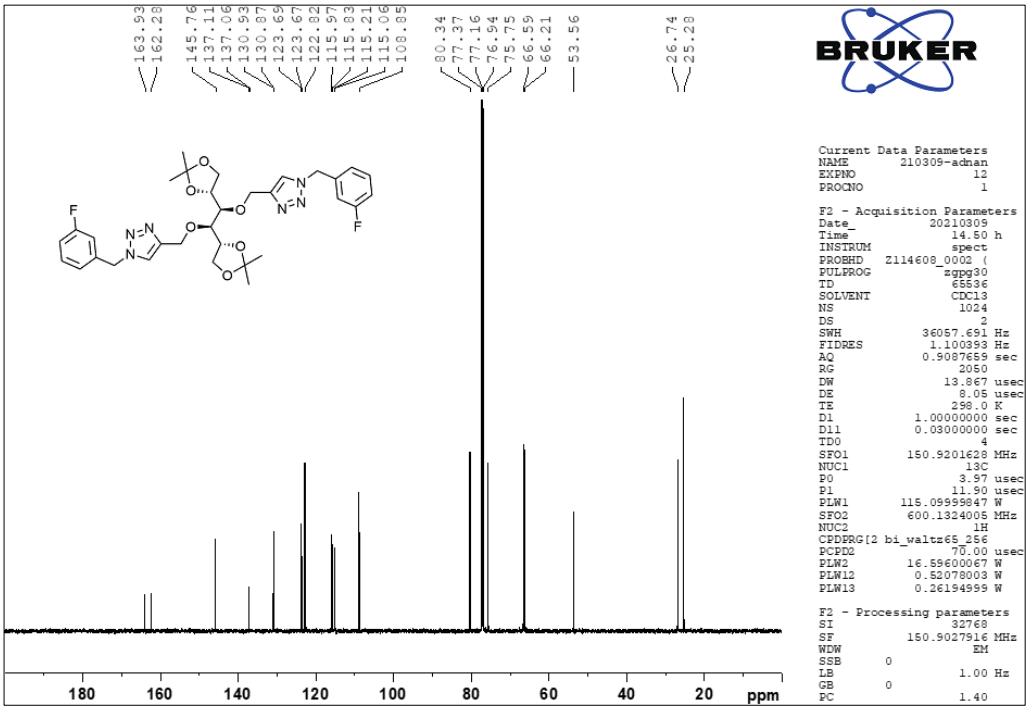

Figure 51. $^{13}C\{^{1}H\}$ NMR spectrum ($CDCl_3$, 150 MHz) of compound **103b**

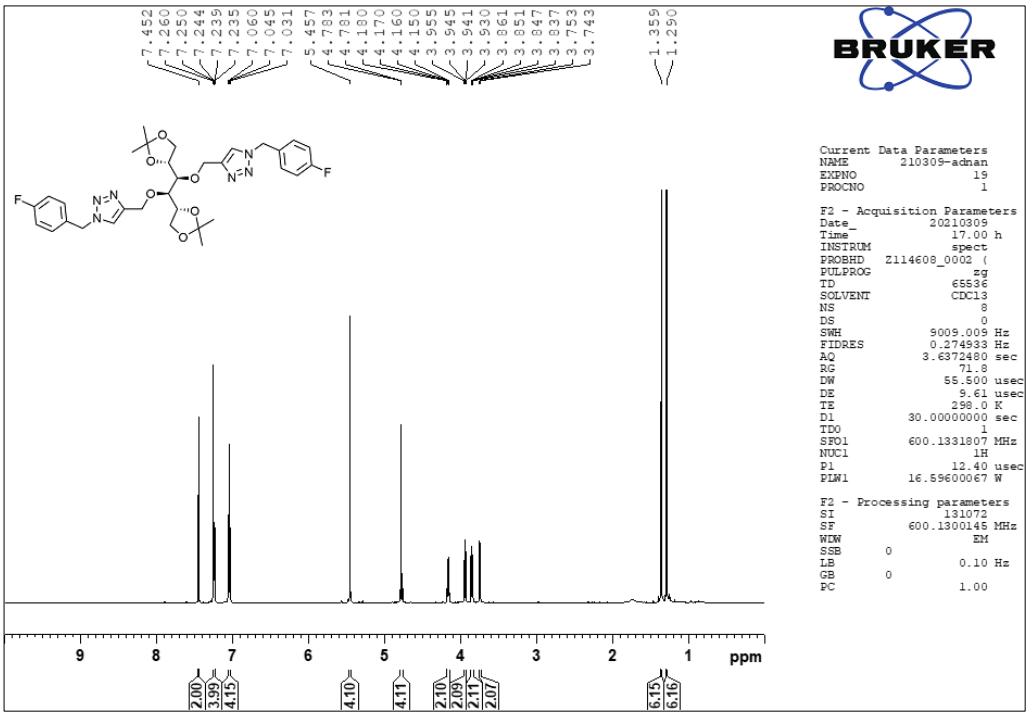

Figure 52. $^{13}C\{^{1}H\}$ NMR spectrum ($CDCl_3$, 150 MHz) of compound **103c**

All ^{19}F NMR spectra (Figures 53–55) showed one fluorine signal due to two symmetrical fluorine atoms at –118.2 ppm, –111.6 ppm, –112.7 ppm for compounds triazole derivatives **103a**, **103b** and **103c** respectively. The multiplicity of the fluorine signal is caused by fluorine-hydrogen splitting.[100]

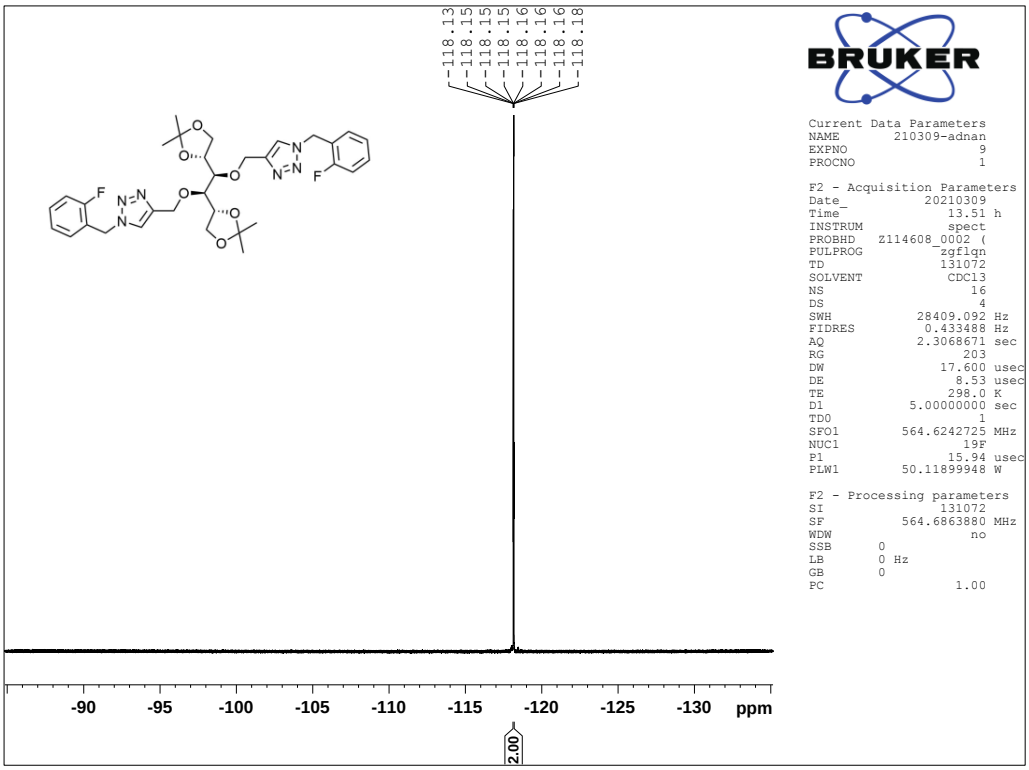

Figure 53. ^{19}F NMR spectrum ($CDCl_3$, 564 MHz) of compound **103a**

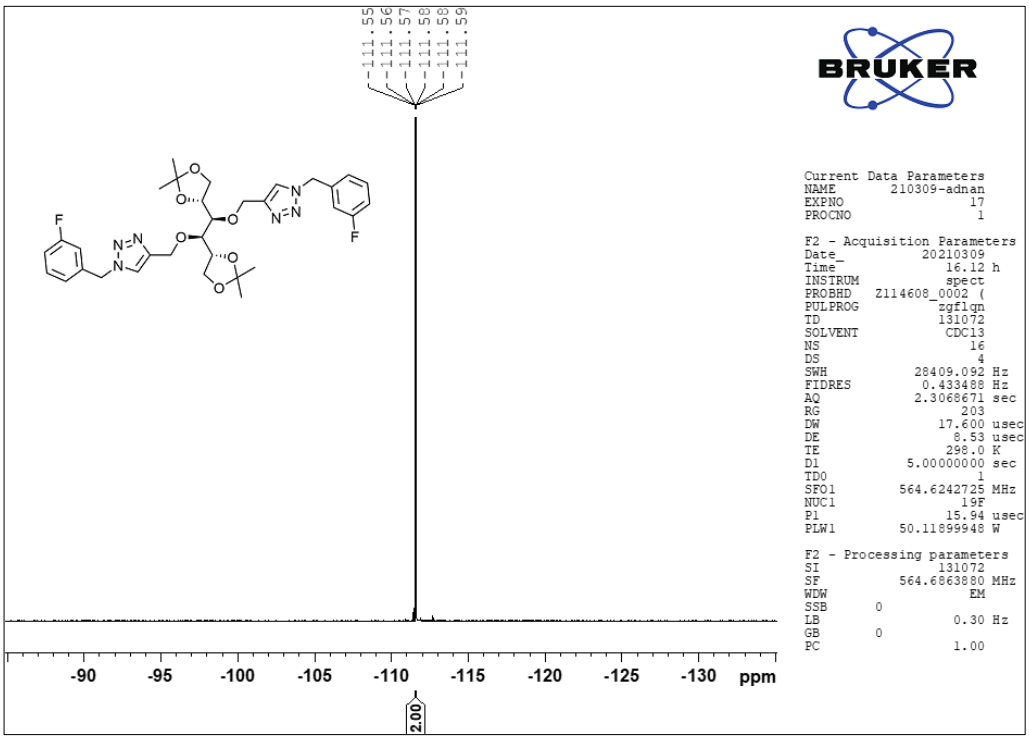

Figure 54. ^{19}F NMR spectrum ($CDCl_3$, 564 MHz) of compound **103b**

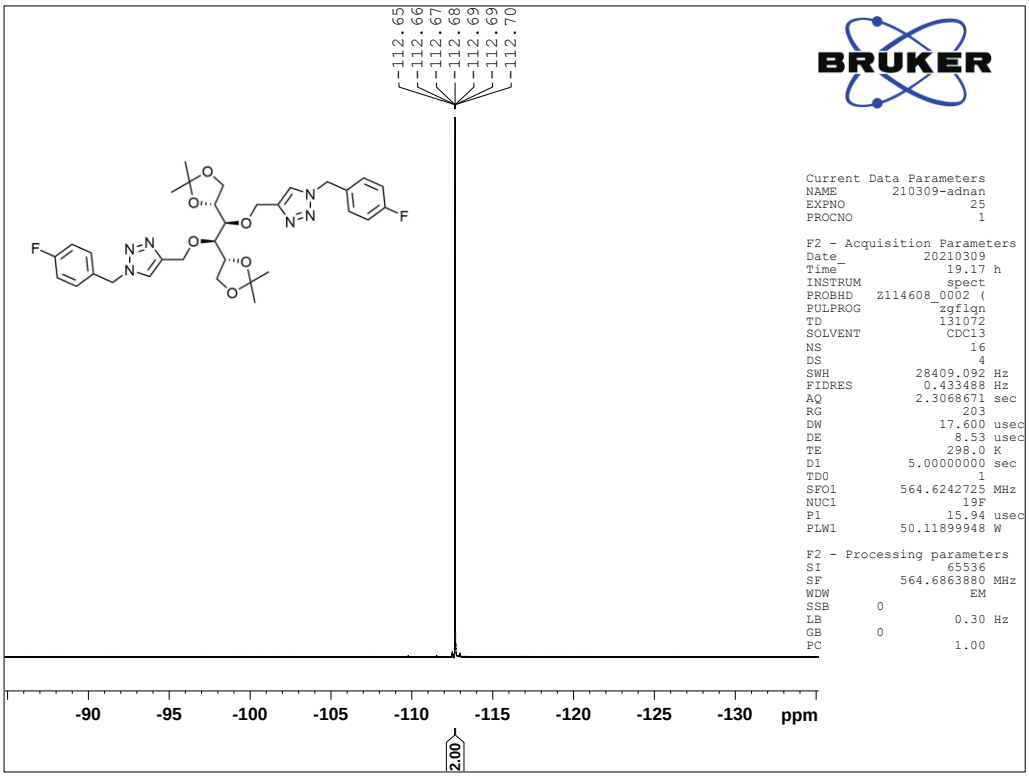

Figure 55. ^{19}F NMR spectrum ($CDCl_3$, 564 MHz) of compound **103c**

The accurate characterization of compounds **103a**–**c** is also achieved by 2D NMR technique ^{1}H–^{1}H COSY, ^{1}H–^{13}C HSQC and ^{1}H–^{13}C HMBC. COSY spectra are important tool to determine proton–proton coupling by showing cross peaks between the protons on neighboured carbons. The zoomed in ^{1}H–^{1}H COSY spectra (Figures 56–58) of compound **103a**–**c** exhibited the cross signals between mannitol core protons and they are almost similar. However, the magnified spectra (Figures 59–61) of the aromatic region exhibit significant differences between the three derivatives **103a**–**c** due to the substitution on the aromatic ring that results in different splitting patterns. This is also clear from the 1D NMR spectra.

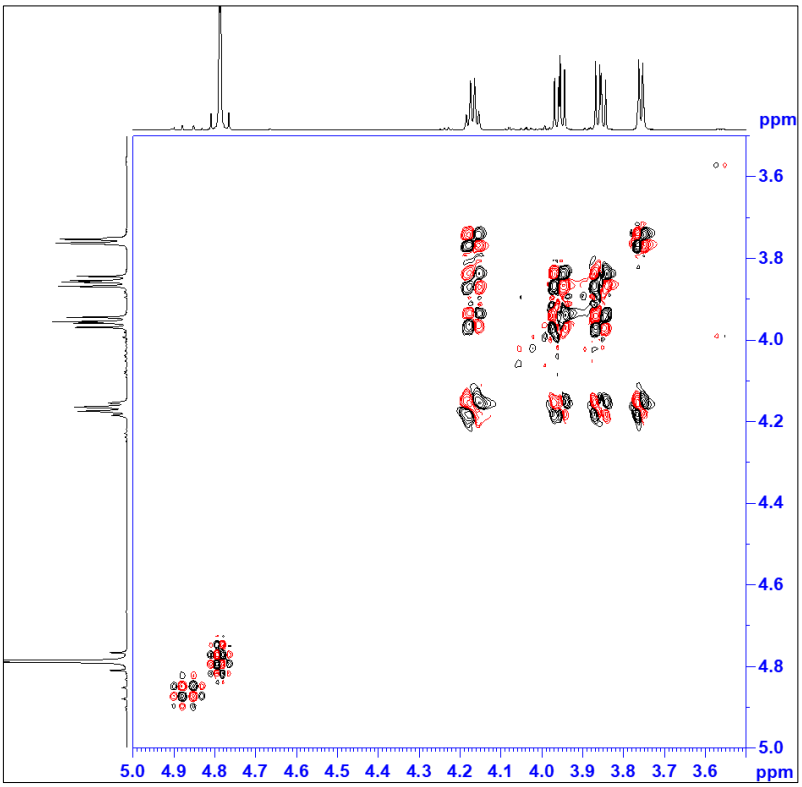

Figure 56. Zoomed in $^{1}H–^{1}H$ COSY (600 MHz, $CDCl_3$) of compound **103a**

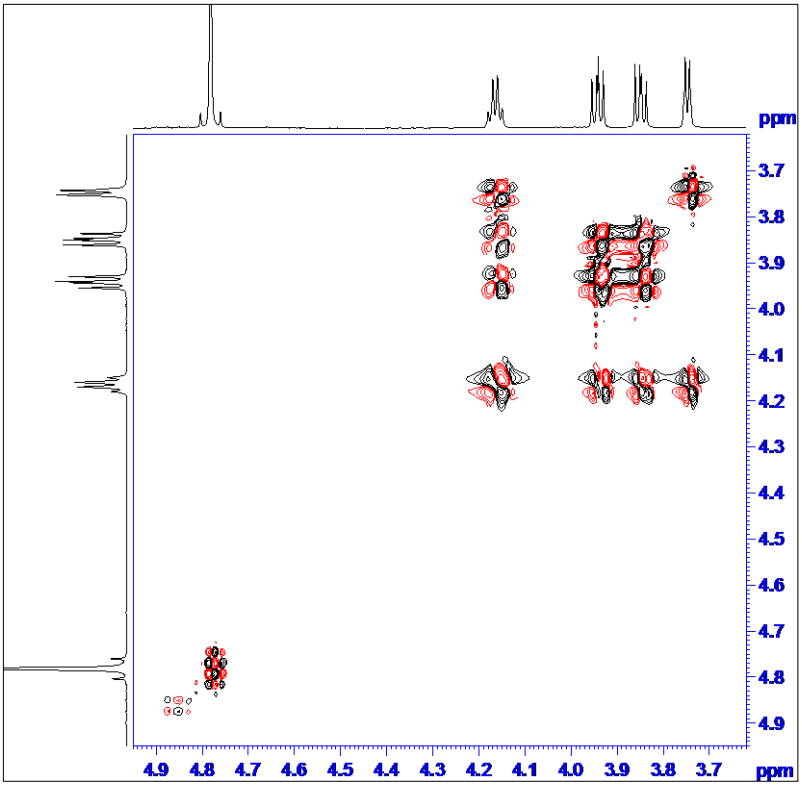

Figure 57. Zoomed in $^{1}H–^{1}H$ COSY (600 MHz, CDCl3) of compound **103b**

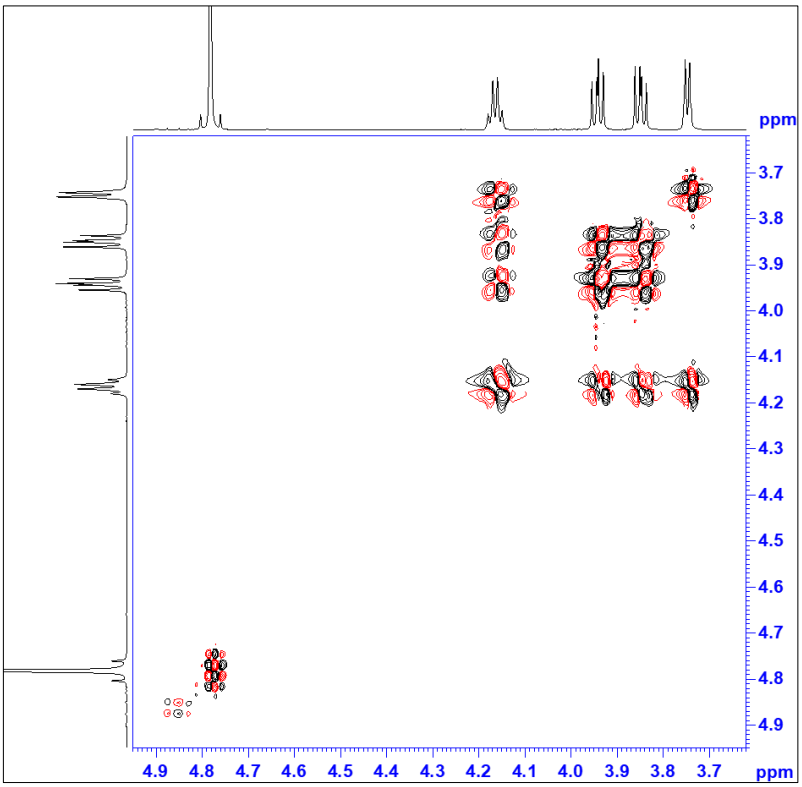

Figure 58. Zoomed in ^{1}H–^{1}H COSY (600 MHz, CDCl3) of compound **103c**

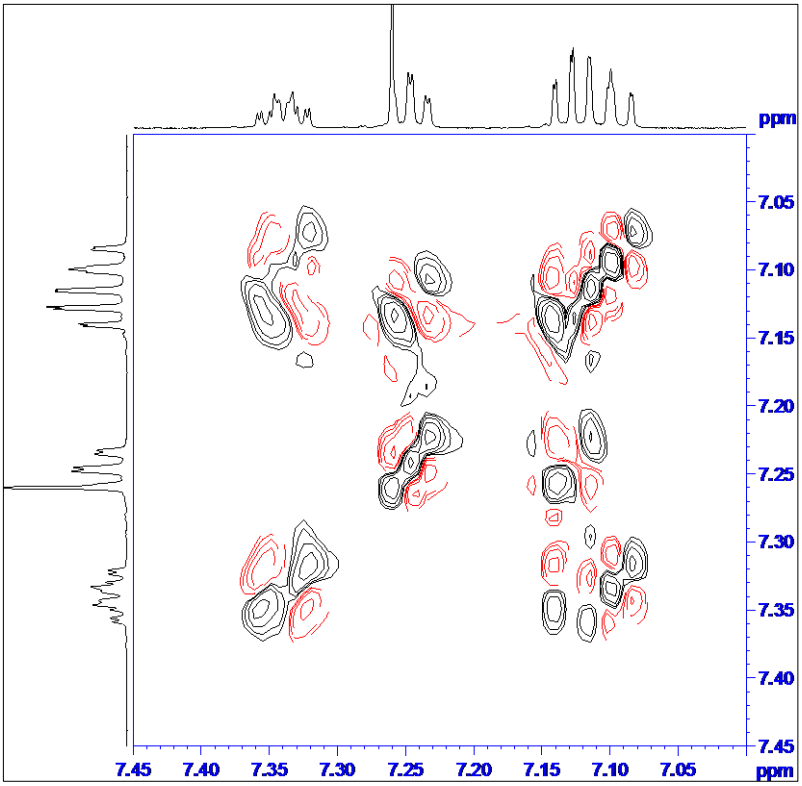

Figure 59. Zoomed in ^{1}H–^{1}H COSY (600 MHz, $CDCl_3$) of compound **103a**

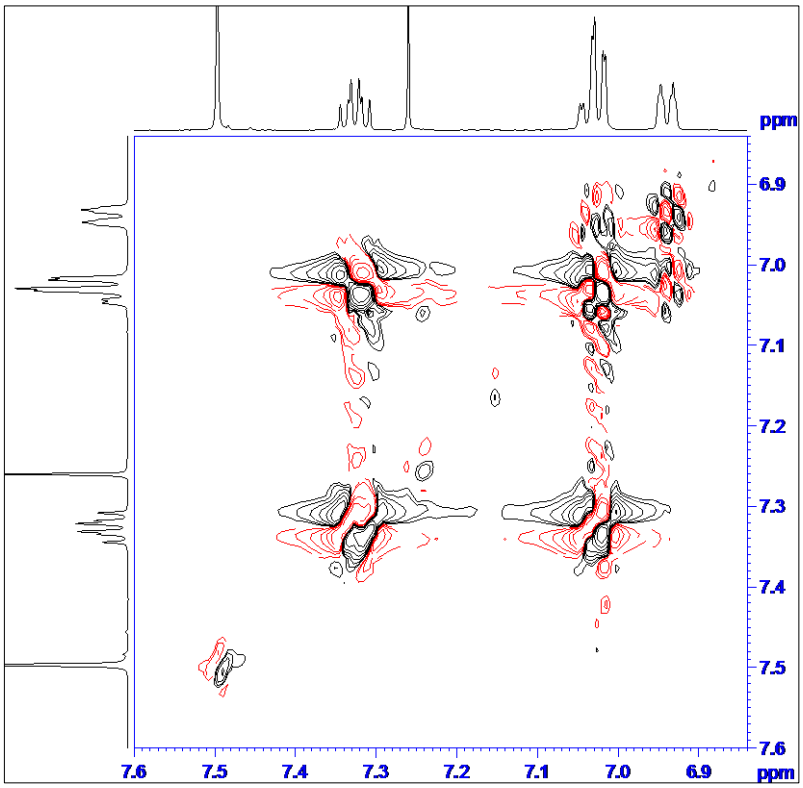

Figure 60. Zoomed in ^{1}H–^{1}H COSY (600 MHz, $CDCl_3$) of compound **103b**

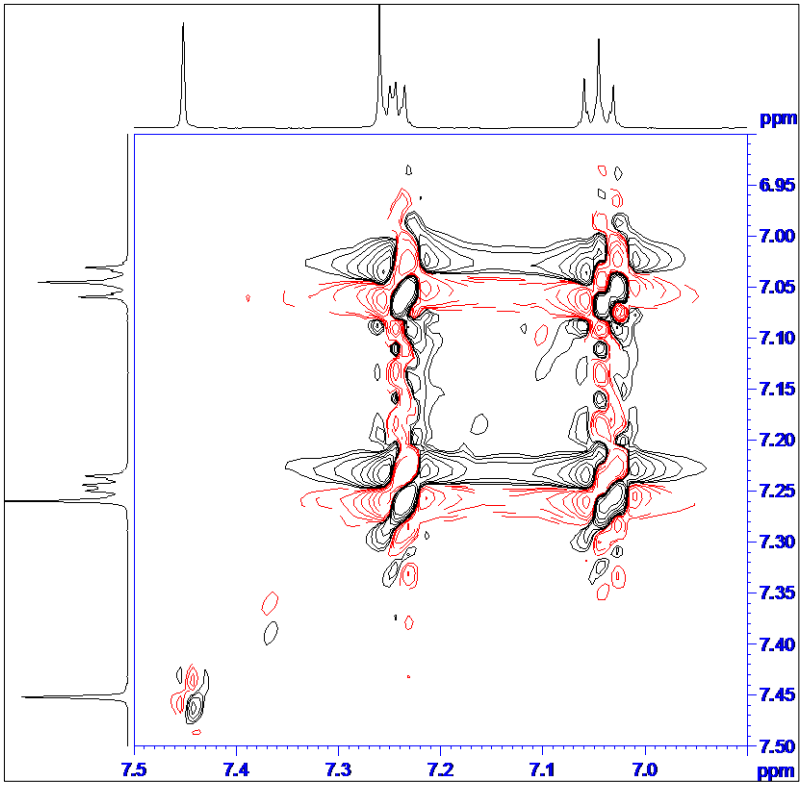

Figure 61. Zoomed in ^{1}H–^{1}H COSY (600 MHz, $CDCl_3$) of compound **103c**

Derivatives **103a**–**c** were also precisely identified using Heteronuclear Single Quantum Coherence HSQC and Heteronuclear Multiple Bond Correlation HMBC (Figures 62–66). All compounds displayed almost similar spectra for the sugar core region. However, the aromatic region exhibited obvious differences between the three compounds.

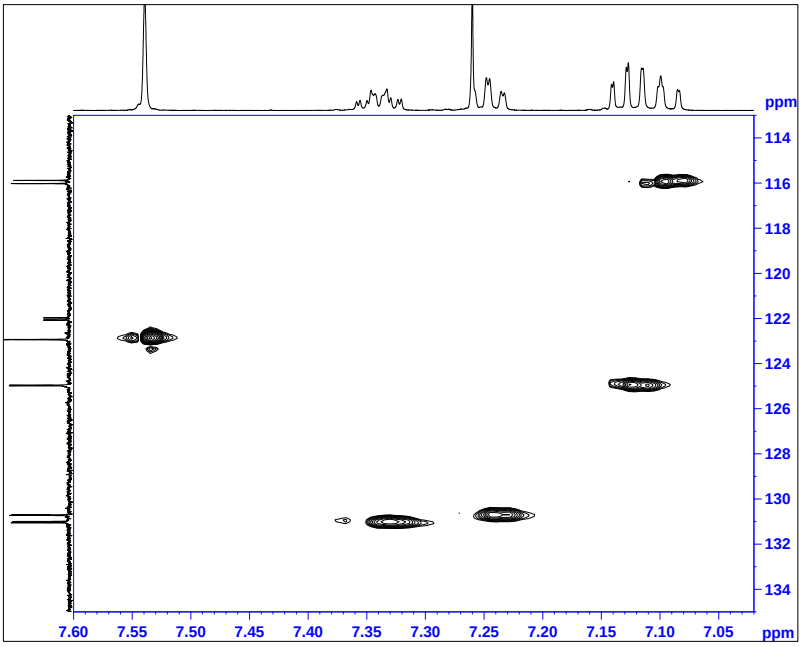

Figure 62. Zoomed in ^{1}H–^{13}C HSQC (600 MHz, $CDCl_3$) of compound **103a**

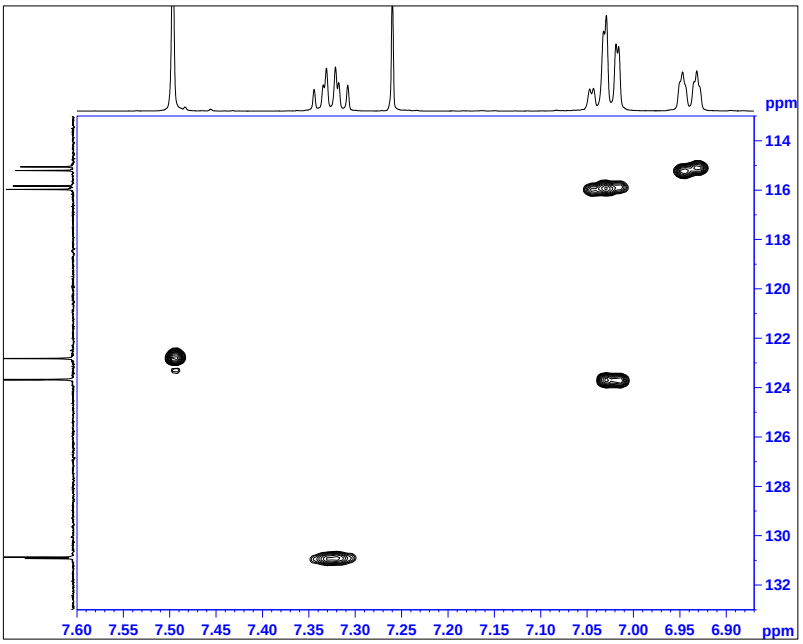

Figure 63. Zoomed in ^{1}H–^{13}C HSQC (600 MHz, $CDCl_3$) of compound **103b**

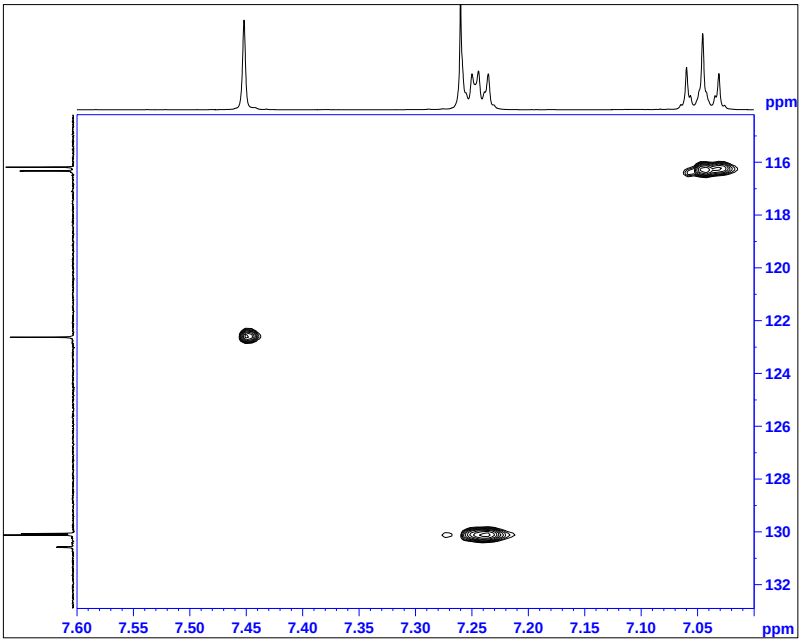

Figure 64. Zoomed in ^{1}H–^{13}C HSQC (600 MHz, $CDCl_3$) of compound **103c**

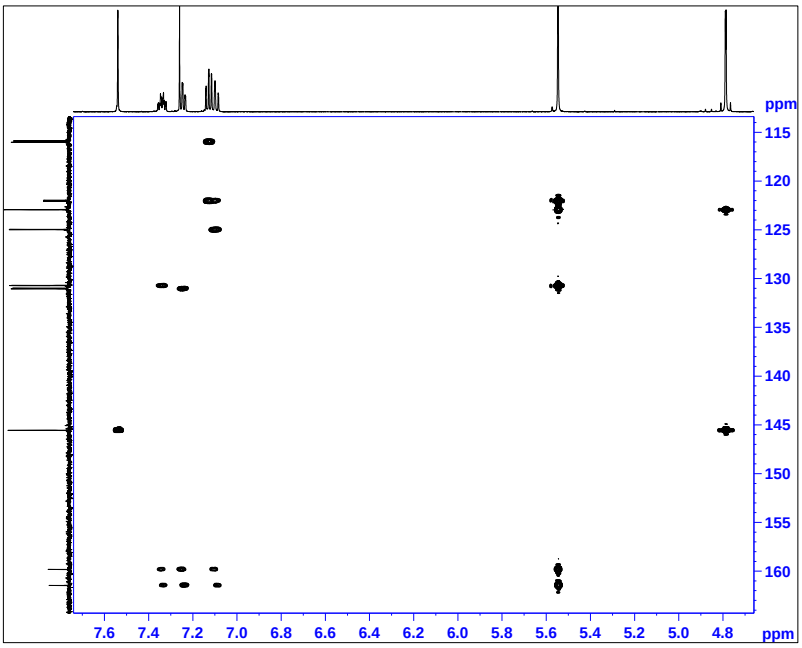

Figure 65. Zoomed in $^{1}H–^{13}C$ HMBC (600 MHz, $CDCl_3$) of compound **103a**

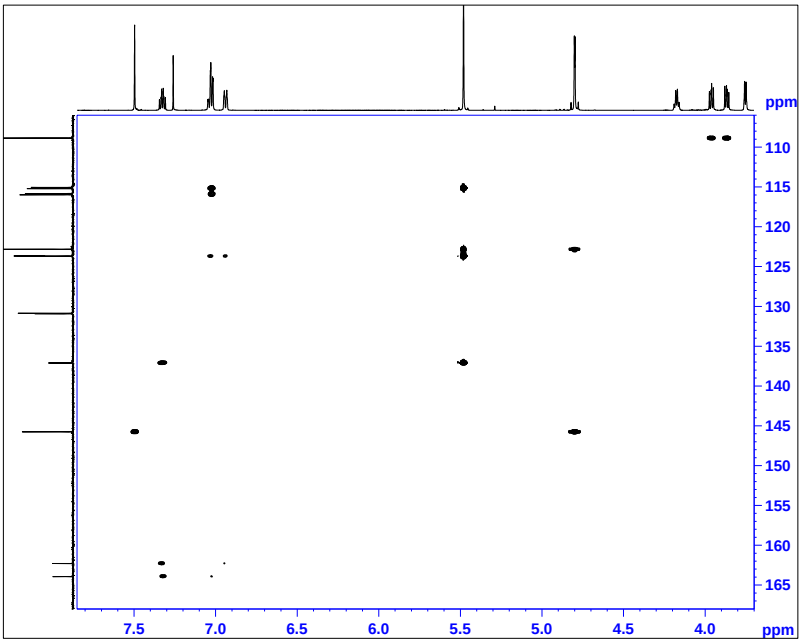

Figure 66. Zoomed in $^{1}H–^{13}C$ HMBC (600 MHz, $CDCl_3$) of compound **103b**

Finally, high resolution mass spectra have been utilized to identify the accurate mass of each derivative. HRMS analysis (Figures 67–69) base peaks at *m*/*z* 663.2707, 663.2714 and 663.2711 were observed for the compounds **103a**, **103b** and **103c** respectively consistent with the formula $C_{32}H_{38}F_2N_6O_6Na^+$.

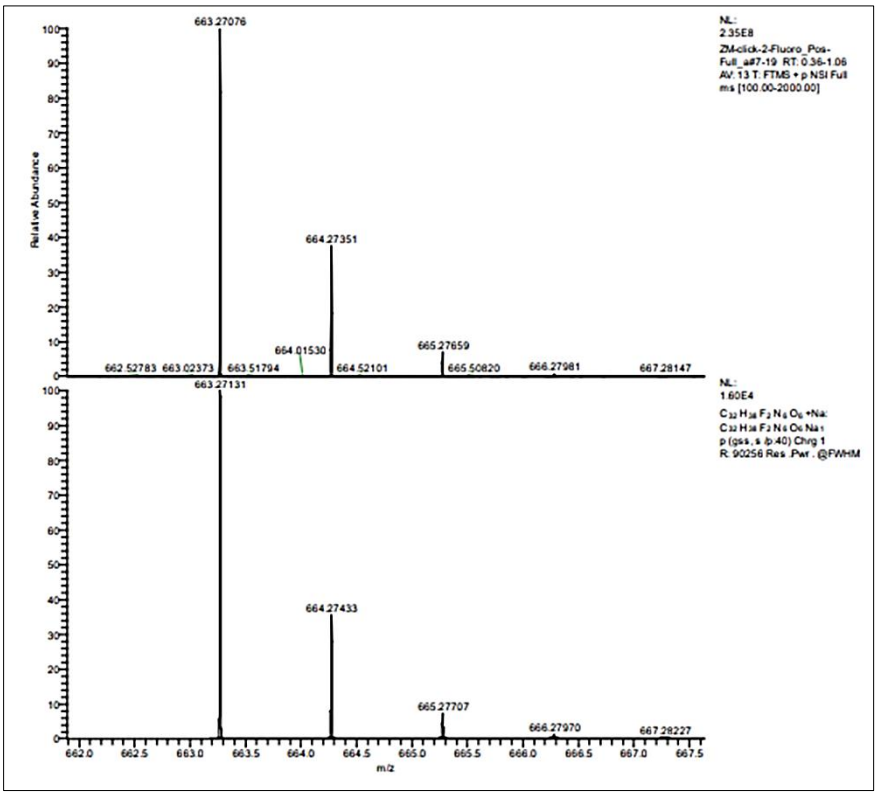

Figure 67. HRMS of compound **103a**

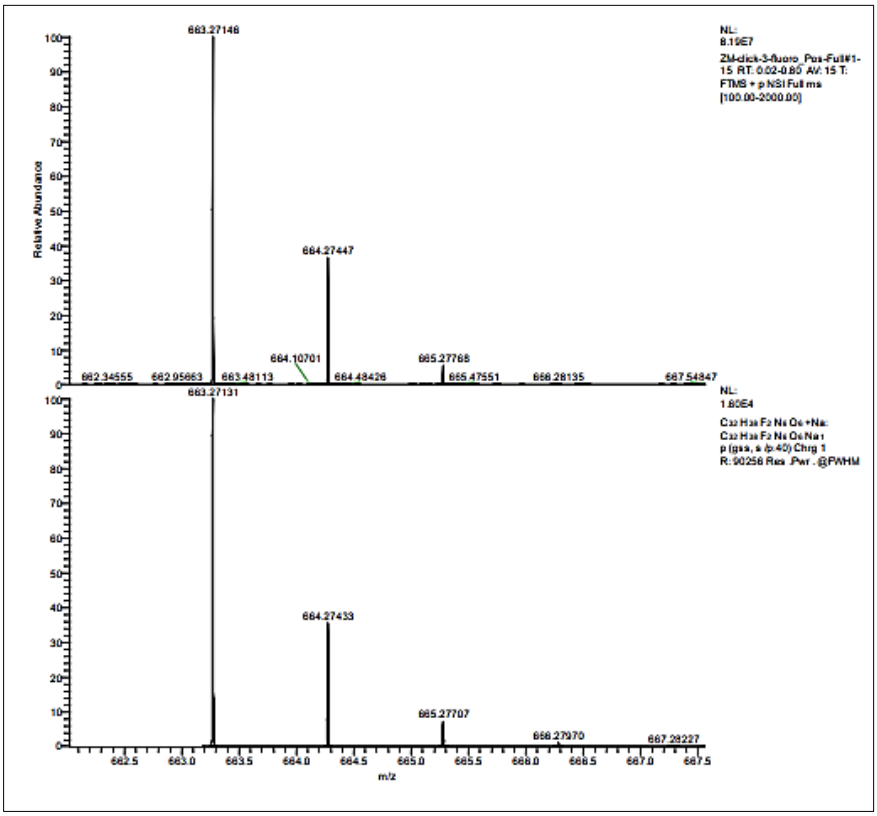

Figure 68. HRMS of compound **103b**

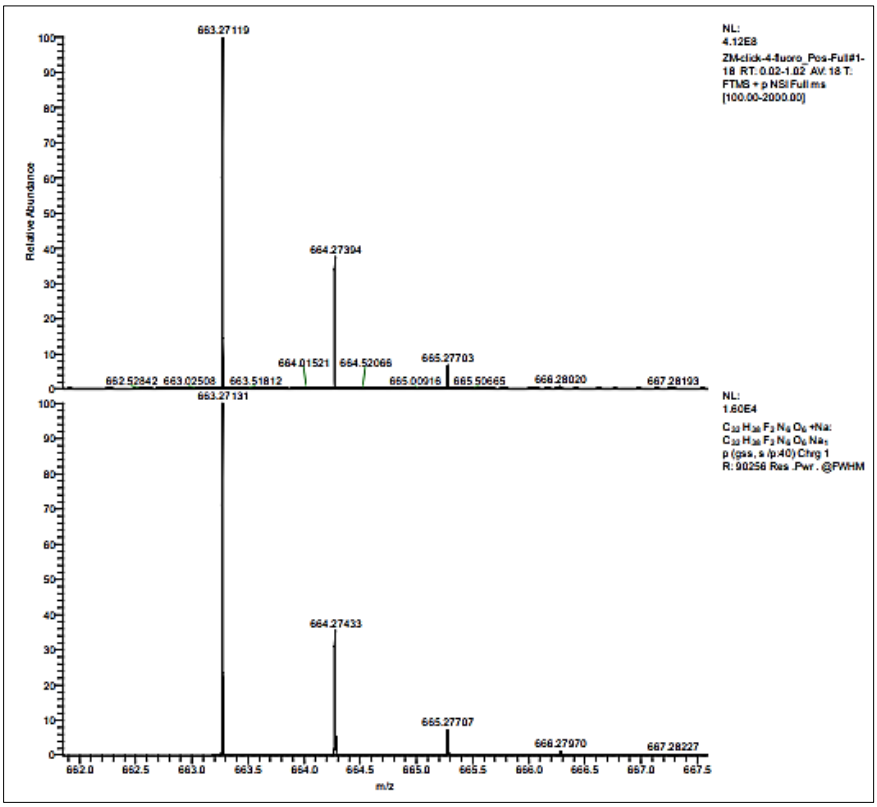

Figure 69. HRMS of compound **103c**

3.4. Acetal removal of bistriazoles

The last step in the synthetic protocol of the current work is the removal of acetal protecting groups. The treatment of compounds **103a**–**c** with acidic resin (Amberlite IR 120 H^+) in a mixture of methanol / water at 60 °C for 72 h produced the deprotected triazole derivatives **104a**–**c** quantitative yields (Scheme 27). The employment of the resin in the step is to avoid the cleavage of other ether linkage because ethers are sensitive to the acid.[101]

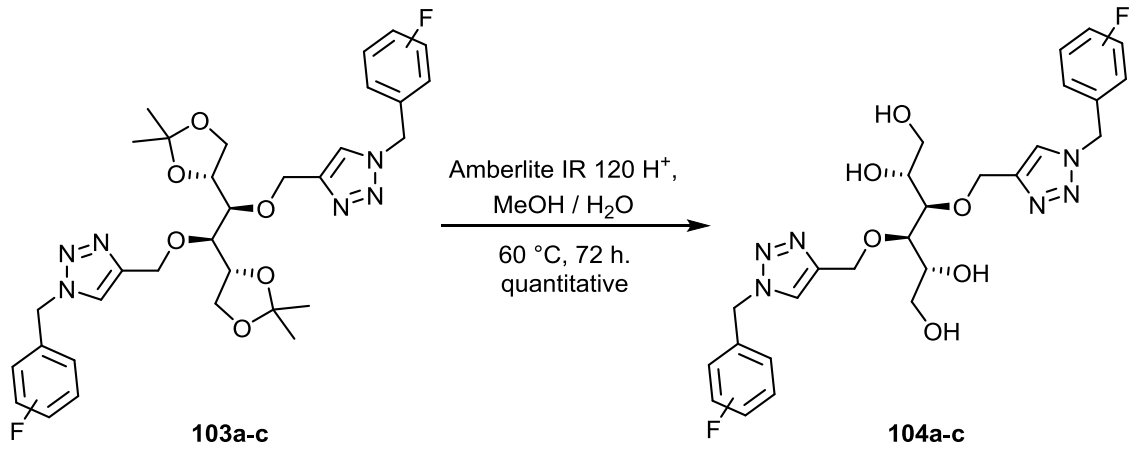

Scheme 27. Acetal removal of bis-1,2,3-triazoles **103 a–c**

The formation of compounds **104 a–c** was confirmed by IR and HRMS. FTIR spectra (Figures 70–72) showed a broad band assigned for the hydroxyl groups between 3360 cm^{-1} and 3433 cm^{-1} whereas the concrete evidence was afforded by high resolution mass spectra HRMS. The HRMS of compound **104a** (Figure 73) exhibited a base peak at *m*/*z* 561.2269 consistent with the formula $C_{26}H_{31}F_2N_6O_6^+$ while HRMS of compounds **104b** and **104c** (Figures 74 and 75) showed base peaks at 583.2086 and 583.2087 respectively consistent with the formula $C_{26}H_{30}F_2N_6O_6Na^+$.

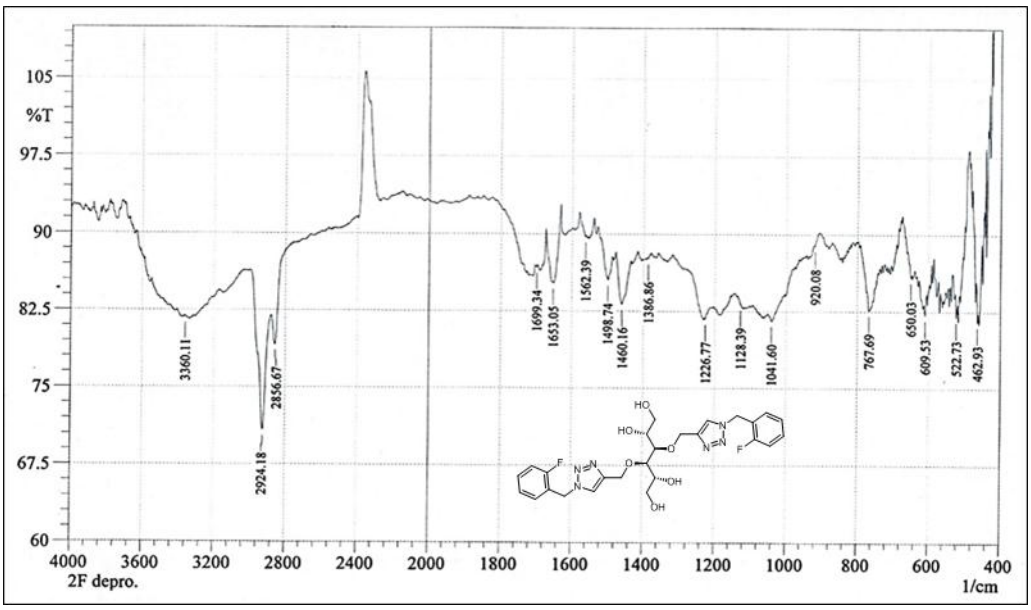

Figure 70. FT-IR spectrum of compounds **104a**

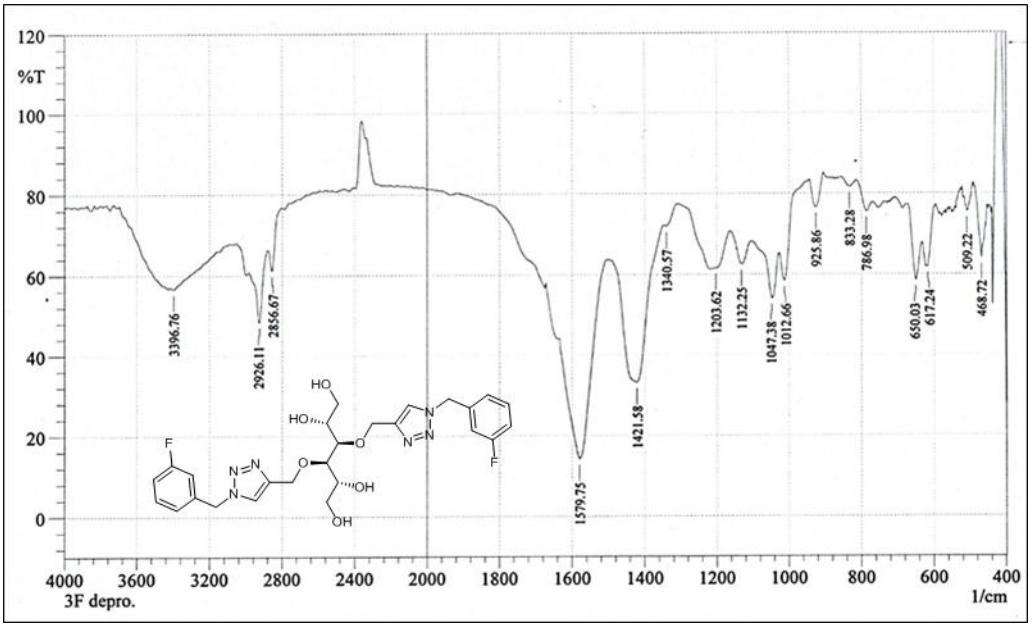

Figure 71. FT-IR spectrum of compounds **104b**

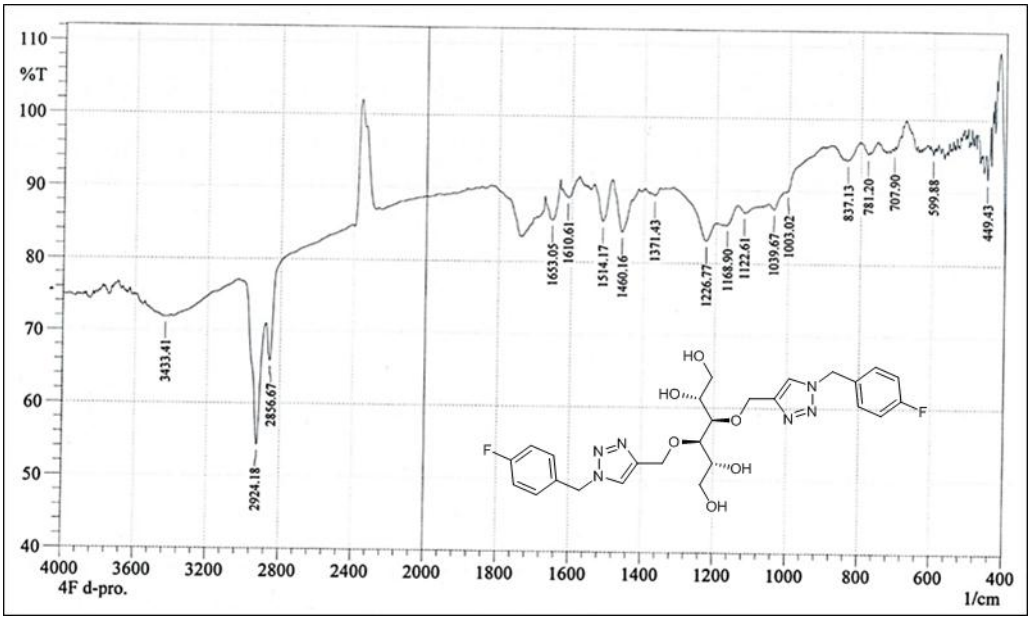

Figure 72. FT-IR spectrum of compounds **104c**

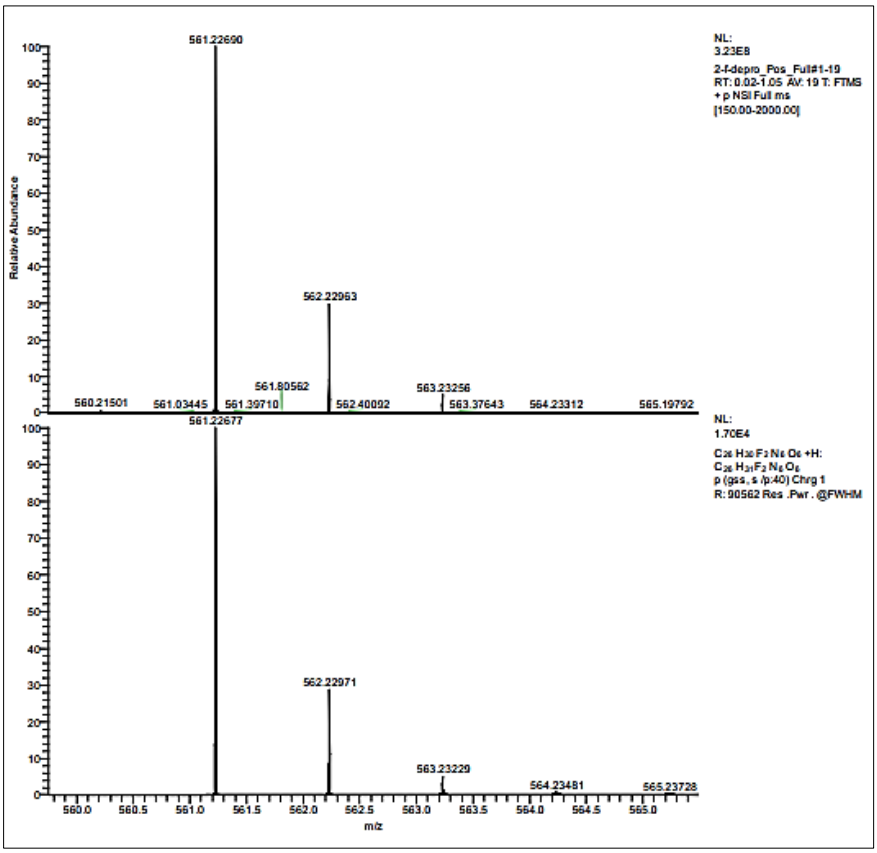

Figure 73. HRMS of compound **104a**

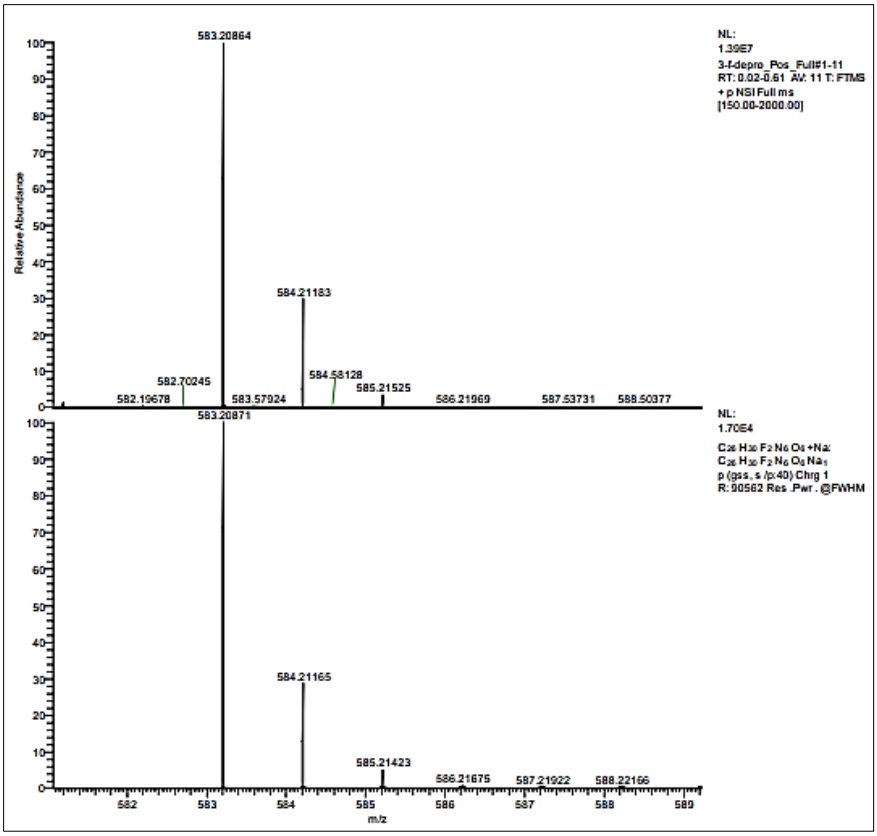

Figure 74. HRMS of compound **104b**

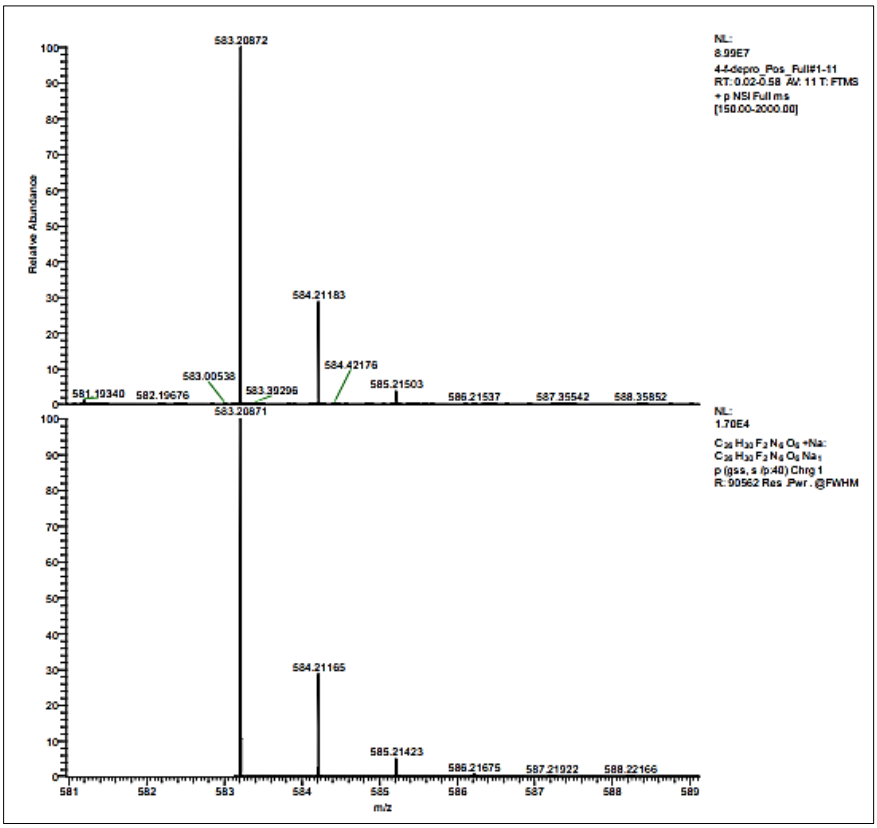

Figure 75. HRMS of compound **104c**

The important physical properties and spectral data of the synthesized compounds are summarized in Table 1.

Table 1. Some of the physical properties and spectral data of the synthesized compounds

Comp No.	Physical state and melting point	R_f and eluent	IR data	NMR data	HRMS	
					calculated	found
99a	Colorless liquid	0.75 (EtOAc)	FTIR (KBr) cm^{-1}: 3352, 3053, 2937, 2881, 2100, 1616, 1587, 1492, 1454, 1348, 1236, 1180, 1103, 1031, 941, 883, 839, 756, 669, 588, 551, 520, 424.	**^{1}H NMR** (600 MHz, $CDCl_3$) δ ppm: 7.36–7.32 (m, 2H, Ar−H), 7.17 (td, J = 7.6, 1.0 Hz, 1H, Ar−H), 7.11 (t, J = 9.1 Hz, 1H, Ar−H), 4.41 (s, 2H, Ar−C**H**$_2$). **^{13}C NMR** (150 MHz, $CDCl_3$) δ ppm: 161.0 (d, J = 247.4 Hz, Ar**C**), 130.5 (d, J = 4.1 Hz, Ar**C**), 130.4 (d, J = 8.6 Hz, Ar**C**), 124.5 (d, J = 3.4 Hz, Ar**C**), 122.8 (d, J = 15.3 Hz, Ar**C**), 115.8 (d, J = 21.7 Hz, Ar−**C**), 48.6 (d, J = 3.2 Hz, Ar−**C**H$_2$). **^{19}F NMR** (564 MHz, $CDCl_3$) δ ppm: −117.9 (m, 1F, Ar−**F**).		
99b	Colorless liquid	0.74 (EtOAc)	FTIR (KBr) cm^{-1}: 3064, 2933, 2879, 2102, 1616, 1593, 1487, 1450, 1344, 1259, 1139, 1103, 1078, 943, 891, 860, 785, 750, 690, 557, 524, 443.	**^{1}H NMR** (600 MHz, $CDCl_3$) δ ppm: 7.36 (m, 1H, Ar−H), 7.11 (m, 1H, Ar−H), 7.06–703 (m, 2H, Ar−H), 4.34 (s, 2H, Ar−C**H**$_2$). **^{13}C NMR** (150 MHz, $CDCl_3$) δ ppm: 163.0 (d, J = 246.6 Hz, Ar**C**), 138.0 (d, J = 7.1 Hz, Ar**C**), 130.5 (d, J = 8.6 Hz, Ar**C**), 123.7 (d, J = 3.0 Hz, Ar**C**), 115.3 (d, J = 21.1 Hz, Ar**C**), 115.1 (d, J = 22.0 Hz, Ar−**C**), 54.2 (Ar−**C**H$_2$). **^{19}F NMR** (564 MHz, $CDCl_3$) δ ppm: −112.3 (m, 1F, Ar−**F**).		
99c	Colorless liquid	0.76 (EtOAc)	FTIR (KBr) cm^{-1}: 3045, 2933, 2879, 2100, 1602, 1510, 1450, 1344, 1226, 1157, 1097, 1016, 941, 881, 852, 823, 767, 665, 540, 480, 420.	**^{1}H NMR** (600 MHz, $CDCl_3$) δ ppm: 7.32–7.28 (m, 2H, Ar−H), 7.01–7.05 (m, 2H, Ar−H), 4.31 (s, 2H, Ar−C**H**$_2$). **^{13}C NMR** (150 MHz, $CDCl_3$) δ ppm: 162.7 (d, J = 248.1 Hz, Ar**C**), 131.3 (d, J = 3.2 Hz, Ar**C**), 130.1 (d, J = 8.1 Hz, Ar**C**), 115.8 (d, J = 21.9 Hz, Ar−**C**), 54.1 (Ar−**C**H$_2$). **^{19}F NMR** (564 MHz, $CDCl_3$) δ ppm: −113.6 (m, 1F, Ar−**F**).		
101	With solid 120–121 ˚C	0.30 (EtOAc)	FTIR (KBr) cm^{-1}: 3464, 3317, 2989, 2935, 2881, 1485. 1458, 1417, 1379, 1255, 1211, 1155, 1072, 1041, 997, 852, 781, 698, 646, 592, 516.	**^{1}H NMR** (600 MHz, MeOH-d_4) δ ppm: 4.14 (ddd, J = 8.3, 6.0, 6.0 Hz, 2H, 2 × (−C**H**O−CH$_2$O)), 4.08 (dd, J = 8.3, 6.3 Hz, 2H, 2 × (−CHO−C**H**$_2$O)), 3.97 (dd, J = 8.4, 5.3 Hz, 2H, 2 × (−CHO−C**H**$_2$O)), 3.64 (d, J = 8.2 Hz, 2H, 2 × (−C**H**OH)), 1.37 (s, 6H, 2 × (−C(C**H**$_3$)$_2$)), 1.33 (s, 6H, 2 × (−C(C**H**$_3$)$_2$)). **^{13}C {^{1}H} NMR** (150 MHz, MeOH-d_4) δ ppm: 110.2 (2 × (−**C**(CH$_3$)$_2$)), 76.5 (2 × (−**C**HO−CH$_2$O)), 72.2 (2 × (−CHO−**C**H$_2$O)), 68.2 (2 ×	285.1308	285.1306

				(−**C**HOH)), 27.2 (2 × (−C(**C**H$_3$)$_2$)), 25.7 (2 × (−C(**C**H$_3$)$_2$)).		
102	white prismatic crystals 51–52 °C	0.56 (EtOAc)	FTIR (KBr) cm^{-1}: 3252, 2985, 2931, 2904, 2115, 1456, 1379, 1348, 1265, 1213, 1163, 1109, 1060, 1018, 964, 918, 862, 817, 675, 515.	**^{1}H NMR** (500 MHz, $CDCl_3$) δ ppm: 4.60 (dd, J = 16.0, 2.2 Hz, 2H, 2 × (−C**H**$_2$C≡CH)), 4.35 (dd, J = 16.0, 2.3 Hz, 2H, 2 × (−C**H**$_2$C≡CH)), 4.21 (dd, J = 11.0, 6.2 Hz, 2H, 2 × (−C**H**O−CH$_2$O)), 4.11 (dd, J = 8.5, 6.3 Hz, 2H, 2 × (−CHO−C**H**$_2$O)), 4.03 (dd, J = 8.0, 6.9 Hz, 2H, 2 × (−CHO−C**H**$_2$O)), 3.84 (d, J = 4.3 Hz, 2H, 2 × (−C**H**O−CH$_2$C≡CH)), 2.45 (t, J = 2.0 Hz, 2H, 2 × (−CH$_2$C≡C**H**)), 1.39 (s, 6H, 2 × (−C(C**H**$_3$)$_2$)), 1.32 (s, 6H, 2 × (−C(C**H**$_3$)$_2$)). **^{13}C NMR** (125 MHz, $CDCl_3$) δ ppm: 108.5 (2 × (−**C**(CH$_3$)$_2$)), 79.9 (2 × (−CH$_2$**C**≡CH)), 78.6 (2 × (−CH$_2$C≡**C**H)), 76.5 (2 × (−**C**HO−CH$_2$O)), 74.9 (2 × (−CHO−**C**H$_2$O)), 66.2 (2 × (−**C**HO−CH$_2$C≡CH)), 59.7 (2 × (−**C**H$_2$C≡CH)), 26.6 (2 × (−C(**C**H$_3$)$_2$)), 25.3 (2 × (−C(**C**H$_3$)$_2$)).	361.1621	361.1621
103a	White solid 98–101 °C	0.53 (EtOAc)	FTIR (KBr) cm^{-1}: 3138, 2987, 2935, 2877, 1620, 1589, 1544, 1494, 1458, 1375, 1232, 1072, 1041, 1024, 889, 846, 761, 655, 513.	**^{1}H NMR** (600 MHz, $CDCl_3$) δ ppm: 7.54 (s, 2H, 2 × H triazole)), 7.34 (dddd, J = 13.6, 7.3, 5.4, 1.7 Hz, 2H, 2 × (Ar−H)), 7.25 (td, J = 7.5, 1.7 Hz, 2H, 2 × (Ar−H)), 7.13 (td, J = 7.6, 1.1 Hz, 2H, 2 × (Ar−H)), 7.10 (dd, J = 8.4, 0.9 Hz, 2H, 2 × (Ar−H)), 5.55 (s, 4H, 2 × (Ar−C**H**$_2$−triazole)), 4.79 (d, J = 12.2 Hz, 2H, 2 × (−CHO−C**H**$_2$−triazole)), 4.785 (d, J = 12.2 Hz, 2H, 2 × (−CHO−C**H**$_2$−triazole)), 4.17 (dd, J = 12.4, 6.2 Hz, 2H, 2 × (−C**H**O−CH$_2$O)), 3.96 (dd, J = 8.5, 6.4 Hz, 2H, 2 × (−CHO−C**H**$_2$O)), 3.86 (dd, J = 8.5, 6.2 Hz, 2H, 2 × (−CHO−C**H**$_2$O)), 3.77−3.75 (m, 2H, 2 × (−C**H**O−triazole)), 1.36 (s, 6H, 2 × (−C(C**H**$_3$)$_2$)), 1.29 (s, 6H, 2 × (−C(C**H**$_3$)$_2$)). **^{13}C NMR** (150 MHz, $CDCl_3$) δ ppm: 160.7 (d, J = 248 Hz, 2 × (Ar**C**)), 145.6 (2 × (−**C** triazole)), 131.0 (d, J = 8.2 Hz, 2 × (Ar**C**)), 130.1 (d, J = 3.2 Hz, 2 × (Ar**C**)), 125.0 (d, J = 3.7 Hz, 2 × (Ar**C**)), 122.9 (d, J = 1.3 Hz, 2 × (−**C** triazole)), 122.0 (d, J = 14.5 Hz, 2 × (Ar**C**)), 116.0 (d, J = 21.1 Hz, 2 × (Ar−**C**)), 108.8 (2 × (−**C**(CH$_3$)$_2$)), 80.3 (2 × (−**C**HO−CH$_2$−triazole)), 75.7 (2 × (−**C**HO−CH$_2$O)), 66.7 (2 × (−CHO−**C**H$_2$O)), 66.2 (2 × (−CHO−**C**H$_2$−triazole)), 47.7 (d, J = 4.4 Hz, 2 × (Ar−**C**H$_2$−triazole)), 26.7 (2 × (−C(**C**H$_3$)$_2$)), 25.3 (2 × (−C(**C**H$_3$)$_2$)). **^{19}F NMR** (564 MHz, $CDCl_3$) δ ppm: −118.2 (m, 2F, Ar−**F**).	663.2713	663.2708

103b	White solid 116–118 °C	0.52 (EtOAc)	FTIR (KBr) cm^{-1}: 3136, 3072, 2987, 2937, 2877, 1647, 1593, 1544, 1492, 1485, 1454, 1373, 1249, 1114, 1024, 887, 783, 750, 682, 513.	**^{1}H NMR** (600 MHz, $CDCl_3$) δ ppm: 7.50 (s, 2H, 2 × H triazole)), 7.33 (ddd, J = 13.8, 7.8, 5.9 Hz, 2H, 2 × (Ar−H)), 7.03 (td, J = 7.5, 7.5, 1.7 Hz, 4H, 2 × (2Ar−H)), 6.94 (dt, J = 9.2, 1.8 Hz, 2H, 2 × (Ar−H)), 5.48 (s, 4H, 2 × (Ar−C**H**$_2$−triazole)), 4.80 (d, J = 12.1 Hz, 2H, 2 × (−CHO−C**H**$_2$−triazole)), 4.797 (d, J = 12.1 Hz, 2H, 2 × (−CHO−C**H**$_2$−triazole)), 4.18 (dd, J = 12.0, 6.0 Hz, 2H, 2 × (−C**H**O−CH_2O)), 3.96 (dd, J = 8.4, 6.4 Hz, 2H, 2 × (−CHO−C**H**$_2$O)), 3.87 (dd, J = 8.4, 6.3 Hz, 2H, 2 × (−CHO−C**H**$_2$O)), 3.75 (broad d, J = 5.5 Hz 2H, 2 × (−C**H**O−triazole)), 1.36 (s, 6H, 2 × (−C(C**H**$_3$)$_2$)), 1.29 (s, 6H, 2 × (−C(C**H**$_3$)$_2$)). **^{13}C NMR** (150 MHz, $CDCl_3$) δ ppm: 163.1 (d, J = 247.6 Hz, 2 × (Ar**C**)), 145.8 (2 × (−**C** triazole)), 137.2 (d, J = 7.1 Hz, 2 × (Ar**C**)), 130.9 (d, J = 8.4 Hz, 2 × (Ar**C**)), 123.7 (d, J = 3.1 Hz, 2 × (Ar**C**)), 122.8 (2 × (−**C** triazole)), 115.9 (d, J = 21.0 Hz, 2 × (Ar**C**)), 115.1 (d, J = 22.7 Hz, 2 × (Ar−**C**)), 108.9 (2 × (−**C**$(CH_3)_2$)), 80.3 (2 × (−**C**HO−CH_2−triazole)), 75.7 (2 × (−**C**HO−CH_2O)), 66.6 (2 × (−CHO−**C**H_2O)), 66.2 (2 × (−CHO−**C**H_2−triazole)), 53.6 (2 × (Ar−**C**H_2−triazole)), 26.7 (2 × (−C(**C**H_3)$_2$)), 25.3 (2 × (−C(**C**H_3)$_2$)). **^{19}F NMR** (564 MHz, $CDCl_3$) δ ppm: −111.6 (ddd, J = 14.6, 8.6, 5.7 Hz, 2F, Ar−**F**).	663.2713	663.2715
103c	White solid 105–107 °C	0.52 (EtOAc)	FTIR (KBr) cm^{-1}: 3136, 3074, 2985, 2877, 1606, 1512, 1460, 1375, 1224, 1072, 1024, 844, 748, 599, 499.	**^{1}H NMR** (600 MHz, $CDCl_3$) δ ppm: 7.45 (s, 2H, 2 × H triazole)), 7.25 (dd, J = 8.6, 3.5 Hz, 4H, 2 × (2Ar−H)), 7.05 (t, J = 8.6 Hz, 4H, 2 × (2Ar−H)), 5.46 (s, 4H, 2 × (Ar−C**H**$_2$−triazole)), 4.783 (d, J = 12.1 Hz, 2H, 2 × (−CHO−C**H**$_2$−triazole)), 4.78 (d, J = 12.1 Hz, 2H, 2 × (−CHO−C**H**$_2$−triazole)), 4.17 (dd, J = 12.3, 6.1 Hz, 2H, 2 × (−C**H**O−CH_2O)), 3.94 (dd, J = 8.5, 6.4 Hz, 2H, 2 × (−CHO−C**H**$_2$O)), 3.85 (dd, J = 8.4, 6.3 Hz, 2H, 2 × (−CHO−C**H**$_2$O)), 3.75 (broad d, J = 5.9 Hz 2H, 2 × (−C**H**O−triazole)), 1.36 (s, 6H, 2 × (−C(C**H**$_3$)$_2$)), 1.29 (s, 6H, 2 × (−C(C**H**$_3$)$_2$)). **^{13}C NMR** (150 MHz, $CDCl_3$) δ ppm: 163.0 (d, J = 248.4 Hz, 2 × (Ar**C**)), 145.7 (2 × (−**C** triazole)), 130.6 (d, J = 3.2 Hz, 2 × (Ar**C**)), 130.9 (d, J = 8.4 Hz, 2 × (Ar**C**)), 130.1 (d, J = 8.2 Hz, 2 × (Ar**C**)), 122.6 (2 × (−**C** triazole)), 116.3 (d, J = 21.6 Hz, 2 × (Ar**C**)), 108.8 (2 × (−**C**$(CH_3)_2$)), 80.3 (2 ×	663.2713	663.2712

				(−**C**HO−CH_2−triazole)), 75.8 (2 × (−**C**HO−CH_2O)), 66.6 (2 × (−CHO−**C**H_2O)), 66.2 (2 × (−CHO−**C**H_2−triazole)), 53.5 (2 × (Ar−**C**H_2−triazole)), 26.7 (2 × (−C(**C**H_3)$_2$)), 25.3 (2 × (−C(**C**H_3)$_2$)). **^{19}F NMR** (564 MHz, $CDCl_3$) δ ppm: −112.7 (tt, J = 8.5, 5.2 Hz, 2F, Ar−**F**).		
104a	White gum	0.15 (DCM / MeOH, 9:1)	FTIR (KBr) cm^{-1}: 3360, 2924, 2856, 1653, 1592, 1562, 1498, 1386, 1226, 1128, 1041, 767, 650, 609, 522, 492.		561.2267	561.2269
104b	White gum	0.17 (DCM / MeOH, 9:1)	FTIR (KBr) cm^{-1}: 3396, 2926, 2856, 1579, 1421, 1340, 1203, 1132, 1047, 1012, 925, 833, 786, 650, 617, 509, 468.		583.2087	583.2086
104c	White gum	0.15 (DCM / MeOH, 9:1)	FTIR (KBr) cm^{-1}: 3433, 2924, 2856, 1653, 1610, 1514, 1460, 1371, 1226, 1168, 1122, 1039, 1003, 837, 781, 707, 599, 449.		583.2087	583.2087

3.5. Cytotoxicity of compounds 103a–103c

The *in vitro* cytotoxicity of compounds **103a**–**103c** is screened against human mesenchymal stem cells using alamarBlue as an Indicator in two concentrations 1.0 mM and 0.5 mM. This is a colorimetric method depends on the reduction of non-toxic indicator resazurin dye (7-hydroxy-10-oxidophenoxazin-10-ium-3-one) (**105**), by dehydrogenase enzymes in the living cells, to the resofurin (**106**) (Scheme 28).[102]

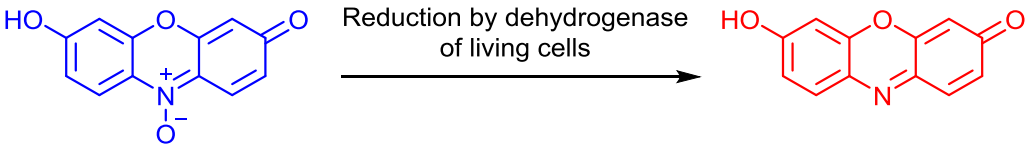

105 **106**

Scheme 28. Reduction of resazurin (**105**) to resofurin (**106**) by dehydrogenase of living cells

The concentration of the red dye resofurin (**106**) and the amount of the fluorescence produced increase as the amount of the living in the assay rises. Table 2 and Figure 76 illustrate that compounds **103a**–**103c** possess fair cytotoxicity. Generally, compounds **103a** and **103c** have higher cytotoxic effect 48% and 40% respectively at 1.0 mM. However, the increase of the concentration of compound **103b** from 0.5 mM to 1.0 mM does not affect the cytotoxicity. This can be attributed to the structures of the compounds. The electron-withdrawing effect extends in the first two compounds because the fluorine atom attaches to the *ortho* and *para* positions, which disturbs the lipophilicity of the molecules and hence affects the diffusion of the molecules into cells through the lipid bilayer membrane.[103]

Table 2. *In vitro* cytotoxicity of compounds **103a**–**103c** against human mesenchymal stem cells

Compound No.	**Cells Viability%**	
	1.0 mM	**0.5 mM**
Control	100%	
103a	52%	69%
103b	79%	72%
103c	60%	77%

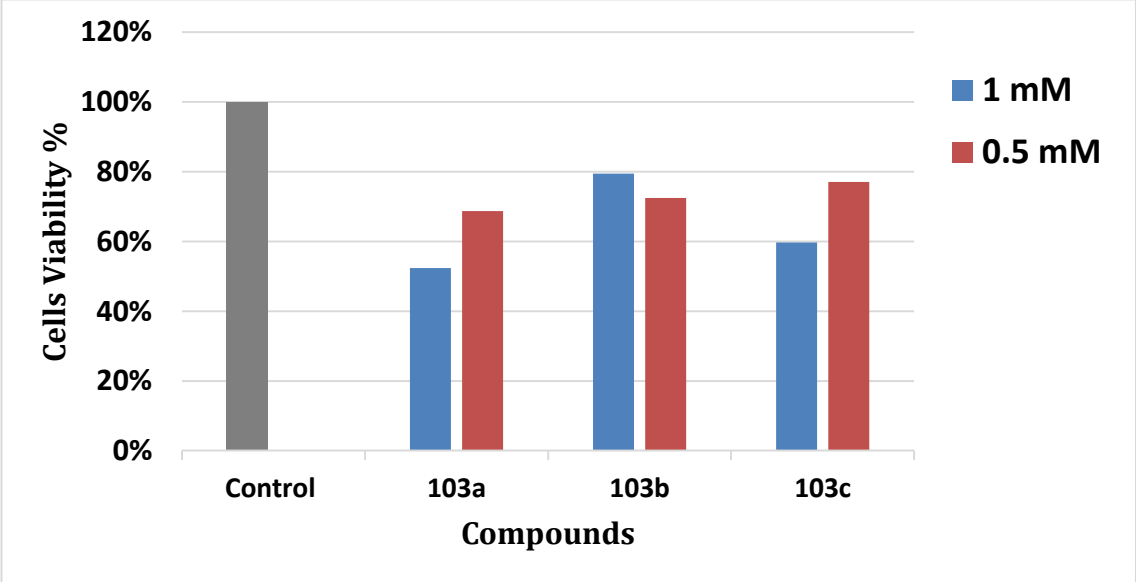

Figure 76. Cytotoxicity studies using alamarBlue assay with MSCs seeded overnight on top of compounds **103a**–**103c**. Control represents the bottom well.

3.6.Conclusion

Triazole are important class of organic compounds that have a wide range of applications. This work included the synthesis of new category of bis-1,2,3-triazoles starting of readily available carbohydrate derivative (D-mannitol). The synthesized molecules were fully characterized by TLC and spectroscopic techniques. Insertion of fluorine containing segment in the molecule increase the lipophilicity as the fluorine is hydrophilic element. This enhanced the properties of molecules towards the biological applications. The cytotoxicity of the protected triazoles **103a**–**103c** against human mesenchymal stem cells was reasonable at two concentrations 0.5 mM and 1.0 mM.

3.7.Future work

It is recommended to study the cytotoxicity of the deprotected set of the bis-1,2,3-triazoles **103a**–**103c** against human mesenchymal stem cells because they have both hydrophilic and hydrophobic parts. This will facilitate the transmission of the molecules inside the cells through the lipid bilayer membrane and consequently affords better results. It is also proposed to profoundly examine the activity of the synthesized compounds against different types of pathogenic bacteria and fungi due to the aforementioned reason. Moreover, the synthesized compounds can be utilized as ligands in the synthesis of various organometallic complexes which have numerous applications such as the medicinal, catalysis or material science fields.

References

References

1- T. L. Gilchrist "*Heterocyclic Chemistry*" 3rd ed. Addison Wesley: Essex, England, 1997. 414 pp.

2- K. C. Dze and F. Samad, *IJRASET,* 2020, **8**, 36–55.

3- P. Arora, V. Arora, H. S. Lamba and D. Wadhwa, *Int J Pharm Sci Res*, 2012, 3, 2947–2954.

4- M. Hossain and A. K. Nanda, *Chem. Sci.*, 2018, **6**, 83–94.

5- S. Saber, M. I. Alhazaa and A. A. Ibrahim, *Catal. Sustain. Energy*, 2015, **2**, 99–115.

6- N. Kerru, L. Gummidi, S. Maddila, K. K. Gangu and S. B. Jonnalagadda, *Molecules*, 2020, **25**, 1909–1950.

7- A. P. Taylor, R. P. Robinson, Y. M. Fobian, D.C. Blakemore, L. H. Jones and O. Fadeyi, *Org. Biomol. Chem.*, 2016, **14**, 6611–6637.

8- S. Tahlan, S. Kumar and B. Narasimhan, *BMC Chemistry*, 2019, **13**, 101–121.

9- R. Sapra, D. Patel and D. Meshram, *Journal of Medicinal and Chemical Sciences*, 2020, 3, 71–78.

10- J. Stagg and M. Smyth, *Oncogene*, 2010, **29,** 5346–5358.

11- F. AL-Niaimi, and N. Y. Z. Chiang, *J. Clin. Aesthet. Dermatol*., 2017, **10**, 14–17.

12- M. Lobanovska and G. Pilla, *Yale J. Bio. Med*., 2017, **90**, 135–145.

13- J. Kanetaka, T. Asano and S. Masamune, *Ind. Eng. Chem.*, 1970, **62**, 24–32.

14- S. Benetti, C. De Risi, G. P. Pollini and V. Zanirato, *Chem. Rev.*, 2012, **112**, 2129–2163.

15- K. I. Fujita, T. Fujii and R. Yamaguchi, *Org. Lett.*, 2004, **6**, 3525–3528.

16- R. Rossi and M. Ciofalo, *Molecules*, 2020, **25**, 5133–5237.

17- A. Saeed, D. Shahzad, M. Faisal, F. A. Larik, H. R. El-Seedi and P. A. Channar, *Chirality*, 2017, **29**, 684–707.

18- M. D. Morrison, J. J. Hanthorn and D. A. Pratt, *Org. Lett.*, 2009, **11**, 1051–1054.

19- V. I. Kelarev, S. G. Shvekhgeimer, V. N. Koshelev, G. A. Shvekhgeimer and A. F. Lunin, *Chem. Heterocycl. Compd*., 1984, **20,** 721–723.

20- H. Gao and J. M. Shreeve, *Chem. Rev.* 2011, **111**, 7377–7436.

21- J. Catalan, R. M. Claramunt, J. Elguero, J. Laynez, M. Menendez, F. Anvia, J. H. Quian, M. Taagepera, and R. W. Taft, *J. Am. Chem. Soc.*, 1988, **110**, 4105–4111.

22- M. Vasiliu, A. J. Arduengo and D. A. Dixon, *J. Phys. Chem. C*, 2012, **116**, 22196–22211.

23- J. A. Maertens, *Clin. Microbiol. Infect.*, 2004, **10**, 1–10.

24- B. Schulze and U. S. Schubert, *Chem. Soc. Rev.*, 2014, **43**, 2522–2571.

25- R. Balabin, *J. Chem. Phys*., 2009, **131**, 154307. DOI:10.1063/1.3249968

26- M. Arshad, *Int J Pharm Pharm Sci*, 2014, **6**, 438–442.

27- J. Huo, H. Hu, M. Zhang, X. Hua, M. Chen, D. Chen, J. Liu, G. Xiao, Y. Wang and Z. Wen, *RSC Adv*., 2017, **7**, 2281–2287.

28- K. Bozorov, J. Zhao and H. A. Aisa, *Bioorg. Med. Chem*., 2019, **27**, 3511–3531.

29- K. T. Potts, *Chem. Rev*., 1961, **61**, 87–127.

30- S. Banerjee, S. Ganguly and K. K. Sen, *J. Adv. Pharm. Edu. Res*., 2013, **3**, 102–115.

31- P. Kaur, R. Kaur and M. Goswami, *Int. Res. J. Pharm*., 2018, **9**, 1–35.

32- C. W. Bird and C. K. Wong, *Tetrahedron Lett*., 1974, **15**, 1251–1252.

33- J. Lee, M. Hong, Y. Jung, E. J. Cho and H. Rhee, *Tetrahedron*, 2012, **68**, 2045–2051.

34- M. Nakka, R. Tadikonda, S. Rayavarapu, P. Sarakula and S. Vidavalur, *Synthesis*, 2015, **47**, 517–525.

35- S. Ueda and H. Nagasawa, *J. Am. Chem. Soc*., 2009, **131**, 15080–15081.

36- J.-Q. Liu, X. Shen, Y. Wang, X.-S. Wang and X. Bi, *Org. Lett*., 2018, **20**, 6930–6933.

37- N. Jatangi, N. Tumula, R. K. Palakodety and M. Nakka, *J. Org. Chem*., 2018, **83**, 5715–5723.

38- B. R. Nemallapudi, D. R. Guda, N. Ummadi, B. Avula, G. V. Zyryanov, C. S. Reddy and S. Gundala, *Polycycl Aromat Compd*, 2021, DOI: 10.1080/10406638.2020.1866038.

39- Q. Wang, X. Shi, X. Zhang and X. Fan, *Org. Biomol. Chem*., 2017, **15**, 8529–8534

40- A. Lebeau, C. Abrioux, D. Bénimèlis, Z. Benfodda, P. Meffre, *Med. Chem*., 2016, **13**, 40–48.

41- R. Huisgen, Angew. *Chem. Int. Ed.*, 1963, **9**, 565–598.

42- K. Martina, S. Tagliapietra, V. V. Veselov and G. Cravotto, *Front. Chem*., 2019, **7**, DOI: 10.3389/fchem.2019.00095

43- J. Adrio and J. C. Carretero, *Chem. Commun*., 2014, **50**, 12434-12446.

44- R. A. Firestone, *J. Org. Chem*., 1968, **33**, 2285–2290.

45- R. Huisgen, *J. Org. Chem*., 1976, **41**, 403–419.

46- D. K. Wedegaertner, R. K. Kattak, I. Harrison and S. K. Cristie, *J. Org. Chem*., 1991, **56**, 4463–4467.

47- F. Sebest, L. Casarrubios, H. S. Rzepa, A. J. P. White and S. Díez-González, *Green Chem*., 2018, **20**, 4023–4035.

48- G. Molteni and A. Ponti, *Molecules*, 2021, **26**, 928, DOI:10.3390/molecules26040928

49- H. C. Kolb, M. G. Finn, and K. Barry Sharpless, *Angew. Chem. Int. Ed*., 2001, **40**, 2004 – 2021.

50- K. Nwe and M. W. Brechbiel, *Cancer Biother. Radiopharm*., 2009, **24**, 289–302.

51- N. M. Meghani, H. H. Amin and B. Lee, *Drug Discov. Today*, 2017, **22**, 1604–1619.

52- N. Ma, Y. Wang, B. Zhao, W. Ye and S. Jiang, *Drug Des. Devel. Ther*., 2015, **9**, 1585–1599.

53- V. V. Rostovtsev, L. G. Green, V. V. Fokin and K. B. Sharpless, *Angew. Chem. Int. Ed*., 2002, **41**, 2596–2599.

54- C. W. Tornøe, C. Christensen and M. Meldal, *J. Org. Chem*., 2002, **67**, 3057–3064.

55- W. G. Kim, M. E. Kang, J. B. Lee, M. J. Jeon, S. Lee, J. Lee, B. Choi, P. M. S. Cal, S. Kang, J. Kee, G. J. L. Bernardes, J. Rohde, W. Choe and S. Y. Hong, *J. Am. Chem. Soc*., 2017, **139**, 12121−12124.

56- A. S. Stalsmeden, A. J. Paterson, I. C. Szigyártó, L. Thunberg, J. R. Johansson, T. Beke-Somfai and N. Kann, *Org. Biomol. Chem*., 2020, **18**, 1957–1967.

57- R. Varala, H. B. Bollikolla and C. M. Kurmarayuni, *Curr. Org. Synth.*, 2021, 18. DOI.:10.2174/1570179417666200914142229

58- S. Kantheti, R. Narayan and K.V. Raju, *RSC Adv*., 2015, **5**, 3687–3708.

59- N. Touj, I. Özdemir, S. Yaşar and N. Hamdi, *Inorganica Chim. Acta*, 2017, **467**, 21–32.

60- I. E. Valverde, A. Bauman, C. A. Kluba, S. Vomstein, M. A. Walter and T. L. Mindt, *Angew. Chem. Int. Ed*., 2013, **52**, 8957–8960.

61- J. E. Doiron, C. A. Le, J. Bacsa, G. W. Breton, K. L. Martin, S. G. Aller and M. Turlington, *ChemMedChem*, 2020, **15**, 1720–1730.

62- A. I. Mohammed, N. H. Mansour and L. S. Mahdi, *Arab. **J**. Chem*., 2017, **10**, S3508–S3514.

63- A. I. Mohammed, R. S. Jwad and N. A. Al-Radha, *Int. J. Chem. Sc.*, 2013, **11**, 1–11.

64- A. I. Mohammed, *Al- Mustansiriya J. Sci*., 2011, **22**, 51–60.

65- G. Singh, G. Sharma, Sanchita, P. Kalra, P. Satija, Pawan, B. Singh, D. Aulakh and M. Wreidt, *ChemistrySelect*, 2020, **5**, 284–292.

66- R. Gondru, S. Kanugala, S. Raj, G. Kumar, M. Pasupuleti, J. Banothu and R. Bavantula, *Bioorg. Med. Chem. Lett*., 2021, **33**, DOI: 10.1016/j.bmcl.2020.127746

67- P. Awolade, N. Cele, N. Kerru and P. Singh, *Mol Divers*., 2020, DOI: 10.1007/s11030-020-10112-3.

68- D. Wang, K. Liu, X. Li, G. Lu, W. Xue, X. Qian, K. Mohamed O, F. Meng, *Eur. J. Med. Chem*., 2021, **211**, 113083, DOI: 10.1016/j.ejmech.2020.113083.

69- D. Vo, K. H. Hong, J. Lee and H. Park, *Bioorg. Med. Chem*., 2021, **29**, 115861, DOI: 10.1016/j.bmc.2020.115861.

70- T. R. Deshmukh, S. P. Khare, V. S. Krishna, D. Sriram, J. N. Sangshetti, V. M. Khedkar and B. B. Shingate, *Synth. Commun*., 2020, **50**, 271–288.

71- G. Huang, C. M. Solano, J. Melendez, S. Yu-Alfonzo, R. Boonhok, H. Min, J. Miao, D. Chakrabarti and Y. Yuan, *Eur. J. Med. Chem*., 2021, **209**, 112889, DOI: 10.1016/j.ejmech.2020.112889.

72- S. Nerella, S. Kankala and B. Gavaji, *Nat. Prod. Res*., 2021, **35**, 9–16.

73- C.P. Kaushika, J. Sangwana, R. Luxmi, D. Kumar, D. Kumar, A. Das, A. Kumar and D. Singh, *J. Mol. Struct*., 2021, **1226**, 129255, DOI: 10.1016/j.molstruc.2020.129255.

74- H. S. Khalaf, H. E. M. Tolan, M. A. A. Radwan, A. M. Mohamed, H. M. Awad and Wael A. El-Sayed, *Nucleosides Nucleotides Nucleic Acids,* 2020, **39**, 1036–1056.

75- F. Seghetti, R. M. C. Di Martino, E. Catanzaro, A. Bisi, S. Gobbi, A. Rampa, B. Canonico, M. Montanari, D. V. Krysko, S. Papa, C. Fimognari and F. Belluti, *Molecules*, 2020, **25**, 3066; DOI:10.3390/molecules25133066.

76- V. N. Holanda, E. M. de Araújo Lima, W. V. da Silva, R. T. Maia, R. de Lima Medeiros, A. Ghosh, V. L. de Menezes Lima and R. C. B. de Figueiredo, *J. Biomol. Struct. Dyn*., 2021, DOI: 10.1080/07391102.2020.1871073.

77- F. Ahmed and H. Xiong, *Dyes Pigm*., 2021, **185**, DOI: 10.1016/j.dyepig.2020.108905.

78- P. Rani, K. Lal and R. Shrivastava, *Asian J. Chem*., 2019, **31**, 2443–2447.

79- D. Ghosh, S. Rhodes, K. Hawkins, D. Winder, A. Atkinson, W. Ming, C. Padgett, J. Orvis, K. Aikena and S. Landge, *New J. Chem*., 2015, **39**, 295–303.

80- S. B. Kamble, P. M. Gawade, P. M. Badani and A. V. Karnik, *Synth. Commun*., 2020, **50**, 602–611.

81- J. Niskanen, M. N. Tousignant, A. J. Peltekoff and B. H. Lessard, *Polymer*, 2021, **212**, 123144, DOI: 10.1016/j.polymer.2020.123144.

82- A. Nahle, R. Salim, F. El Hajjaji, M. R. Aouad, M. Messali, E. Ech-chihbi, B. Hammoutid and M. Taleb, *RSC Adv*., 2021, **11**, 4147–4162.

83- A. Al-shargabia, G. Yeapa, W. A. K. Mahmood, C. Hanc, H. Linc and M. M. Ito, *Liquid Crystals*, **47**, 219–230.

84- D. V. Francis, D. H. Miles, A. I. Mohammed, R. W. Read and X. Wang, *J. Fluor. Chem.*, 2011, **132**, 898–906.

85- J. Kuszmann, É. Tomori and I. Meerwald, *Carbohydr. Res.*, 1984, **128**, 87–99.

86- A. I. Mohammed, Z. H. Abboud and A. H. O. Alghanimi, *Tetrahedron Lett.*, 2012, **53**, 5081–5083.

87- M. J. Mohammed, A. A. H. Kadhum, A. I. Mohammed and S. H. Abbood Al-Rekabi, *J. Chem. Soc. Pak.*, 2020, **42**, 103–108.

88- M. R. Altıokka and H. L. Hoşgün, *Ind. Eng. Chem. Res.*, 2007, **46**, 1058–1062.

89- E. V. Tret'yakova, E. V. Salimova and L. V. Parfenova, *Nat. Prod. Res.*, 2020, DOI: 10.1080/14786419.2020.1762187.

90- A. Rani, G. Singh, A. Singh, U. Maqbool, G. Kaur and J. Singh, *RSC Adv.*, 2020, **10**, 5610–5635.

91- S. Yoshida, *Org. Biomol. Chem.*, 2020, **18**, 1550–1562.

92- W. Peng and S. Zhu, *Tetrahedron*, 2003, **59**, 2003, 4395–4304.

93- S. Oae and Y. Kadoma, *Phosphorus, Sulfur, Silicon Relat. Elem.*, 1997, **123**, 293–300.

94- T. A. Hamlin, M. Swart and F. M. Bickelhaupt, *ChemPhysChem*, 2018, **19**, 1315–1330.

95- N. Muller and D. T. Carr, *J. Phys. Chem.*, 1963, **67**, 112–115.

96- D. H. McDaniel, *Inorg. Chem.*, 1979, **18**, 1412.

97- C. P. Reddy and R. B. Rao, *Tetrahedron*, 1982, **38**, 1825–1826.

98- A. Diamanti, Z. Ganase, E. Grant, A. Armstrong, P. M. Piccione, A. M. Rea, J. Richardson, A. Galindo and C. S. Adjiman, *React. Chem. Eng*., 2021, **6**, 1195–1211.

99- A. I. Mohammed, *Asian J. Chem*., 2012, **24**, 5585–5588.

100- J.W. Emsley, L. Phillips and V. Wray, *Prog. Nucl. Mag. Res. Sp*., 1976, **10**, 83–752.

101- B. C. Ranu and S. Bhar, *Org. Prep. Proc. Int*., 1996, **28**, 371–409.

102- S. N. Rampersad, *Sensors*, 2012, **12**, 12347–12360.

103- W. J. Dunn and Svante Wold, *Bioorg. Chem*., 1980, **9**, 1980, 505–523.

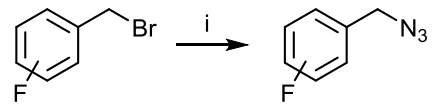

98a-c **99a-c**

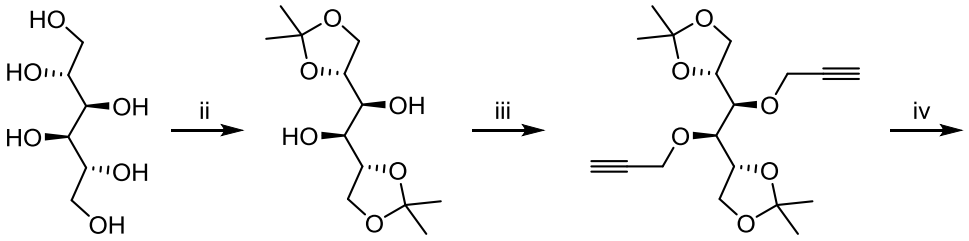

100 **101** **102**

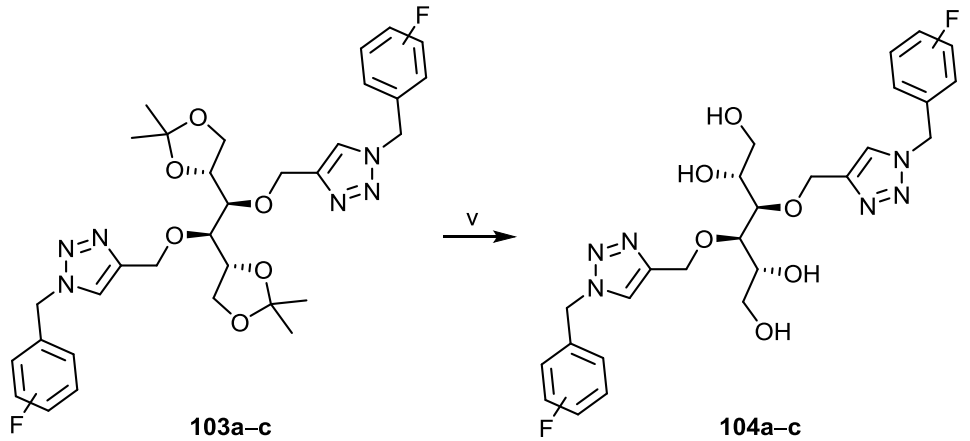

103a–c **104a–c**

Reagents and conditions: **i**] NaN_3, DMSO, 50 °C, 24 h; 88-91%ii] acetone, $ZnCl_2$, r.t., 24 h, 54%; **iii**] propargyl bromide, DMF, –20 °C–r.t.,24 h, 84%; iv] **99a–c**, Na ascorbate, $CuSO_4$•$5H_2O$, DMSO, 50 °C, 36 h, 77–81%; v] Amberlite IR 120 H+, MeOH / H_2O, 60 °C, 72 h.quantitative.

الخلاصة

تضمن العمل الحالي تحضير مشتق 3,2,1- ترايازول جديد ابتداءا من المانيتول

(mannitol based bis-1,2,3-triazoles) و دراسة سميتها ، في البداية تم تخليق أزيدات أروماتية (99a-c) بناتج ممتاز من خلال تفاعل بروميدات البنزين مع أزيد الصوديوم في مذيب DMSO . و في خطوة منفصلة ، تم تفاعل D-Mannitol المتوفر تجاريا مع الأسيتون بوجود كلوريد الزنك ليعطي :

1,2:5,6-di-O-isopropargyl-1,2:5,6-di-O-isopropylidene-D-mannitol 101

بنسبة انتاج (54%) و الذي تمت معالجته مع بروميد البروبرجيل في مذيب DMF لينتج

(3,4-bis-O-propargyl-1,2:5,6-di-O-isopropylidene-D-mannitol 102)بكمية جيدة جدا .

أعطى تفاعل الإضافة الحلقية للألكاين الثنائي 102 المحفز بواسطة النحاس مع أزيدات 99a-c مشتقات 3,2,1- ترايازول الثنائي (103a-c) نتائج جيدة جدا تقريبا .

الخطوة الأخيرة في التحضير كانت إزالة مجموعة الأسيتال لمركبات (103a-c) لتوفير مشتقات الترايازول الغير محمية (104a-c) بنواتج كمية .

تم تشخيص المركبات المحضرة بواسطة TLC، FT-IR، NMR، COSY ، HSQC ، HMBC و HRMS و تم فحص المركبات (103A-C) في المختبر ضد الخلايا الجذعية اللحمية البشرية و وجد انها تمتلك سمية خلوية معتدلة .

جمهورية العراق
وزارة التعليم العالي والبحث العلمي
جامعة كربلاء
كلية العلوم

تحضير و دراسة الفعالية الحيوية لمشتقات ثنائي 3,2,1-ترايازول بدءا من سكر المانتول

رسالة مقدمة الى
مجلس كلية العلوم – جامعة كربلاء
كجزء من استكمال متطلبات نيل درجة الماجستير
علوم في الكيمياء

من قبل

زينب محمد كاظم

بكالوريوس علوم في الكيمياء 2015 / جامعة بابل

اشراف

الأستاذ المساعد
د.عدنان إبراهيم محمد

1443 2021